Investigations into *Synechocystis* Chlorophyll Synthase

The University Of Sheffield.

Jack William Chidgey

A thesis submitted for the degree of Doctor of Philosophy

Department of Molecular Biology and Biotechnology,

University of Sheffield

September 2014

Summary

The first stage of photosynthesis involves the capture of light by pigment molecules bound within membrane-associated protein complexes. Arguably the most important of these pigments are the chlorophylls, tetrapyrrole molecules with a centrally-coordinated Mg^{2+} ion, a fifth ring and a long hydrophobic tail. Chlorophyll biosynthesis occurs in a stepwise manner, starting with chelation of the Mg^{2+} and ending with the addition of the tail via a reaction catalysed by chlorophyll synthase (CS). Then, there is handover of newly-synthesised chlorophylls to the apparatus for assembling photosynthetic complexes, in a poorly-understood process that likely involves CS.

This handover process was investigated by FLAG-tagging the *Synechocystis* CS. Following immunoprecipitation an enzymatically active protein-pigment complex was retrieved containing the high-light-inducible protein HliD, the membrane insertase YidC and the putative photosystem II assembly factor Ycf39. This is the first evidence for a link between Chl biosynthesis and YidC-dependent co-translational insertion of nascent light-harvesting polypeptides into membranes.

Analysis of similar pull-down experiments carried out on cells before and after light shock revealed that CS continues to interact with the HliD and YidC proteins during light shock whilst the interaction of CS with Ycf39 is abolished. Further analysis indicated that the light shock treatment causes a rearrangement of the remaining proteins implying different chlorophyll handover systems may be employed during assembly and repair of light harvesting and reaction centre complexes.

Preliminary kinetic characterisation of FLAG-purified CS was carried out using a chlorophyllide substrate produced by a *Rba. sphaeroides* mutant. K_m values of 25.7 µM ± 19.2 and 66.8 ± 33.1 µM for chlorophyllide and geranylgeranyl pyrophosphate, respectively, were obtained.

An artificial gene was designed encoding a polypeptide representing the loop regions of CS; the expressed, purified polypeptide was used to raise a synthase antibody, which will be useful for future studies of this enzyme.

Acknowledgements

Foremost thanks must go to Prof. Neil Hunter for his constant guidance, encouragement and enthusiasm throughout the course of my PhD.

Huge thanks must also go to Dr. Roman Sobotka, who welcomed me into his laboratory in the Czech Republic and whose expertise has been invaluable to a large portion of my work.

Throughout the course of my PhD I have been lucky enough to use a number of techniques and pieces of specialist equipment. Without the following people I wouldn't have known where to start: Dr. Phil Jackson (mass spectrometry), Dr. Nate Adams (enzymology), Dr. Amanda 'Mo' Brindley (protein purification), Dr. Chris Marklew (HPLC), Lizzy Martin, Dr. Dave Mothersole, Dr. Dan Canniffe (molecular biology), Dr. Jana Kopečná (2D electrophoresis) and Dr. John Olsen (spectroscopy). Thank you all.

My work was funded by a grant from the BBSRC, without which none of this would have been possible.

Thanks to all members of the Hunter Lab, past and present for making life in the lab enjoyable. Particularly: 'Dangerous' Dave Mothersole for taking me under his wing, Dan 'Kenneth' Canniffe for always being there with an extreme expletive to brighten a grey day (eee), 'Admiral' Chris 'Gooch' Marklew for his in-depth song reviews ('bit flaccid this one, int'it?'), Craig for his thought provoking questions ('If you threw a chicken out of a plane, would it die?') and Dave 'Spurs' Armstrong for his regimentally organised social events and being co-owner of Jack and Dave's Craft Brewery. Thanks also to my friends in the department over the past four years: the Kelly lot past and present, Ash, Laura and Pedro.

Thanks to Mum, Granny, Grandad, Paul and Shila. To Dad, Claire and Rachel.

Last, but by no means least, thanks to Alyssa for her constant support.

Table of contents

Summary 2

Acknowledgements 2

Table of contents 4

List of Figures 10

Chapter 1 10

Chapter 3 11

Chapter 4 11

Chapter 5 12

Chapter 6 13

List of Tables 13

Chapter 2 13

Chapter 6 13

List of abbreviations 14

Chapter 1: Introduction 16

1.1. Principles of photosynthesis 16

1.1.1. A brief introduction to photosynthesis 16

1.1.2. Oxygenic Photosynthesis 17

1.1.3. Photosystem II 17

1.1.4. Photosystem I (PSI) 19

1.1.5. Anoxygenic Photosynthesis 19

1.2. Model organisms used in this study 21

1.2.1. Cyanobacteria 21

1.2.2. *Synechocystis* sp. PCC 6803 21

1.2.3 Purple photosynthetic bacteria 23

1.2.4 *Rhodobacter sphaeroides* 23

1.3. Chlorophyll (Chl) and Bacteriochlorophyll (Bchl): Function and Biosynthesis... 24
1.3.1. Introduction to (Bacterio)Chlorophylls 24
1.3.2. Early Stages of Chlorophyll biosynthesis 25
1.3.3. The haem/chlorophyll branchpoint of tetrapyrrole biosynthesis 26
1.3.4. Magnesium Chelatase 28
1.3.5. Magnesium protoporphyrin methyltransferase 29
1.3.6. Mg-protoporphyrin monomethylester cyclase 30
1.3.7. Reduction of protochlorophyllide 32
1.3.8. Light-dependent reduction of protochlorophyllide 32
1.3.9. Light independent reduction of protochlorophyllide 33
1.3.10. Reduction of the 8-vinyl group of chlorophyllide 34
1.3.11. Addition and reduction of the polyprenyl tail 36
1.3.12. Bacteriochlorophyll-specific modifications to the macrocycle 39
1.4. Carotenoids 40
1.5. Thylakoid membrane structure and biogenesis 43
1.6. Photosystem II 45
1.6.1 PSII Structure and function 45
1.6.2. PSII Assembly 47
1.6.3. PSII Repair 48
1.6.4. Delivery and recycling of chlorophyll during PSII assembly and repair 48
1.7. Photosystem I 51
Chapter 2: Materials and Methods 53
2.1. Standard buffers, Reagents and Media 53
2.2. *Escherichia coli* strains, growth and plasmids 53
2.3. *Synechocystis* strains and growth 53
2.4. *Rhodobacter sphaeroides* strains and growth 53
2.5. Competent *E. coli* cells 54

2.5.1. Chemically competent E. coli cells 54
2.5.2. Electrocompetent *E. coli* cells 54
2.6. Genetic transformation of cells 54
2.6.1. Chemical transformation of *E. coli* 54
2.6.2. Electroporation of *E. coli* 55
2.6.3. Transformation of *Synechocystis* 55
2.7. Nucleic acid manipulation 55
2.7.1. Preperation of plamid DNA 55
2.7.2. Polymerase chain reaction 55
2.7.3. Restriction enzyme digests 56
2.7.4. Agarose gel electrophoresis of DNA 56
2.7.5. Recovery of DNA from agarose gels 57
2.7.6. Ligation of DNA fragments 57
2.7.7. DNA sequencing 57
2.8. Mutagenesis 57
2.8.1. 3xFLAG-tagging of *Synechocystis* genes 57
2.8.2. Deletion of *Synechocystis* genes 57
2.8.3. Mutagenesis of Rhodobacter sphaeroides 58
2.9. Protein Analysis 59
2.9.1. Determination of protein concentration 59
2.9.2. SDS-polyacrylamide gel electrophoresis (PAGE) 59
2.9.3. Clear Native (CN)-PAGE 59
2.9.4. 2D-gel electrophoresis 59
2.9.5. Immunoblot analysis of proteins: Blotting procedure 60
2.9.6. Immunoblot analysis of proteins: Immunodetection 60
2.9.7. Preparation of samples for mass spectrometry (in-solution) 60
2.9.8. Perpetration of samples for mass spectrometry (in-gel) 61

2.9.9. Mass spectrometry 61
2.9.10. Quantitative mass spectrometry 62
2.9.11. Analysis of kinetic data 63
2.10. Protein Purification 63
2.10.1. Purification of His_6-tagged proteins 63
2.10.2. Purification of FLAG-tagged proteins from *Synechocystis* 64
2.11. HPLC gel filtration of protein complexes 64
2.12. FPLC gel filtration 65
2.13. Pigment analysis 65
2.13.1. Extraction of pigments from whole cells or protein preparations 65
2.13.2. Extraction of pigments from growth media 65
2.13.3. HPLC analysis of pigments 65
2.13.4. Separation of chlorophyll precursors 65
2.13.5. Separation of chlorophyllide and chlorophyll 66
2.14. Spectroscopy 66
2.14.1. Absorbance spectroscopy 66
2.14.2. Low temperature fluorescence spectroscopy 66
Table 2. Strains 69
Chapter 3: A cyanobacterial chlorophyll synthase-HliD complex associates with the Ycf39 Protein and the YidC/Alb3 insertase 73
3.1. Summary 73
3.2. Introduction 74
3.3. Results 75
3.3.1. FLAG-tagging of the *chlG* gene 75
3.3.2. Deletion of native *chlG* from the FLAG-*chlG* strain 75
3.3.3. Purification of chlorophyll synthase and putative interaction partners using FLAG-affinity chromatography 79

3.3.4. Construction of a *Synechocystis* mutant strain expressing FLAG-tagged YidC. 79

3.3.5. 'Reciprocal' pull-downs using FLAG-tagged chlorophyll synthase interaction partners 82

3.3.6. Spectral analysis of the FGΔG eluate 83

3.3.7. Analysis of the FGΔG eluate by CN-PAGE and size exclusion chromatography 83

3.3.8. Analysis of the pigments associated with FLAG-chlorophyll synthase 87

3.3.9. Chlorophyll synthase activity of the purified FLAG-CS complex 88

3.4. Discussion 88

3.11.1 The HliD Compontent 90

3.11.2. The YidC component 91

3.11.3. The Ycf39 component 92

3.11.4. The Sll1167 component 93

3.11.5. Future work 93

Chapter 4: Analysis of the effects of light shock on chlorophyll synthase and its interaction partners 94

4.1. Summary 94

4.2. Introduction 95

4.3. Results 96

4.3.1. Light shock of FGΔG *Synechocystis* cells 96

4.3.2. FLAG-CS pull-downs from pre- and post-light shock cells 96

4.3.3. Further analysis of the composition of the pre- and post-light shock FLAG-CS eluates by size exclusion chromatography. 97

4.3.4. Analysis of the distribution of CS and its interaction partners in WT thylakoid membranes before and after light shock. 103

4.3.5. Quantification of CS interaction partners in WT thylakoid membranes before and after light shock by mass spectrometry 106

4.4. Discussion 106

4.4.1. Interaction of CS with YidC and HliD is not dependent on the presence of Ycf39 107

4.4.2. Light shock causes a rearrangement of CS containing complexes 108

4.4.3. Future work 109

Chapter 5: Chlorophyll synthase assays: substrate production, experimental design and preliminary characterisation of purified chlorophyll synthase 110

5.1. Summary 110

5.2. Introduction 111

5.3. Results 111

5.3.1. Construction of a Chlorophyllide-producing *Rba. sphaeroides* mutant ... 112

5.3.2. Deletion of *bchC* and *bchX* 115

5.3.3. Deletion of *bchF* from the Δ*bchC*/Δ*bchX* mutant 115

5.3.4. Preliminary analysis of the Δ*CXF* mutant 115

5.3.5. Supplementing the growth medium of the Δ*CXF* mutant with Tween 80116

5.3.6. Investigations into the Chlide : Pchlide ratio in the Δ*CXF* mutant 118

5.3.7. Purification of Chlide from the Δ*CXF* mutant 120

5.3.8. Development of a CS assay 122

5.3.9. Determination of optimum protein concentration for CS assays 122

5.3.10 Determination of optimum detergent concentration for the enzyme assay 124

5.3.11. Preliminary characterisation of CS 124

5.4. Discussion 126

5.4.1. Future work 128

Chapter 6: Design and purification of an artificial antigen containing the extra-membranous regions of *Synechocystis* chlorophyll synthase, antibody production and subsequent immunoblot trials 130

6.1. Summary 130

6.2. Introduction 131

6.3. Results 131

6.3.1. Bioinformatic analysis of the secondary structure of chlorophyll synthase and design of an artificial loop-only protein 132

6.3.2. Overexpression and purification of the artificial CS protein 135

6.3.3. Further purification of G-loop by size exclusion chromatography 136

6.3.4. Antibody production and trails 138

6.4. Discussion 139

Chapter 7: General Discussion 142

References 1455

List of Figures

Chapter 1

Figure 1. Electron transport in photosynthesis 18

Figure 2. Electron transport in purple bacteria 20

Figure 3. Transmission electron micrograph of an ultra thin section of a *Synechocystis* cell 22

Figure 4. Transmission electron micrograph of an ultra thin section of a *Rhodobacter sphaeroies* cell 22

Figure 5. The structure of Chlorophyll *a* 24

Figure 6. Chlorophyll (Chl) *a* and Bacteriochlorophyll (Bchl) *a* 25

Figure 7. The chlorophyll biosynthesis pathway 27

Figure 8. The reaction catalysed by magnesium chelatase 28

Figure 9. The reaction catalysed by magnesium protoporphyrin methyltransferase .. 30

Figure 10 . The reaction catalysed by Mg-protoporphyrin monomethylester cyclase 31

Figure 11. The reaction catalysed by Protochlorophyllide oxidoreductase. 34

Figure 12. The reaction catalysed by C8-vinyl reductase 35

Figure 13. The reaction catalysed by chlorophyll synthase 36

Figure 14. The bacteriochlorophyll specific reactions catalysed by chlorophyllide oxidoreductase and the BchC and BchF enzymes 40

Figure 15. Structure of thylakoid membranes 44

Figure 16. Structure and assembly of photosystem II 46

Figure 17. Proposed model for selective D1 replacement during PSII repair in *Synechocystis* 50

Figure 18. The crystal structure of *Synechococcus elongatus* PSI at 2.5 Å 52

Chapter 3

Figure 1. 3x FLAG-tagging of the *chlG* gene in *Synechocystis* 76

Figure 2. Deletion of the native *chlG* gene from the FLAG-*chlG* strain using the megaprimer method 77

Figure 3. Analysis of the FGΔG strain 78

Figure 4. Analysis of the protein components of the FGΔG eluate 80

Figure 5. C-terminal 3x FLAG-tagging of the *yidC* gene in *Synechocystis* 81

Figure 6. Reciprocal pull-down experiments using FLAG-tagged YidC and Ycf39 81

Figure 7. Spectral analysis of the FGΔG eluate 82

Figure 8. Clear native and 2D electrophoresis of the FGΔG eluate 85

Figure 9. HPLC gel filtration of the FGΔG eluate and immunodetection of eluted proteins 86

Figure 10. Pigment analysis of the FGΔG eluate by reverse phase chromatography .. 87

Figure 11. Activity of the FLAG-purified chlorophyll synthase complex 87

Chapter 4

Figure 1. Spectroscopic analysis of the FG/ΔG strain before and after light shock treatment 98

Figure 2. Analysis of pre- and post-light shock FLAG-CS eluates 99

Figure 3. Size exclusion chromatography of the ML and LS FLAG-CS eluates 100

Figure 4. Size exclusion chromatography of the ML and LS FLAG-CS eluates 101

Figure 5. Relative distribution of the components of the ML and LS FLAG-CS eluates during size exclusion chromatography 102

Figure 6. Two dimensional gel electrophoresis of WT thylakoid membranes before and after light shock..... 104

Figure 7. Quantification of CS interaction partners in WT thylakoid membranes before and after light shock by mass spectrometry..... 105

Chapter 5

Figure 1. The reaction catalysed by CS..... 113

Figure 2. A. The Bchl-specific steps of Bchl biosynthesis..... 113

Figure 3. Deletion of *bchX* and *bchC* from *Rba. sphaeroides* using the pK18mobsacB suicide vector 114

Figure 4. The Δ*CXF* mutant is orange in colour and excretes chlorophyll precursors into the growth medium..... 116

Figure 5. HPLC pigment analysis of the *ΔbchC*/Δ*bchX* and Δ*CXF* strains 117

Figure 6. Analysis of the supernatant of Δ*CXF* cultures supplemented with Tween 80 119

Figure 7. Induction of the Δ*CXF* strain after high oxygen culture..... 121

Figure 8. The absorption spectra of Chlide (in acetone) purified from the Δ*CFX* strain. 121

Figure 9. Variation of enzyme quantity..... 123

Figure 10. The effect of β-DDM variation on CS activity..... 123

Figure 11. Sample assays from the each of the two sets of CS assays 125

Figure 12. Secondary plots of steady state rates against substrate concentration for Chlide and GGPP 126

Chapter 6

Figure 1. Secondary structure predictions of Synechocystis CS using TMHMM and PRED-TMR prediction software 133

Figure 2. Secondary structure predictions of Synechocystis CS using TMpred and HMMTOP prediction software 134

Figure 3. The chlorophyll synthase amino acid sequence annotated based on secondary structure predictions 135

Figure 4. SDS-PAGE of purified G-loop 136

Figure 5. Size exlusion chromatography of nickel purified G-loop protein 137

Figure 6. Immunoblot trials of the antibody raised against the G-loop protein 138

Figure 7. Sequence alignment of (bactrio)chlorophyll synthases from *Synechocystis*, *Arabidopsis* and *Rba*. s*phaeroides* 1389

Figure 8. Identity of *Arabidopsis* and *Rba*. *sphaeroides* (bacterio)chlorophyll synthase to Synechocystis CS within the G-loop regions 140

List of Tables

Chapter 2

Table 1. Growth media 67

Table 2. Bacterial Strains 69

Table 3. Plasmids 70

Table 4. Primers 71

Chapter 6

Table 1. K_m values of Chl biosynthesis enzymes 138

List of abbreviations

ABC	Ammonium bicarbonate
ACN	Acetonitrile
ADP	Adenosine Diphosphate
ALA	5-aminolevulinic acid
AU	Absorbance units
a.u.	Arbitrary units
ATP	Adenosine triphosphate
Bchl	Bacteriochlorophyll
β-DDM	*n*-Dodecyl β-D-maltoside
BSA	Bovine serum albumin
Chl	Chlorophyll
Chl_{GG}	Geranylgeranyl-chlorophyll
COR	Chlorophyllide *a* reductase
CN-PAGE	Clear native polyacrilamide gel electrophoresis
CS	Chlorophyll synthase
DNA	Deoxyribonucleic acid
DTT	Dithiothreitol
EDTA	Ethylenediaminetetraacetic acid
E. coli	*Eschererichia coli*
GGPP/PPP	Geranylgeranyl pyrophopsphate/phytol pyrophosphate
HEPES	(4-(2-hydroxyethyl)-1-piperazomeethanesulphonic acid
Hlip	High light inducible protein
HPLC	High performance liquid chromatography
kb	Kilobase
kDa	Kilodalton

LB	Luria-Bertani medium
LC-MS/MS	Liquid chromatography - tandem mass spectrometry
LPOR	NADPH-protochlorophyllide oxidoreductase
MgCH	Magnesium chelatase
MgProto	Mg-Protoporphyrin
MS	Mass spectrometry
MT	*S*-adenosyl-L-methionine:Mg-protoporphyrin IX methyltransferase
NADP	Nicotinamide adenine dinucleotide phosphate
OEC	Oxygen evolving complex of PSII
PC	Plastocyanin
Pchlide	Protochlorophyllide
PCR	Polymerase chain reaction
PSI/II	Photosystem I/II
p.s.i.	Pounds per square inch
QconCAT	Quantification concatamer
rpm	Revolutions per minute
Rba.	*Rhodobacter*
SDS-PAGE	Sodium dodecyl sulphate polyacrylamide gel electrophoresis
Synechocystis	*Synechocystis* sp PCC 6803
WT	Wild type

Chapter 1: Introduction

1.1. Principles of photosynthesis

1.1.1. A brief introduction to photosynthesis

Photosynthesis is the process by which biological organisms capture and store light energy in a form which can then be used to drive cellular processes. Almost all life on earth is dependent directly or indirectly on photosynthesis. The exceptions to this are the chemolithotrophs such as sulphur-reducing bacteria which utilise inorganic compounds as reducing equivalents for metabolic biosynthesis.

The exact mechanism of photosynthesis varies depending on the organism in question. However, there can broadly be considered to be two different 'types' of photosynthesis: oxygenic and anoxygenic. As the names suggest oxygenic photosynthesis generates molecular O_2 whereas anoxygenic does not. Cyanobacteria, algae and plants carry out oxygenic photosynthesis whilst all other photosynthetic prokaryotes are anoxygenic.

Photosynthesis is a light-induced reduction-oxidation reaction. CO_2 is assimilated into organic matter according to the following equation:

$$CO_2 + 2H_2A \xrightarrow{\text{Light}} CH_2O + 2A + H_2O$$ Equation 1. (van Niel, 1962)

Here, H_2A is a reducing compound and CH_2O is an organic compound which functions as an energy store for the organism. The reaction is driven by light energy which is captured by the organism via pigment molecules such as chlorophyll (Chl) (discussed at length in Section 1.3.) Incident light raises electrons within reaction centres of photosynthetic protein complexes to a higher energy state. In oxygenic organisms these electrons are passed along an electron transport chain to an NADP reductase which catalyses the reduction of NADP to NADPH. The energy derived from the electron transport chain is also utilised to generate a proton-motive force which is responsible for the generation of ATP from ADP. These processes are collectively known as the light-dependent reactions. The high energy compounds evolved by the light-dependent reactions feed in to the dark reactions, where they are utilised in

carbon fixation. In anoxygenic photosynthesis electrons are transported in a cyclic fashion yielding only ATP.

1.1.2. Oxygenic Photosynthesis

In oxygenic photosynthesis the reducing compound (see Equation 1) is H_2O. The water molecule is 'split' by the oxygen evolving complex (OEC) of photosystem II (PSII) yielding oxygen as a waste product. The mechanisms of oxygenic photosynthesis detailed in Figure 1.

1.1.3. Photosystem II

PSII is one of the two reaction centre complexes of oxygenic photosynthetic organisms; the structure, function and assembly of PSII is discussed further in Section 1.6. The primary electron donor receives excitation energy either by direct absorption of a photon of incident light of suitable wavelength or via excitation energy transfer from other photosynthetic pigments in PSII. PSII contains two primary electron donors; a special pair of chlorophylls termed P680 and a Chl situated near to P680 called Chl_{D1}. Although it has been shown that both can act as primary electron donors, the preferred route and exact roles of the two donors remain unknown (Acharya *et al*., 2012).

The excited electron transfers from the primary electron donor to the electron acceptor, pheophytin (a Mg-less chlorophyll molecule). The electron then passes from one electron acceptor to the next along an electron transport chain consisting of two plastoquinone molecules (denoted Q_A and Q_B), the FeS group of the cytochrome b_6f complex and plastocyanin (PC). The quinone molecules accept protons from the stromal side of the membrane during reduction. The cytochrome b_6f complex then oxidises the quinone allowing the release of its protons on the lumenal side of the membrane; these protons are utilised in the chemiosmotic synthesis of an ATP molecule via the ATP synthase (Figure 1).

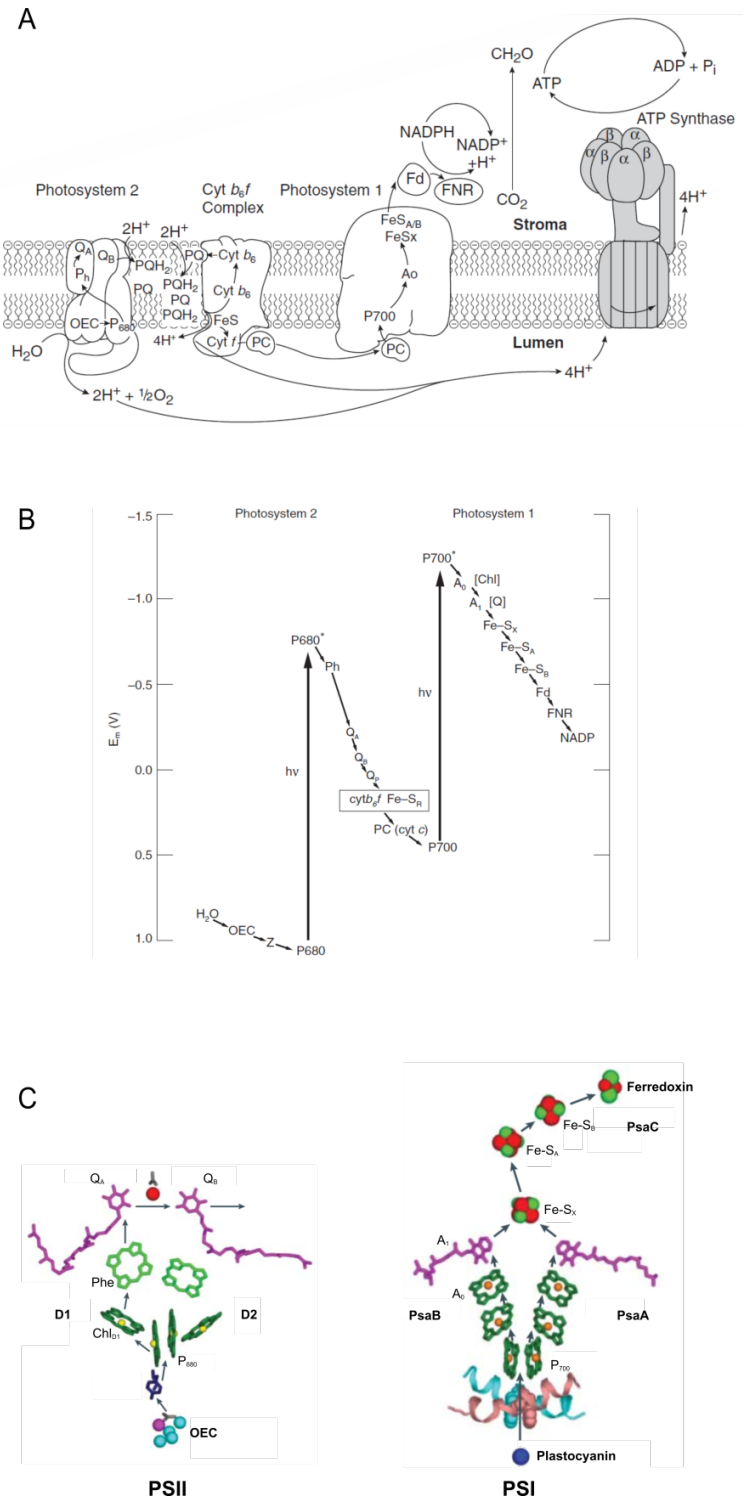

Figure 1. Electron transport in photosynthesis.

A. Schematic diagram showing the light dependent reactions of oxygenic photosynthesis; abbreviations are discussed in Sections 1.3.3. and 1.3.4.

B. z-scheme showing the electron transport chains of PSII and PSI. Modified from Blankenship (2002).

C. Electron transport pathways of PSII (left) and PSII (right) showing cofactors. Modified from Nelson and Ben-Shem (2004).

The OEC serves to replenish electrons lost by P680 by utilising the oxidising power of P680 in its oxidised state ($P680^+$) to split water to give $2H^+ + 2e^- + ½O_2$. Because the OEC is situated on the luminal side of the photosynthetic membrane the protons evolved in this reaction can be used for ATP production.

1.1.4. Photosystem I (PSI)

Similar to PSII, PSI has a special pair reaction centre denoted P700 (again because of the wavelength of its absorption maximum). This is excited in a similar way to PSII and donates an electron to the primary electron acceptor, a special chlorophyll molecule (A_0). From there the electron is passed along another electron transport chain of phylloquinone (A_1), three iron-sulphur centres (Fe-S_x, Fe-S_A and Fe-S_B), ferredoxin (Fd) and to ferredoxin NADP reductase (FNR). FNR uses the energy obtained from electron transfer to reduce NADP to NADPH.

The electrons donated by P700 after excitation are replenished by electrons from the PSII-associated electron transport chain via plastocyanin, 're-setting' the system. The energy storage compounds generated in the light-dependent reactions are then utilised to fix carbon from atmospheric CO_2 into organic compounds which are stored until required by the organism. The structure, function and assembly of PSI is discussed further in Section 1.7.1.

1.1.5. Anoxygenic Photosynthesis

Whilst the basic principles of photosynthesis are shared by both the oxygenic and anoxygenic systems there are fundamental mechanistic differences which will be discussed.

The majority of photosynthetic prokaryotes (the exception being cyanobacteria) carry out anoxygenic photosynthesis; these include purple photosynthetic bacteria, green-sulphur bacteria, green non-sulphur bacteria and heliobacteria. They only have one 'photosystem', which limits them to cyclic electron transfer and lack the ability of the oxygenic organisms to oxidise water, this means that other reducing compounds are used including H_2S, H_2, iron containing compounds, organic compounds and nitrite (Griffin *et al*., 2007). Anoxygenic organisms utilise bacteriochlorophyll for light

harvesting rather than the chlorophyll of their oxygenic counterparts; the two are similar in both their biosynthesis and function, as will be discussed in Section 1.2.

Figure 2A. shows the electron transfer pathway in purple bacteria. Light is either directly absorbed by or transferred to the special pair of bacteriochlorophyll molecules of the reaction centre complex. Excited electrons are accepted by a pheophytin molecule and transferred to a quinone (Q_A), which is tightly bound within the reaction centre, converting it to a semiquinone radical. From there the electron transfers to a second quinone (Q_B) this time loosely bound; Q_B accepts two electrons in this fashion and its reduction is coupled to the uptake of two protons. The fully reduced hydroquinol (Q_BH_2) can freely diffuse to the nearby cytochrome bc_1 complex, where it is oxidised, releasing protons on the other side of the membrane. These protons are then used for ATP synthesis. The electrons lost in the oxidation of Q_BH_2 pass to the soluble cytochrome c_2 protein which returns the electrons to the reaction centre, resetting the system. As with the previous example the ATP generated in the light-dependent reactions is utilised in the dark reactions to fix carbon.

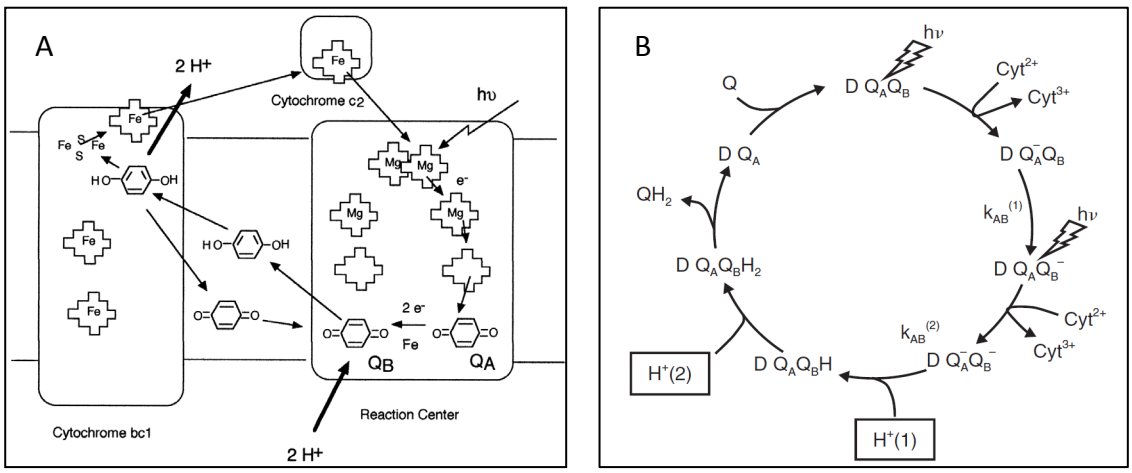

Figure 2. Electron transport in purple bacteria

A. Schematic diagram showing the light dependant reactions of anoxygenic photosynthesis.

B. The quinone cycle of anoxygeninc photosynthesis. Modified from Okamura *et al*., 2000. Abbreviations are discussed in Section 1.1.5.

1.2. Model organisms used in this study

1.2.1. Cyanobacteria

Cyanobacteria, previously known as 'blue-green algae' are aquatic, gram-negative prokaryotes capable of oxygenic photosynthesis. Oxygen produced by cyanobacteria was responsible for the oxygenation of the earth's atmosphere and oceans 2.4 billion years ago allowing aerobic respiration and therefore the evolution of large, complex organisms (Buick, 2008). It is generally accepted that ancestors of cyanobacteria gave rise to plant plastids via endosymbiotic events (Douglas, 1998). The relative simplicity of cyanobacteria coupled with the similarity of their photosystems compared to those of eukaryotic photosynthetic organisms make them useful model organisms for the study of oxygenic photosynthesis.

1.2.2. *Synechocystis* sp. PCC 6803

Synechocystis sp. PCC 6803 (henceforth *Synechocystis*) is a fresh water cyanobacterium capable of photoautotrophic growth in the presence of light, and heterotrophic growth in the presence of a carbon source such as glucose. Heterotrophic growth can be carried out in complete darkness provided the cells receive a 5-minute pulse of blue light every 24 hours (Anderson and McIntosh, 1991).

Synechocystis cells are spherical and contain a network of inner cell membranes called thylakoid membranes (Figure 3) (discussed further in Section 1.5.). The thylakoid membranes are the site of photosynthesis containing the PSI, PSII, cytochrome b_6f and ATPase protein complexes. *Synechocystis* has become an important model organism for the study of photosynthesis; it is naturally competent allowing easy transformation of foreign DNA via homologous recombination, it was the first photoautotrophic organism to have its full genome sequenced (Kaneko *et al*., 1996) and its ability to grow heterotrophically allows genetic manipulation of important photosynthetic protein complexes including PSI and PSII (Vermaas *et al*., 1988; Yu *et al*., 1995).

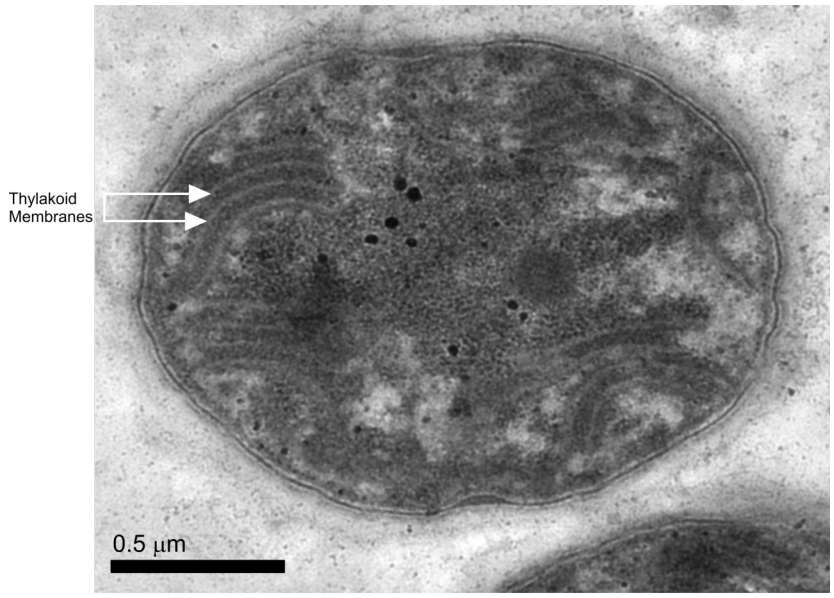

Figure 3. Transmission electron micrograph of an ultra thin section of a *Synechocystis* cell. Thylakoids are highlighted.

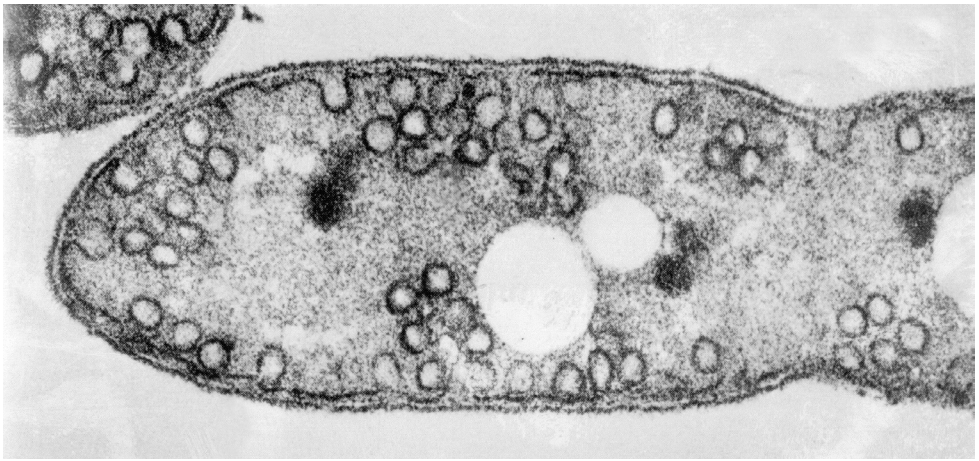

Figure 4. Transmission electron micrograph of an ultra thin section of a *Rhodobacter sphaeroides* cell. The ICM vesicles are clearly visible. Taken from: http://www.news.wisc.edu/newsphotos/images/bacterium_microscopic02.jpg

1.2.3 Purple photosynthetic bacteria

Purple bacteria are Gram negative prokaryotes that inhabit aquatic and terrestrial environments and carry out anoxygenic photosynthesis. They are extremely versatile metabolically and can grow photoautotrophically, photoheterotrophically, fermentatively or by aerobic or anaerobic respiration. Purple bacteria are able to utilise a variety of reductants (see Equation 1) and are subdivided based on their ability to reduce sulphur compounds into sulphur and non-sulphur purple bacteria (Brune, 1995). In order to carry out photosynthesis, low oxygen conditions are required; as development of the photosynthetic apparatus is repressed by molecular oxygen (Cohen-Bazire *et al*., 1957). Under low oxygen conditions morphological changes occur in which the cytoplasmic membrane undergoes multiple invaginations which form vesicles called intracytoplasmic membranes (Tucker *et al*., 2010; Figure 4). The photosynthetic apparatus is located within these intracytoplasmic membranes.

1.2.4 *Rhodobacter sphaeroides*

Rba. sphaeroides is a rod shaped, non-sulphur purple bacterium. It has been isolated from deep lakes, soil, mud, sludge, sewage and waste lagoons (Siefert *et al*., 1978; Cooper *et al*., 1975). Its optimum growth conditions are anaerobic photoheterotrophy and aerobic chemoheterotrophy whilst it is also capable of diazotrophic growth and fermentation (Blankenship *et al*., 1995).

As a model organism for studies into photosynthesis *Rhodobacter sphaeroides* offers numerous advantages, including a fully sequenced and well annotated genome allowing specific genetic manipulation of genes of interest. Its ability to grow aerobically allows mutagenesis and removal of essential photosynthetic genes, and the vast majority of its photosynthetic genes are situated within a gene cluster aiding discovery of novel genes with photosynthetic roles.

1.3. Chlorophyll (Chl) and Bacteriochlorophyll (Bchl): Function and Biosynthesis

1.3.1. Introduction to (Bacterio)Chlorophylls

Photosynthesis is utterly dependent on pigments, without which light could not be harvested. Photosynthetic pigments vary widely in their spectroscopic properties based on their structures. The most abundant and arguably most important group of photosynthetic pigments are the chlorophylls (Chl) and bacteriochlorophylls (Bchl).

Chlorophylls (Chls) are tetrapyrrole molecules containing a central Mg^{2+} ion within the macrocycle. They are the most abundant pigments on Earth and as such chlorophyll metabolism is the only biochemical processes that can be seen from outer space with an estimated 10^8 tons of chlorophyll produced (and degraded) per year (Porra, 1997; Rüdiger, 1997). There are numerous different types of (bacterio)chlorophyll (e.g. Chl *a*, Chl *b*, Chl *c*) which vary spectrally allowing a broad range of wavelengths to be harvested, however the model organisms discussed in this work (*Synechocystis* and *Rba. sphaeroides*) synthesise only (B)Chl *a* (Figure 6). According to the International Union of Pure and Applied Chemistry (IUPAC) nomenclature the five rings of the chlorophyll are lettered A to E, with each of the substituent positions on the macrocycle numbered clockwise (Figure 5).

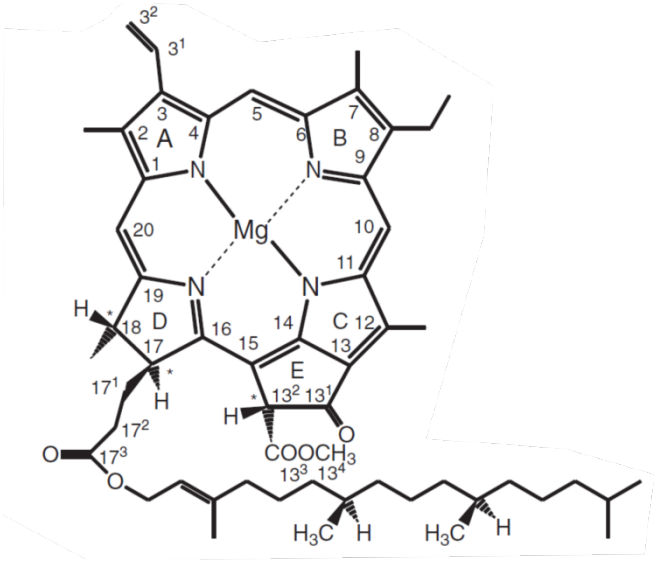

Figure 5. The structure of Chlorophyll *a*. Carbon atoms and rings are labelled according to the IUPAC system

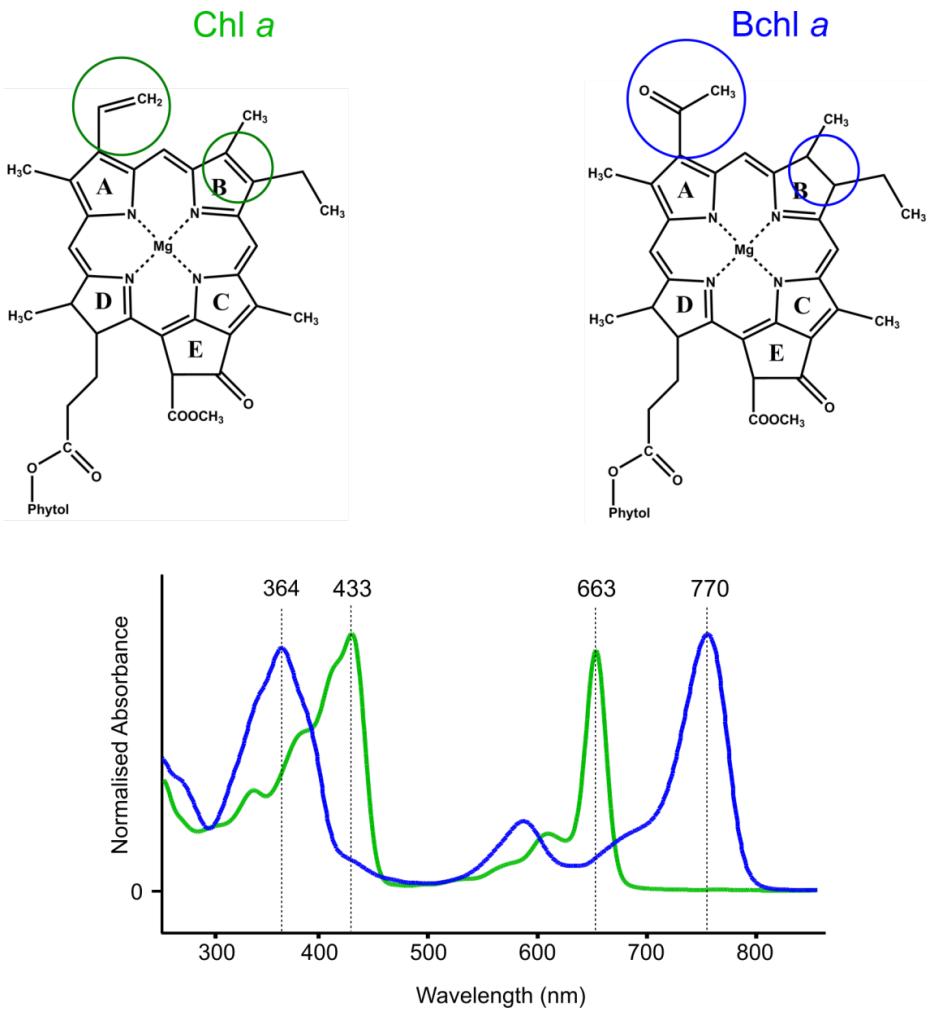

Figure 6. Chlorophyll (Chl) *a* and Bacteriochlorophyll (Bchl) *a*. Differences between the two molecules are represented by coloured circles. The absorbance spectra are shown (Chl *a* – green; Bchl *a* – blue), demonstrating the difference in absorption profile caused by the Bchl specific modifications.

1.3.2. Early Stages of Chlorophyll biosynthesis

The biosynthesis of Chl *a* has 17 enzymatic steps (summarised in Figure 7) beginning with the formation of 5-aminolevulinic acid (ALA) from glutamate. Biosynthesis of ALA is considered to be the first committed step in the tetrapyrrole biosynthesis and happens one of two ways; either from glycine and succinate or from glutamate via L-glutamyl-tRNA (Beale, 2006). In chlorophyll biosynthesis the latter route is generally used and is interesting as it is one of the very few biosynthetic pathways in which tRNA is used, other than in protein synthesis.

Two molecules of ALA are converted to porphobilinogen (PBG) via an asymmetric condensation reaction catalysed by ALA dehydrogenase. Four PBG molecules are then condensed to one hydoxymethylbilane I (HMB) by HMB sythase. HMB is linear and unstable and so spontaneously cyclises to urogen I in the absence of uroporphyrinogen III synthase (UROS) (Battersby *et al*., 1979). UROS 'flips' what will become ring D of the finished tetrapyrrole moving the propionate chain to the bottom of the molecule and closes the ring forming the first tetrapyrrole of the pathway, uroporphyrinogen III.

Uroporphyrinogen III lies at a branchpoint in tetrapyrrole biosynthesis. Decarboxylation by uroporphryinogen III decarboxylase to give coproporphyrinogen leads to chlorophyll and haem biosynthesis, whereas C-methylation is the first committed step of vitamin B_{12} synthesis (Battersby, 1994). Two more enzymatic steps catalysed by coproporphrinogen III oxidative reductase and protoporphrinogen IX oxidase lead to the formation of protoporphyrin IX (Proto), the precursor to chlorophyll and haem.

1.3.3. The haem/chlorophyll branchpoint of tetrapyrrole biosynthesis

The steps described thus far have been common between both the haem and chlorophyll biosynthesis pathways; it is at this stage that the two paths diverge. This is dependent upon which divalent metal ion is inserted in to the Proto macrocycle; if Fe^{2+} is inserted, the pathway continues toward haem and bilin production. Mg^{2+} insertion leads to chlorophyll biosynthesis.

The chelation of Fe^{2+} is carried out by ferrochelatase (FeCH), whereas the Mg^{2+} chelation is carried out by magnesium chelatase (MgCH). The FeCH reaction has no requirement for energy input although it cannot spontaneously occur. The reaction catalysed by MgCH on the other hand requires the hydrolysis of approximately 14 ATP molecules (Reid and Hunter, 2004), making it an energetically expensive reaction. It has been proposed that this high energy input is required to remove the hydration shell from the Mg^{2+} ion (Gibson *et al*., 1995; Jensen *et al*., 1996; Reid and Hunter, 2004).

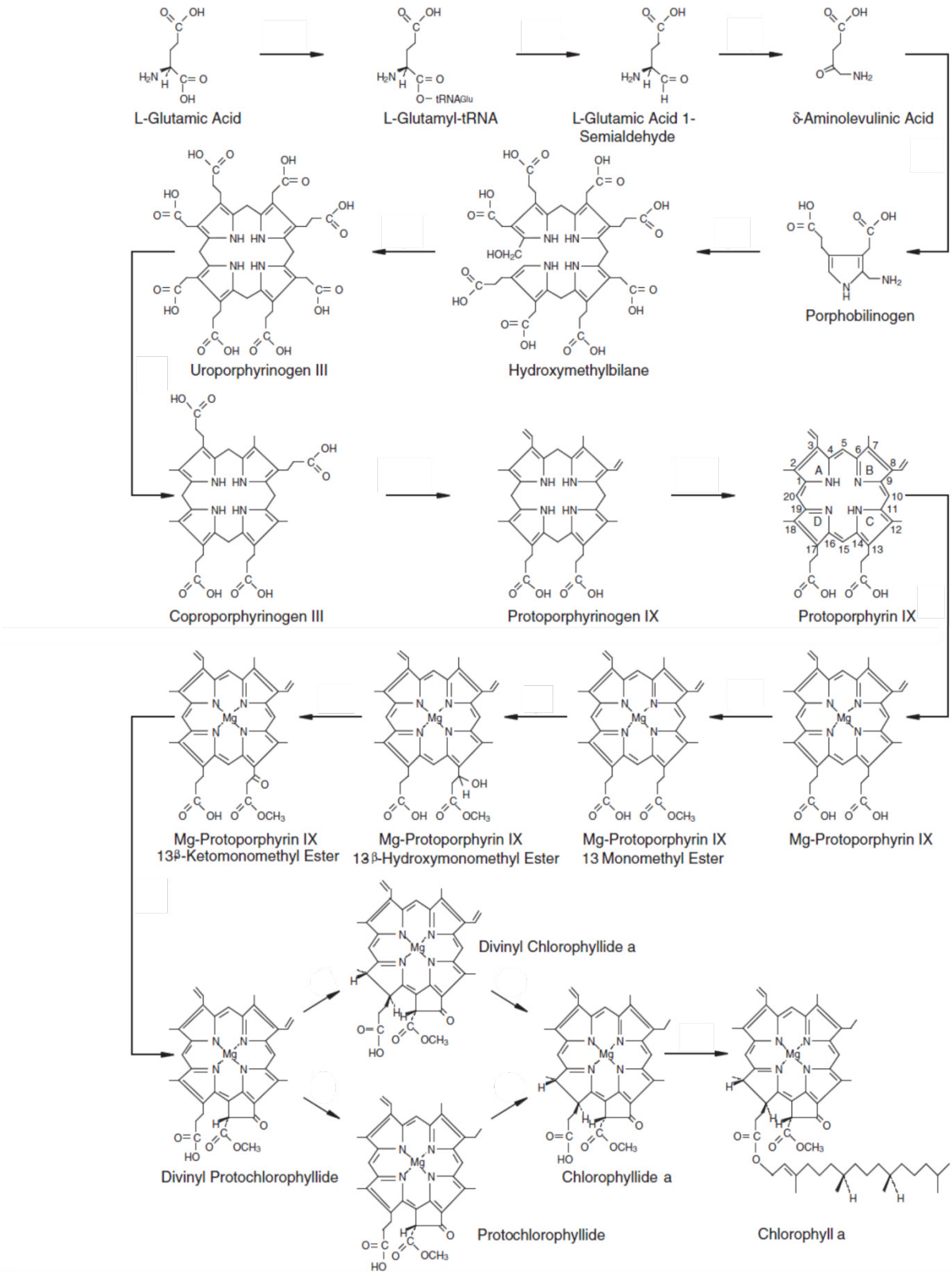

Figure 7. The chlorophyll biosynthesis pathway. Modified from Blankenship, (2008).

1.3.4. Magnesium Chelatase

MgCH is a multi-subunit enzyme which catalyses the ATP dependent insertion of a magnesium ion in to the macrocycle of Proto to yield Mg-protoporphyrin (MgProto). The reaction catalysed by MgCH is shown in Figure 8.

Mutation of the *bchI*, *bchH* and *bchD* genes in *Rhodobacter sphaeroides* and *Rhodobacter capsulatus* revealed an inability of the mutant strains to synthesise MgProto, indicating a role in magnesium chelation (Coomber *et al*., 1990; Naylor *et al*., 1999). This was confirmed by *in vitro* assay using recombinant versions of the proteins obtained by overexpression in *E. coli* (Gibson *et al*., 1995). The *Synechocystis* homologues of the equivalent purple bacteria genes, *chlI*, *chlH* and *chlD*, were then shown to have similar roles using the same technique (Jensen *et al*., 1996).

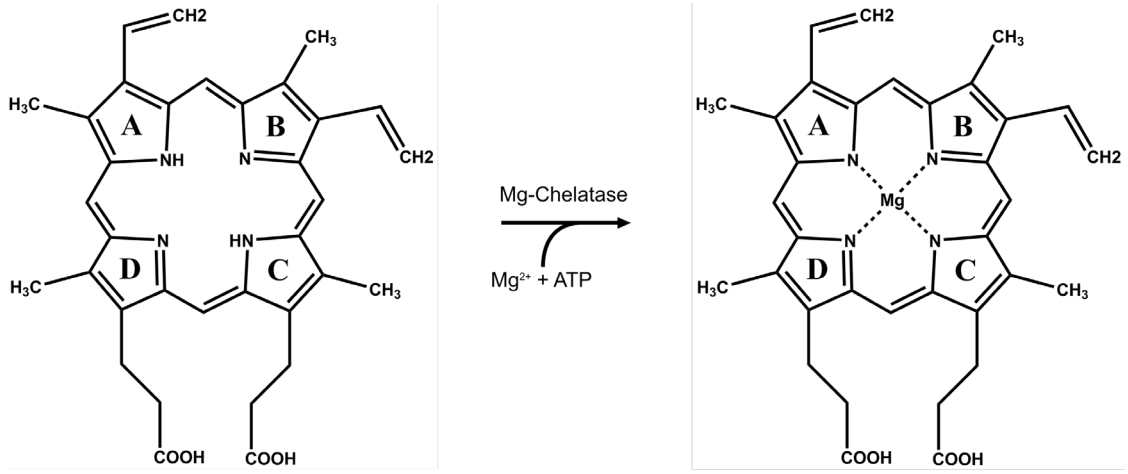

Figure 8. The reaction catalysed by magnesium chelatase

Whilst the exact mechanisms of MgCH catalysis remain elusive it has been possible, through *in vitro* assays using recombinant protein, to establish roles for various individual components of the complex. Chl/BchH has been shown to bind porphyrins and to contain the MgCH active site (Karger *et al*., 2001) but exhibits no ATPase activity (Sirijovski *et al*., 2006). Chl/BchI is an ATPase, providing the free energy required for the energetically unfavourable insertion of Mg^{2+}. Chl/BchI also contains a metal binding site, although it remains unclear whether this is the route taken by the Mg^{2+} during catalysis (Reid *et al*., 2003). Chl/BchD is similar to the Chl/BchI subunit in

that it also contains an ATPase domain and a metal binding site. Mutation of the metal binding site of the *Rba. capsulatis* BchD protein leads to a loss of MgCH activity indicating an essential role in catalysis (Axelsson *et al*., 2006). The ATPase component of *Synechocystis* ChlD is not an active, although it does play an essential allosteric regulatory role in MgCH catalysis (Adams and Reid, 2013). MgCH is regulated by the Gun4 protein which appears to have a role in the regulation of Chl biosynthesis (Davison *et al*., 2005).

1.3.5. Magnesium protoporphyrin methyltransferase

The next stage three stages of chlorophyll biosynthesis involve the modification of the 13-propionate side chain of Mg-proto eventually leading to the formation of an isocyclic ring; the fifth, E ring of the chlorophyll molecule. The first step involves methylation of the carboxyl group by *S*-adenosyl-L-methionine:Mg-protoporphyrin IX methyltransferase (MT). MT catalyses the transfer of a methyl group from *S*-adenosyl-L-methionine (SAM) to MgProto, yielding magnesium protoporphyrin monomethyl ester (MgPME) and *S*-adenosyl-L-homocysteine (Figure 9).

MT is encoded by the *chl*/*bchM* gene, as evidenced by assays using *Rba. capsulatus* (Bollivar *et al*., 1994a) and *Rba. sphaeroides* (Gibson and Hunter, 1994) BchM overexpressed in *E. coli*. The cyanobacterial equivalent was found by complementation of a *Rba. capsulatus* Δ*bchM* mutant with a cosmid library prepared from *Synechocystis* genomic DNA (Smith *et al*., 1996). This gene, annotated *chlM*, has 29% identity with its bacterial counterpart.

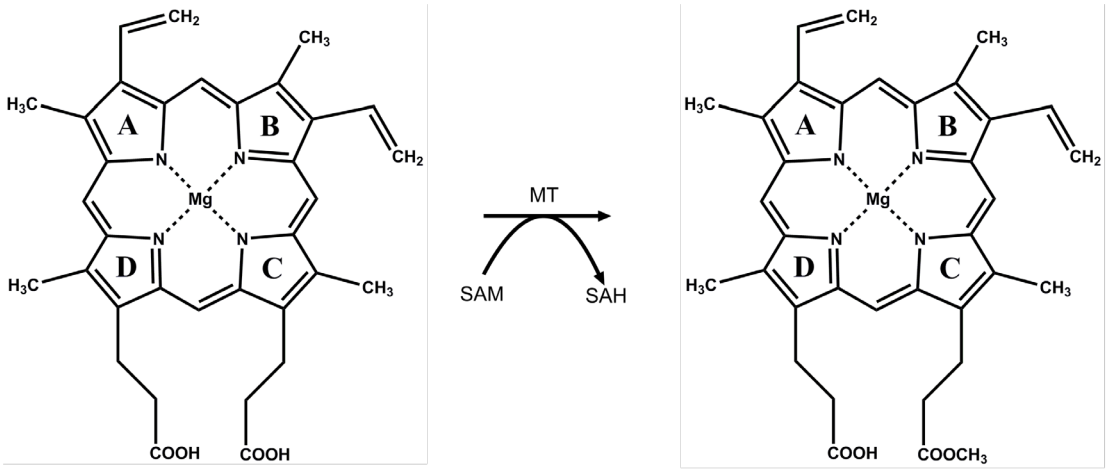

Mg-Protoporphyrin **Mg-Protoporphyrin monomethyl ester**

Figure 9. The reaction catalysed by magnesium protoporphyrin methyltransferase.

1.3.6. Mg-protoporphyrin monomethylester cyclase

MgPME is converted to protochlorophyllide (Pchlide) by MgPME cyclase (cyclase) inducing a colour shift from red to the characteristic green of chlorophylls. Whilst the exact mechanisms of catalysis are not fully understood the cyclase is proposed to catalyse two further modifications to the 13-propionate side chain of MgPME; a hydroxylation followed by oxidation to form keto-propionate. In the final step of catalysis the activated methylene group is ligated to the γ-meso carbon of the porphyrin ring (Wong *et al*., 1985). The proposed reaction sequence is shown in Figure 10.

Molecular genetic studies of photosynthetic bacteria have revealed the *acsF* and *bchE* gene products as oxygenase and hydratase-type cyclases respectively (Porra *et al*., 1996; Pinta *et al*., 2002). Homologues of these two cyclase types are found throughout the photosynthetic organisms. *bchE* is found in numerous photosynthetic bacteria (Xiong *et al*., 2000) whilst *acsF* is generally found in plants (Tottey *et al*., 2003). Some organisms such as *Rubrivivax gelatinosus* contain both (Ouchane *et al*., 2004), the distribution of the aerobic and anaerobic cyclases appears to be consistent with the natural environment of the organism. There is evidence that atmospheric oxygen is incorporated into newly formed Pchlide by the aerobic cyclase (Walker *et al*., 1989) whereas in the anaerobic reaction oxygen is derived from water (Porra *et al*., 1995).

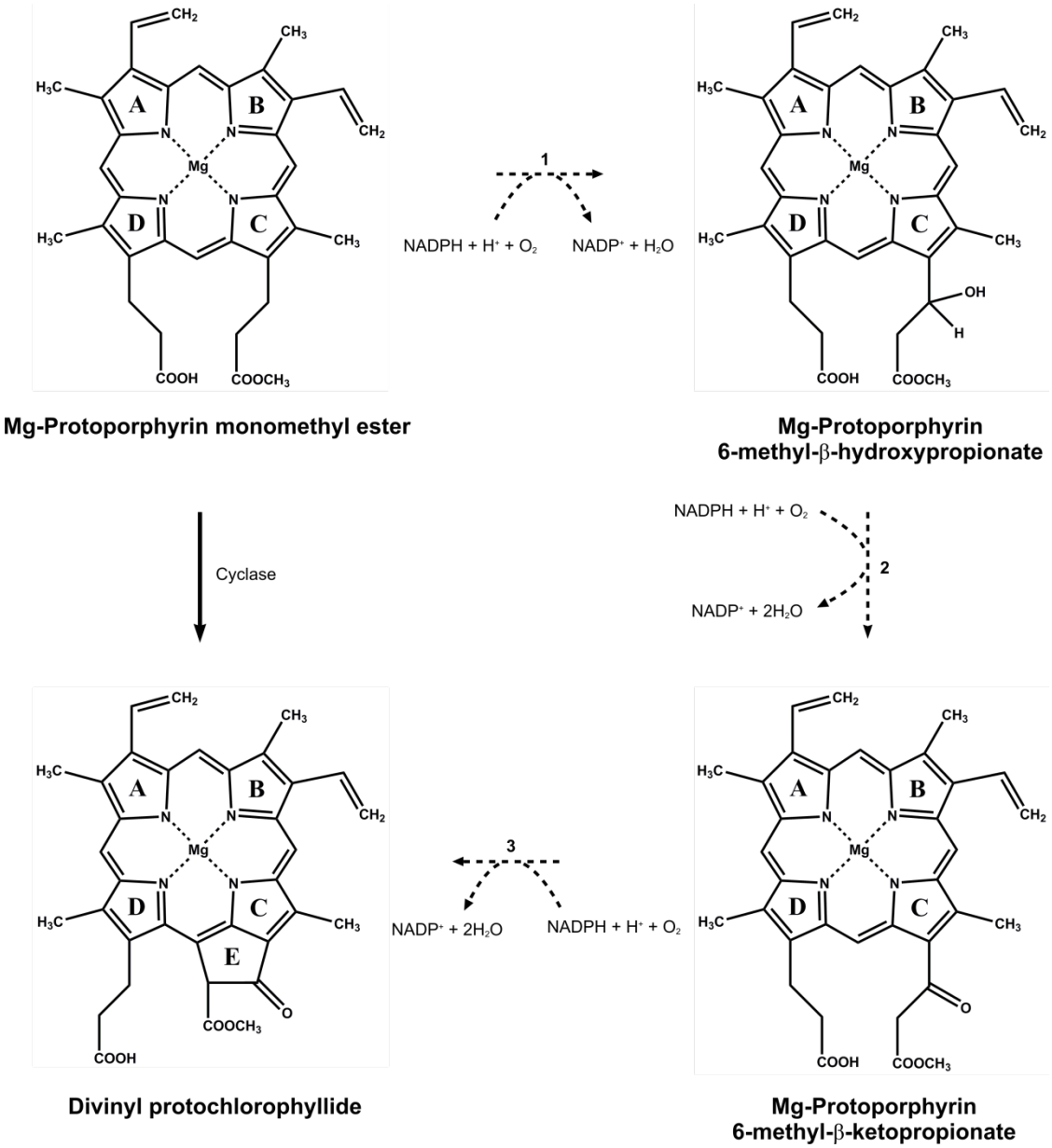

Figure 10 . The reaction catalysed by Mg-protoporphyrin monomethylester cyclase. Solid arrow indicates known reaction; dotted arrows indicate the proposed reaction sequence as shown in (Hollingshead *et al*., 2012).

Although the enzyme remains enigmatic, cyclase activity has been observed in cucumber chloroplasts (Wong and Castelfranco, 1984), wheat etioplasts (Nasrulhaq-Boyce *et al*., 1987) and C*hlamydomonas reinhardtii* (Bollivar and Beale, 1996). It has,

however, never been possible to purify an active cyclase implying that there are one or more as yet undiscovered essential cyclase components. Various studies have demonstrated an absolute requirement of both soluble and membrane fractions for cyclase activity in cucumber (Wong and Castelfranco, 1984), C*hlamydomonas reinhardtii*, *Synechocystis* (Bollivar and Beale, 1996) and barley (Rzeznicka *et al*., 2005), although in all cases further purification of the membrane component proved impossible.

Synechocystis has two *acsF* homologues, *sll1214* and *sll1874*, which are essential for growth under aerobic and micro-oxic conditions respectively (Minamizaki *et al*., 2008; Peter *et al*., 2009). Pull-down experiments with these proteins led to the discovery of Ycf54 (*slr1780*) as an essential cyclase component (Hollingshead *et al*., 2012). However, Ycf54 is a soluble protein leaving the integral membrane cyclase component a mystery.

1.3.7. Reduction of protochlorophyllide

The addition of hydrogen across the C17-C18 double bond of Pchlide yields chlorophyllide (Chlide) (Figure 11). The reaction can be catalysed by two different enzymes, one of which has an absolute requirement for light, and one which requires no light (Bogorad, 1950). The first, NADPH-protochlorophyllide oxidoreductase (LPOR), is one of only two known light-dependent enzymes along with DNA photolyase (Begley, 1994; Heyes and Hunter, 2005) and appears to be found in all Chl producing organisms. The other enzyme, 'dark' protochlorophyllide reductase (DPOR) is light-independent and is found in all Chl producing organisms with the exception of angiosperms. Bchl producing organisms appear to have only DPOR (Suzuki and Bauer, 1995).

1.3.8. Light-dependent reduction of protochlorophyllide

Discovery of LPOR as a light-activated enzyme was prompted by the observation that angiosperms fail to synthesise Chl in the dark, activating Chl biosynthesis only after exposure to light. Thus, light activation of POR is an important regulatory step in development of the photosynthetic apparatus (Lebedev and Timko, 1998). Prokaryotic Chl producing organisms with the capability to reduce Pchlide in the dark

have a single POR encoding gene (Rowe and Griffiths, 1995) whereas angiosperms, which rely fully on the light-activated version, contain three homologues of the gene denoted *PORA*, *PORB* and *PORC*. There is evidence that *PORA* expression decreases after the onset of germination, whilst *PORB and PORC* are constitutively expressed (Masuda *et al*., 2003). However, Paddock and co-workers (2010) have demonstrated that *PORA* is capable of fully complementing a Δ*PORB*/Δ*PORC* mutant leaving the exact roles of each homologue enigmatic.

1.3.9. Light independent reduction of protochlorophyllide

The light-independent DPOR is a multi-subunit enzyme consisting of three protein components. Pchlide accumulation was observed in *Rhodobacter capsulatus* mutants perturbed at three loci, denoted *bchL*, *bchN* and *bchB* (Yang and Bauer, 1990; Coomber *et al*., 1990; Burke *et al*., 1993a). Homologous genes have since been found in cyanobacteria, algae and non-flowering plants and annotated *chlL*, *chlN* and *chlB*. Bioinformatic analysis of these genes indicates a high degree of similarity with the *nifH*, *nifD* and *nifK* subunits of nitrogenase, which converts molecular nitrogen to ammonia. In nitrogenase the NifH protein forms a homodimer in which two Cys residues from each subunit form a binding site for the co-ordination of a [4Fe-4S] cluster. This Fe cluster functions as an ATP-dependent electron donor to a molybdenum-iron (MoFe cluster) situated within a NifD-NifK heterodimer.

Various studies have demonstrated that the Bch/ChlL, Bch/ChlN and Bch/ChlB appear to behave very similarly to their nitrogenase counterparts. Bch/ChlL share the same highly conserved Cys residues with NifK and form a strong homodimer, whilst Chl/BchN and Chl/BchB form a strong heterodimer (Nomata *et al*., 2005; Bröcker *et al*., 2010). The main divergence between the nitrogenase and DPOR subunits comes at the MoFe cluster binding region, which in DPOR is replaced with two Pchlide binding sites, as shown by crystallographic data (Muraki *et al*., 2010; Bröcker *et al*., 2010). It has therefore been hypothesised that Bch/ChlL functions as an ATP-dependent reductase for Bch/ChlN-BchB/ChlB which reduces Pchlide with electrons from Bch/ChlL.

It remains unclear why some organisms contain copies of both LPOR and DPOR. Studies using the cyanobacterium *Leptolyngbya boryana* (Yamazaki *et al*., 2006) demonstrated that the contribution of LPOR increases at higher light whereas DPOR contributes more under anaerobic conditions. Thus, the type of POR utilised may be a response to environmental conditions. It has also been hypothesised that evolution of an 'aerobic' POR was essential during the oxygenation of the atmosphere.

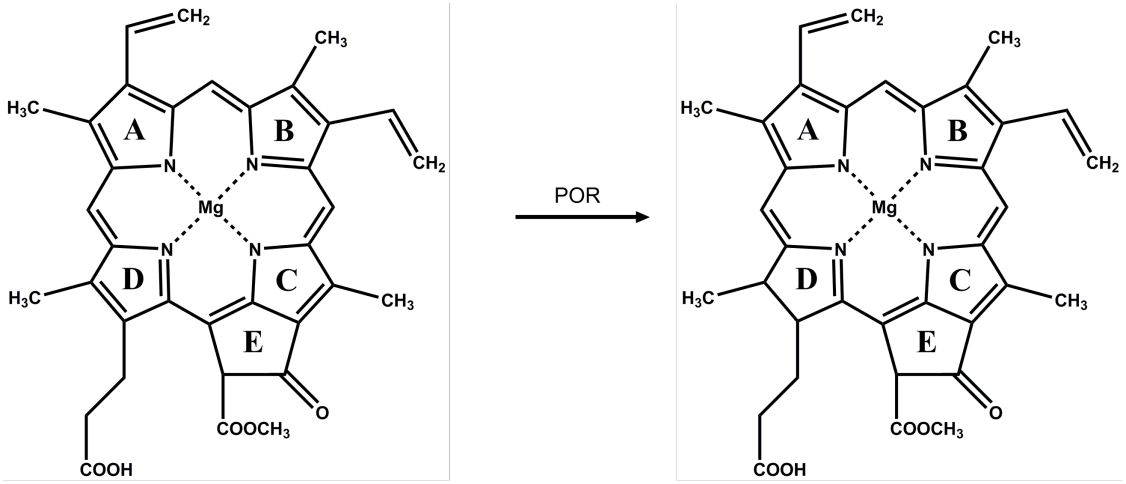

Figure 11. The reaction catalysed by Protochlorophyllide oxidoreductase.

1.3.10. Reduction of the 8-vinyl group of chlorophyllide

C8-vinyl reductase (8VR) catalyses the conversion of the 8-vinyl group (8V) of Chlide to an ethyl group (8E), confining the π-electron system of the macrocycle and causing a ~10 nm shift in the Soret band.

Mutants in the *Arabidopsis thaliana* AT5G18660 gene showed an accumulation of 8V Chls rather than 8E (Nagata *et al*., 2005; Nakanishi *et al*., 2005). Overexpression of the same gene in *E. coli* yielded a lysate with the capability to reduce 8V Chlide to 8E Chlide reinforcing the notion that the gene product was an 8VR. Since, homologues of the gene, designated *bciA*, have been discovered in rice (Wang *et al*., 2010), *Chlorobaculum tepidum* (Chew and Bryant, 2007) and *Rba. sphaeroides* (Canniffe *et al*., 2013).

Although *Synechocystis* and other freshwater cyanobacteria utilise 8E Chl they do not contain an orthologue of the *bciA* gene, pointing to the existence of a second 8VR, termed *bciB*, which has been discovered in *Synechocystis* and is encoded by the *slr1923* gene (Ito *et al*., 2008; Islam *et al*., 2008). 8E Bchl was found in *Rba. sphaeroides* Δ*bciA* mutants, indicating the presence of a third class of 8VR. This was found to be Childe *a* oxidoreductase (COR) encoded by the *bchX*, *bchY* and *bchZ* gene) which already has a known function in the bacteriochlorophyll-specific reactions (discussed further in section 1.3.12.) (Tsukatani *et al*., 2013).

It has been shown using in vitro assays that BciA enymes require NADPH and that they exhibit substrate flexibility (Wang *et al*., 2013). This has led to confusion regarding the preferred route of (B)Chl biosynthesis; whether the 8VR acts on Pchlide (before POR) or Chlide (after POR). A recent study suggests that the preferred substrate for both BciA and BciB is C8-vinyl Chlide (Canniffe *et al*., 2014).

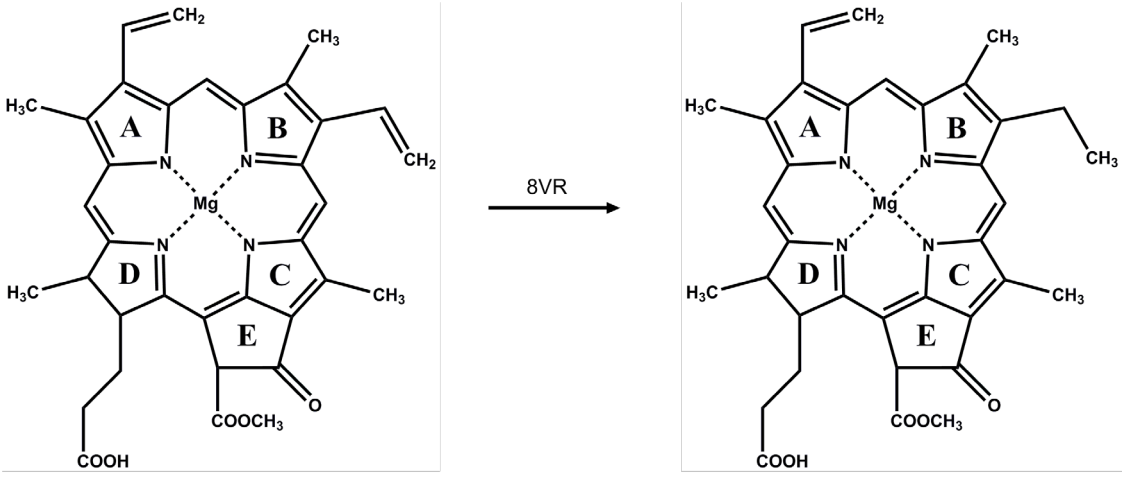

Divinyl chlorophyllide **Monovinyl chlorophyllide**

Figure 12. The reaction catalysed by C8-vinyl reductase.

1.3.11. Addition and reduction of the polyprenyl tail

The final steps of Chl biosynthesis involve the addition of a tetraprenyl 'tail' to the propionate residue at the C17 position of Chlide via an esterification reaction catalysed by chlorophyll synthase (CS). The tail does not alter the spectral properties of the Chl (Chlide and Chl share the same absorption and fluorescence spectra); it does however greatly increase the hydrophobicity of the Chl molecule, which favours insertion into the hydrophobic cores of Chl binding light-harvesting complexes. The phytyl tails have been shown to play a role in the alignment and orientation of Bchls in the *Rhodopseudomonas acidophila* LH2 complex as shown by x-ray crystallographic data (Freer *et al*., 1996).

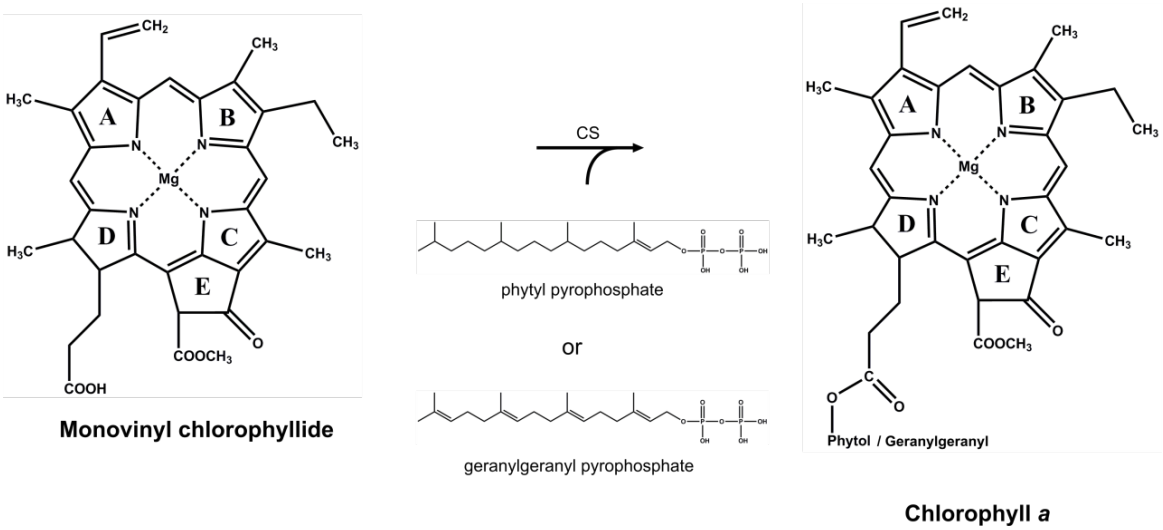

Figure 13. The reaction catalysed by chlorophyll synthase

Although the finished Chl has a phytyl tail, CS can catalyse the addition of either phytol or geranylgeranyl via their activated forms geranylgeranyl pyrophosphate (GGPP) or phytyl pyrophosphate (PPP) (Figure 13). The geranylgeranyl tail of geranylgeranyl-chlorophyll (Chl_{GG}) must be further reduced to form mature Chl, in a reaction catalysed by geranylgeraniol reductase (GGR). It remains unclear exactly which order the two steps happen in, GGPP is reported as the preferred substrate for etiolated seedlings indicating that esterification precedes reduction (Schoch, 1978) whereas in green plants PPP appears to be favoured (Soll *et al*., 1983) suggesting that

reduction occurs before esterification. It has been proposed that these different orders of esterification and reduction predominate at different stages of growth and substrate availability (Rüdiger, 1987).

CS activity was first demonstrated in membrane fractions from Oat (*Avena sativa*) (Rüdiger *et al*., 1980). Multiple subsequent studies performed on the same system (Benz *et al*., 1980; Schoch *et al*., 1980; Benz and Rüdiger, 1981) demonstrated a preference for GGPP over PPP. Assays were also carried out on spinach (*Spinacia oleracea*) material (Soll *et al*., 1983) and CS activity was observed exclusively in the membrane fraction. The genetic locus for the *Rba. capsulatus* CS was identified after the observation that mutations to the ORF led to an accumulation of Bchlide (Bollivar *et al*., 1994b), the gene was annotated *bchG* and its function as a CS along with the *Synechocystis* homologue, *chlG*, was confirmed by heterologous expression in *E. coli* (Oster *et al*., 1997). Similar experiments were carried out on the *Arabidopsis chlG* gene product (Oster and Rüdiger, 1997), found that CS was exclusively in the membrane fraction, agreeing with earlier studies suggesting that CS was an integral membrane protein. The amino acid sequences of all known CSs contain the highly conserved DRXXD motif, characteristic of polyprenyl transferases (Garcia-Gil *et al*., 2003). Each photosynthetic organism studied thus far has had only one detectable CS gene in their genome, with the exception of *Chloroflexus aurantiacus* which has two *bchG* genes yielding CSs with differing substrate specificities (Schoch *et al*., 1999).

Schmid and co-workers (2001; 2002) carried out detailed characterisation of recombinant oat CS in which they demonstrated an absolute requirement of magnesium for activity and noted that esterification with GGPP was favoured early on in the assay timecourse whilst in the later stages PPP predominated. They also demonstrated that catalysis proceeds via a 'ping-pong' type reaction in which a first substrate, in this case tetraprenyl-PP, binds the enzyme causing a conformational change allowing the binding of (B)Chlide and therefore catalysis.

Although the *bchG* and *chlG* encoded CS enzymes share a reasonably high level of similarity (30% identity between the *Synechocystis* and *Rba. sphaeroides* versions) BchG can accept Bchlide but not Chlide whereas the opposite is true of ChlG (Oster *et al*., 1997). Substrate specificity has been further tested with the use of modified Chlide structures; modifications of the A and B rings are tolerated including the addition of bulky side chains whilst modification of ring E is not (Helfrich *et al*., 1994).

Expression of antisense *CHLG* RNA in tobacco (*Nicotiana tabacum*) mutants causes a downregulation of transcript levels of all Chl biosynthesis enzymes as well as ALA synthesis and FeCH and MgCH activity (Shalygo *et al*., 2009a). Thus, reduction of *CHLG* levels caused a feedback-controlled inactivation of the initial and rate limiting step of the Chl biosynthesis pathway indicating an important regulatory role for CS.

GGR catalyses the NADPH and ATP dependent reduction of three of the four C-C double bonds within the geranylgeranyl molecule (Schoch and Schäfer, 1978). The product of the *bch/chlP* gene is essential for the reduction of these double bonds yielding phytol from geranylgeranyl as shown in *Rba. capsulatus* (Bollivar *et al*., 1994c) and *Synechocystis* (Addlesee *et al*., 1996). *Synechocystis chlP* was found to complement a *Rhodobacter sphaeroides* Δ*bchP* knock-out mutant. Addlesee and Hunter (1999) demonstrated the first successful in vitro reduction of $Bchl_{GG}$ to Bchl using *Rhodobacter sphaeroides* BchP expressed in *E. coli*. Deletion of the *Synechocystis chlP* gene yields a mutant that accumulates Chl_{GG} (Shpilyov *et al*., 2005). This mutant is incapable of photoautotrophic growth due to instability and rapid degradation of the photosystems. It is therefore proposed that the increased rigidity of the polyprenyl tail disrupts pigment-protein interactions within the photosystems leading to photooxidative damage. However, the photosynthetic bacterium *Rhodospirillum rubrum* uses $Bchl_{GG}$ in its light-harvesting complexes (Addlesee and Hunter, 2002), indicating that this pigment is tolerable to some photosynthetic complexes (Qian *et al*., 2003).

1.3.12. Bacteriochlorophyll-specific modifications to the macrocycle

The Bchl *a* biosynthesis pathway takes the same route as that of Chl *a* up to Chlide (with regards the intermediate progression along this pathway; some steps are achieved via different cyclase and POR enzymes as listed above). At this point two Bchl-specific modifications are made; the first, a reduction of the C7=C8 double bond of ring B, yields 3-vinyl-bacteriochlorophyllide (3V-Bchlide). The second modification converts the C3-vinyl group to an acetyl group yielding Bchlide which is then esterified to Bchl as discussed previously (Section 1.3.1). These modifications cause a shift in the absorption profile (shown in Figure 6).

The reduction of the C7=C8 double bond of Chlide is carried out by Chlide *a* reductase (COR). Directed mutagenesis and phenotypic analysis of the resultant mutants suggests that three genes are essential for this reduction; *bchX*, *bchY* and *bchZ* (Burke *et al*., 1993; McGlynn and Hunter, 1993). The deduced amino acid sequences of these genes indicate a nitrogenase-like enzyme (previously discussed in Section 1.3.9.); BchX from *Rhodobacter capsulatus* shares 31.5% identity with the NifH protein of *Azotobacter vinelandii* whilst BchY and BchZ show lower, yet appreciable, similarity to NifD and NifK respectively. Nomata and co workers (2006) purified the three COR components and demonstrated the formation of 3V-Bchlide *in vitro*, observing that the reaction requires ATP and a reductant (in this case dithioinite).

The conversion of the C3-vinyl to an acetyl group appears to be a two step process catalysed by the *bchF* and *bchC* gene products. The *bchF* gene product catalyses the addition of a hydroxyl group to the vinyl side chain of ring A (Taylor *et al*., 1983; Zsebo and Hearst, 1984) whilst the *bchC* gene product oxidises the newly formed hydroxyl group yielding a acetyl group.

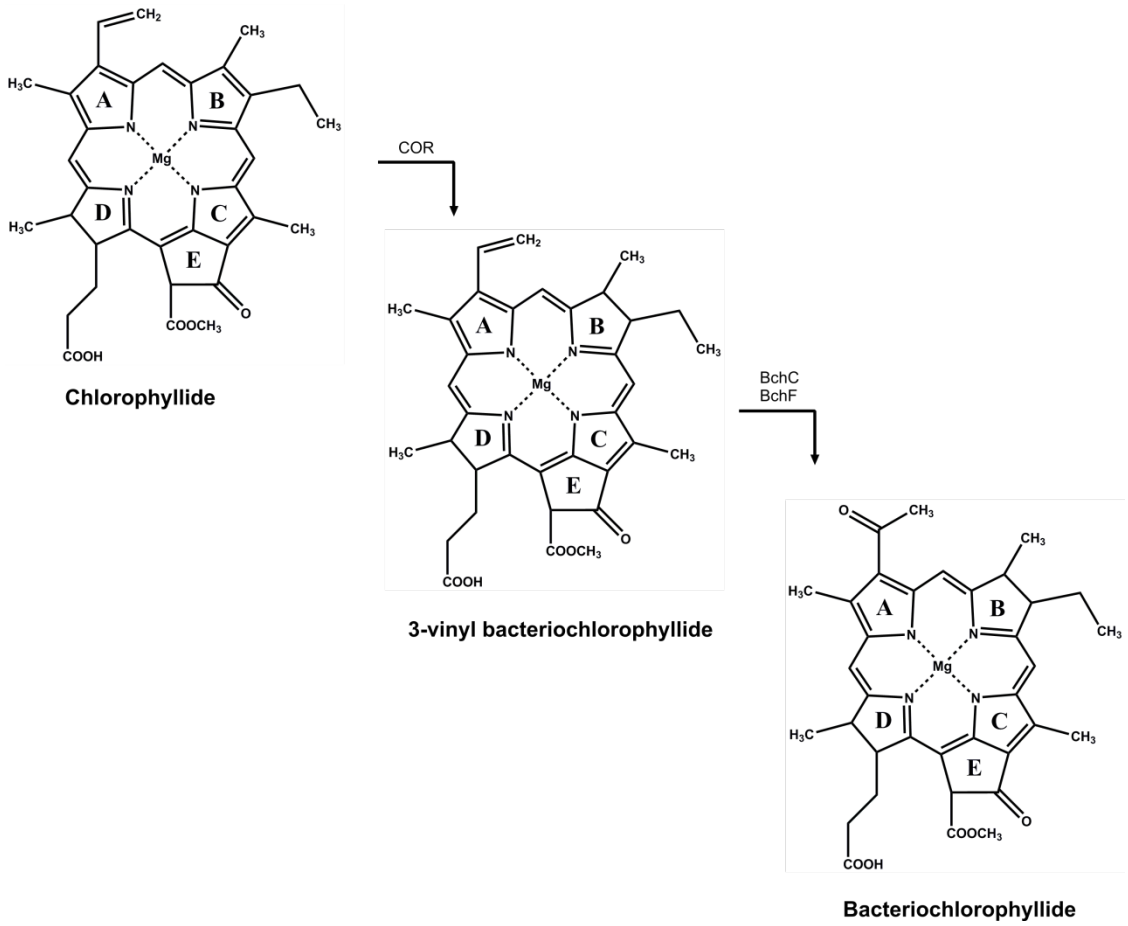

Figure 14. The bacteriochlorophyll specific reactions catalysed by chlorophyllide oxidoreductase and the BchC and BchF enzymes

1.4. Carotenoids

Carotenoids are a structurally diverse class of red, yellow and orange pigment molecules and are found in all known photosynthetic organisms, as well as many nonphotosynthetic organisms (Frank *et al*., 2000). Carotenoids from photosynthetic organisms are extended molecules with a delocalised π electron system usually containing oxygen atoms, usually as part of hydroxyl or epoxide groups. Carotenoids from oxygenic organisms tend to contain ring structures at each end.

In carotenoids biosynthesis large molecules are built up using five-carbon branched-chain isoprene units. Successive condensation reactions yield phytoene, a 40-carbon compound. Phytoene is colourless due to the fact that its double bonds do not form an extended conjugated system. The second part of carotenoid biosynthesis involves

desaturation of phytoene increasing the number of conjugated double bonds and therefore shifting the absorption to the visible region. Carotenoid biosynthesis is outlined in Figure 15.

Carotenoids have two major roles; first, they act as accessory pigments absorbing light in the 450-570 nm range, between the two major peaks of chlorophyll and passing energy to a chlorophyll molecule. The second role for carotenoids is photoprotection; the process by which excess energy is dissipated in a safe manner. Carotenoids are able to quench triplet excited states of chlorophylls before they are able to react with oxygen to form reactive oxygen species, they can also quench singlet oxygen molecules if they do arise. A third role exists for these pigments; in some complexes carotenoids are an essential structural element, such as the LH2 complex of some phototrophic bacteria and in the LHCII complex of plants (Lang and Hunter, 1994; Havaux, 1998).

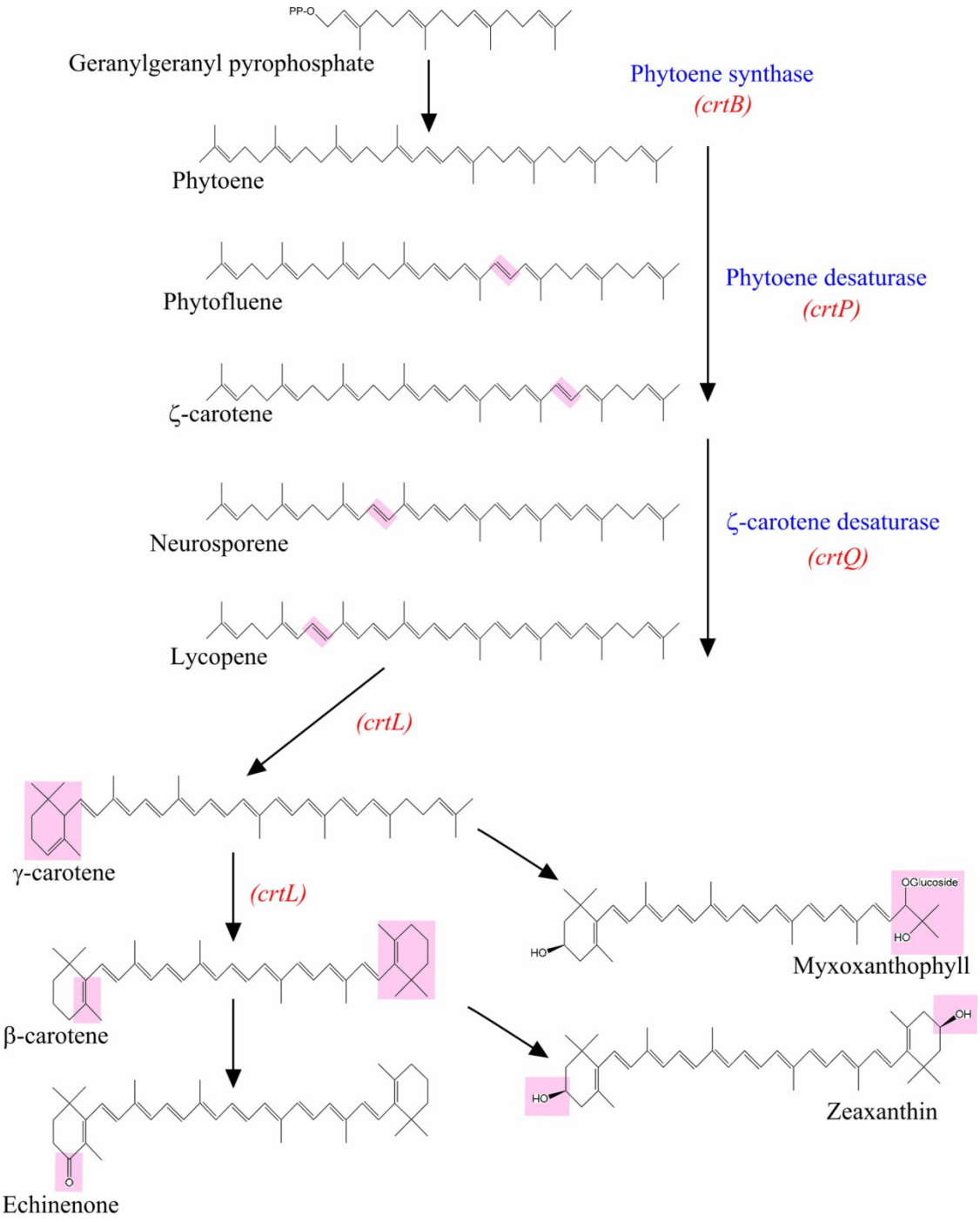

Figure 15. The carotenoid biosynthesis pathway of *Synechocystis*. Modifications are highlighted in magenta.

1.5. Thylakoid membrane structure and biogenesis

Thylakoid membranes are the site of photosynthesis in almost all oxygenic photosynthetic organisms. They contain the four main bioenergetic components of the light dependent reactions of photosynthesis (photosystem I (PSI), photosystem II (PSII), cytochrome b_6f and ATP synthase) (Figure 16A.) along with accessory light harvesting complexes such as LHC complexes in plants and the phycobilisomes in cyanobacteria. In *Synechocystis* the thylakoid membranes form layered sheets located at the periphery of the cell and converge at various sites near the cytoplasmic membrane (Figure 16B).

The biogenesis of thylakoid membranes is an area of great interest, but the topic remains poorly understood. It is a complex process that requires close interplay of protein synthesis, PSII and PSI assembly and chlorophyll biosynthesis (discussed in Sections 1.6/7. and 1.3. respectively). The current hypothesis suggests that they form at specialised regions of the cytoplasmic membrane, termed PratA defined membrane (PDA) (Nickelsen *et al*., 2011), which invaginate yielding mature thylakoids PratA is discussed further in section 1.6.2.

The *VIPP1* (vesicle-inducing protein in plastids 1) gene was discovered in *Pisum sativum* by Li and co-workers (1994)**.** The gene is well conserved among oxygenic photosynthetic organisms. Deletion of *hcf155* encoding the *Arabadopsis thaliana* VIPP1 abolishes thylakoid formation and leads to formation of vesicles (Kroll *et al*., 2001) . This results in a loss of photosynthesis which is rescued by complementation with the *VIPP1* gene implying an essential role for VIPP1 in thylakoid biogenesis. Deletion of the *Synechocystis* Vipp1 homologue, encoded by the *sll0617* gene causes a similar phenotype; loss of thylakoid formation and absence of light-dependent oxygen evolution (Westphal *et al*., 2001). It has recently been demonstrated that the Vipp1 protein is not essential for thylakoid biogenesis in *Synechocuccus sp*. PCC 7002, however the Δ*vipp1* mutant created had greatly reduced amounts of PSI implying a role for Vipp1 in PSI assembly (Zhang *et al*., 2014). Bryan and co-workers (2014) demonstrated that *Synechocystis* Vipp1 relocalises under high-light induced stress to defined puncta within the cytoplasm and thylakoid membranes implying a role in high-light stress response.

The *Synechocystis* Slr1471 protein, part of the Oxa1/Alb3/YidC family of insertase proteins, has also been shown to play a role in thylakoid biogenesis. Deletion of the *slr1471* gene is impossible, implying an essential role in cell viability; it has, however, been possible to create a partial knock-out strain (Spence *et al*., 2004) and a strain in which the native protein is fused to green fluorescent protein (GFP) yielding an impaired version of the protein (Ossenbühl *et al*., 2006). In both instances thylakoid biogenesis was perturbed; the latter study went on to propose a role for Slr1471 in PSII assembly (discussed further in Section 1.6.2.).

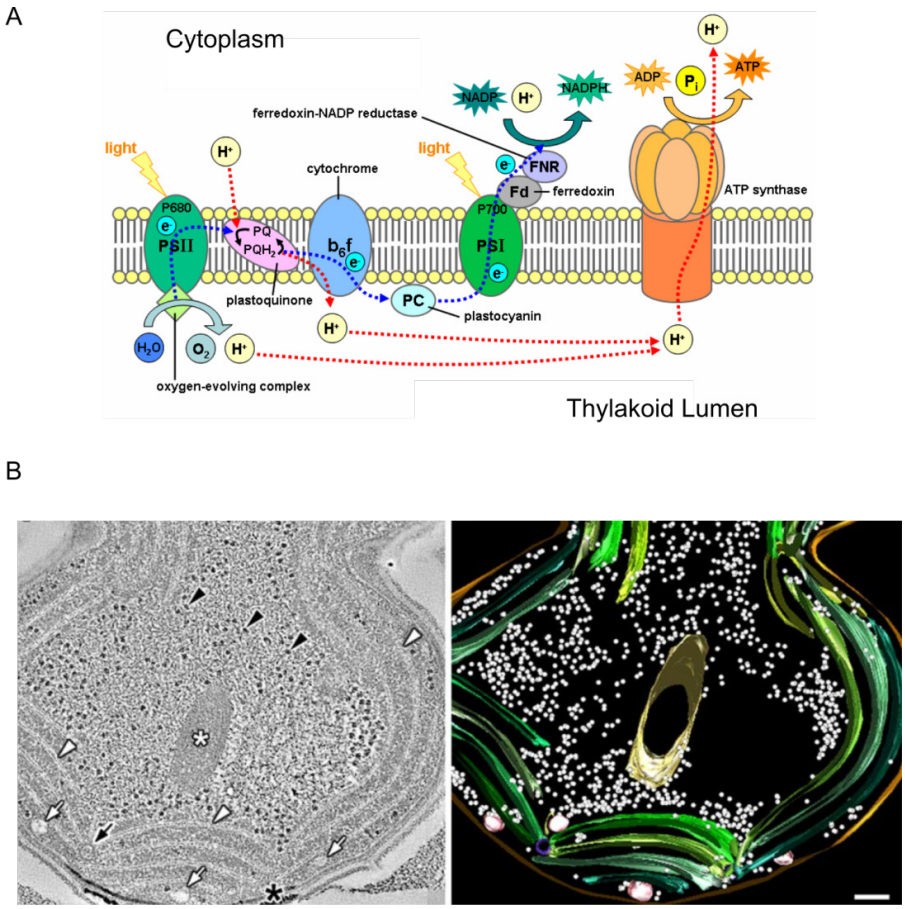

Figure 15. Structure of thylakoid membranes

A. Schematic showing the major bioenergetic components of thylakoid membranes. Components of the electron transport pathway are discussed further in Sections 1.1.3. and 1.1.4. **B**. Transmission electron micrograph (left) of a *Synechocystis* cell, representative of a series of images used to create a tomographical reconstruction of the thylakoid membranes (right). Figure taken from Meene *et al*. (2006).

1.6. Photosystem II

1.6.1 PSII Structure and function

PSII is a membrane protein complex situated within the thylakoid membranes of oxygenic photosynthetic organisms. The crystal structure has been resolved on numerous occasions (Zouni *et al*., 2001; Ferreira *et al*., 2004; Guskov *et al*., 2009), the highest resolution achieved to date being 1.9 Å (Umena *et al*., 2011). These structures reveal a 20-subunit complex consisting of two 'core' subunits in the D1 (PsbA) and D2 (PsbD) proteins which bind the cofactors that are involved in electron transfer (see Section 1.1.3: Figure 1). These are flanked by Chl *a* binding proteins CP43 (PsbC) and CP47 (PsbB) which act as light harvesting complexes, transferring energy to the reaction centre pigments (Bricker, 1990). The PsbE and PsbF subunits contain the histidine ligands responsible for binding haem, forming cytochrome b_{559} (Nelson and Yocum, 2006) which is not involved in the primary electron transport pathway due to its slow photo-oxidation and photo-reduction. It has been hypothesised that this secondary electron transfer chain has a role in photoprotection (Burda *et al*., 2003). The OEC consists of four Mn atoms, five O atoms and a Ca atom in a cubane-like structure coordinated to the D1 and CP43 proteins on the lumenal side of the membrane (Figure 16B). The OEC of cyanobacteria is stabilised by the presence of the extrinsic proteins PsbO, PsbV and PsbU with the plant equivalents being PsbO, PsbP and PsbQ. Interestingly there is evidence that cyanobacterial homologues of PsbP and PsbQ appear to be involved with the biogenesis of optimally active PSII (Thornton *et al*., 2004). The remaining PSII components are small intrinsic proteins which are required for the assembly and stability of the complex (Nelson and Yocum, 2006). Along with the protein subunits discussed above the PSII complex contains 35 chlorophylls, 2 pheophytins, 11 β-carotenes, 2 plastoquinones, 2 haems and a non-haem iron.

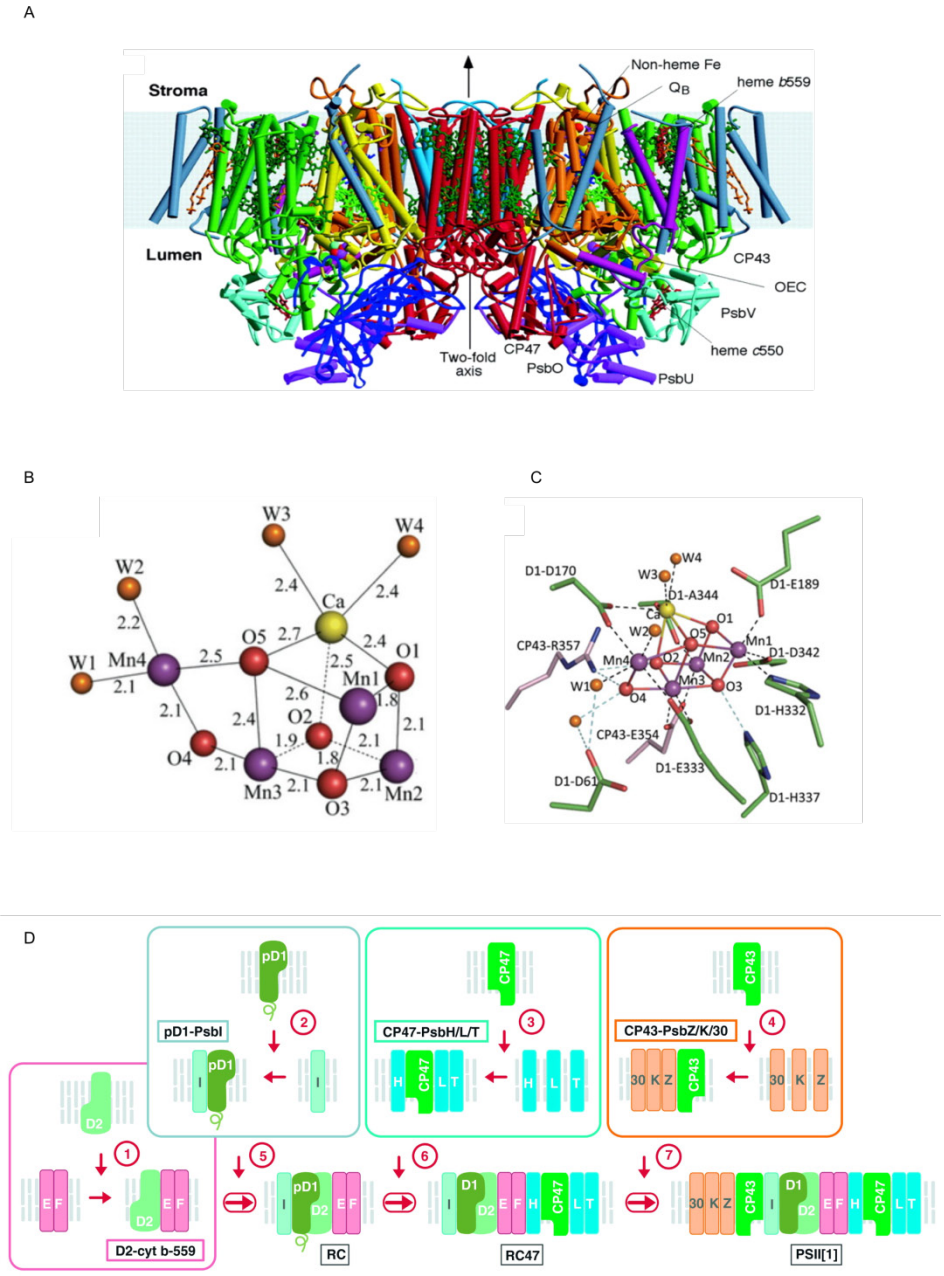

Figure 16. Structure and assembly of photosystem II

A. Crystal structure of *Thermosynechococcus elongatus* PSII with a resolution of 3.5 Å Helices are represented as cylinders: yellow – D1, orange – D2, red – CP47, green – CP43. Taken from Ferreira *et al*. (2004).

B. The structure of the oxygen evolving complex from Thermosynechococcus vulcanus. Numbers, bond length (Å); W, water molecules.

C. Coordination of the oxygen evolving complex to the D1 and CP43 proteins. Green, D1; pink, CP43. B. and C. Are modified from Umena *et al*., 2011

D. The proposed route of PSII assembly. Taken from Komenda *et al*. (2012).

1.6.2. PSII Assembly

As a large, membrane bound, multisubunit protein complex containing a variety of cofactors, PSII requires precise coordination of the various subunits and cofactors to function correctly. Thus, assembly of PSII is a complex process involving multiple pre-complexes (Komenda *et al*., 2012). PSII also requires regular repair due to photodamage sustained by the D1 subunit.

The exact mechanisms of PSII assembly are not fully understood, however recent studies have allowed a picture to be built up. A study by Boehm and co-workers (2011) demonstrated the presence of CP43 and CP47 preassembled with their respective immediate interaction partners (PsbK and Psb30 with CP43 and PsbH, PsbL and PsbT with CP47) and preloaded with most or all of their Chl and β-carotene pigments prior to incorporation into the nascent PSII complex. PsbI has been shown to form a complex with the D1 precursor (pD1) protein (Dobáková *et al*., 2007) whilst D2 and the cytochrome b_{559} complex interact forming a fourth precomplex. The proposed route for PSII assembly is detailed in Figure 16B. The D2 and D1 precomplexes join to create the reaction centre (RC), to which the CP47 precomplex is added yielding the RC47 complex, followed by the CP43 precomplex which finally yields PSII.

There are numerous well conserved assembly factors associated with PSII assembly; the Ycf48 protein binds to pD1 and promotes RC formation (Komenda *et al*., 2008), Psb27 binds and stabilises CP43 (Komenda *et al*., 2012), Psb28 binds CP47 (Dobáková *et al*., 2009a, p. 28) and the PAM68 protein appears to have a role in D1 biogenesis (Armbruster *et al*., 2010). The CtpA protease cleaves the C-terminal precursor domain of pD1, forming mature D1. The *Synechocystis* Oxa1/Alb3/YidC (discussed further in section 1.5) is essential for pD1 integration. The cyanobacterial-specific protein PratA co-purifies with pD1 and is apparently involved with early stages of PSII biogenesis (Klinkert *et al*., 2004; Schottkowski *et al*., 2009).

1.6.3. PSII Repair

Damage to PSII by light is termed PSII photoinhibition. This damage is caused by either by the formation of the triplet state of the primary electron donor (P680) creating singlet oxygen species (acceptor-side inhibition) or because electron donation from water oxidation to the $P680^+$ cannot match the rate of P680 oxidation leaving the $P680^+$ and other nearby oxidising species relatively long lived (donor-side inhibition) (Nixon *et al*., 2010). This damage appears to mainly affect the D1 subunit which has rapid turnover times and is therefore the focus of PSII repair (Ohad *et al*., 1984; Komenda *et al*., 2000).

Repair is carried out via the selective removal and degradation of damaged D1. Whilst the mechanisms of initiation of PSII disassembly remain unclear, it has been shown that FtsH proteases have an important role in D1 degradation and that the exposed N-terminal domain of the D1 protein plays an essential role in efficient degradation of damaged D1 (Silva *et al*., 2003; Komenda *et al*., 2007). The current model for PSII repair is detailed in Figure 17.

1.6.4. Delivery and recycling of chlorophyll during PSII assembly and repair

It has long been speculated that there must be close interplay between the synthesis of light harvesting complexes and the chlorophyll biosynthesis pathway. This belief has been reinforced by numerous studies which suggest that cotranslational insertion of Chl into light-harvesting proteins is required for correct protein folding and for correct incorporation of Chl proteins into membranes (Eichacker *et al*., 1996; Müller and Eichacker, 1999). The availability of *de novo* Chl molecules is required for the synthesis of Chl proteins in *Synechocystis* (Kopečná *et al*., 2013).

Numerous proteins have been linked with roles in coupling PSII assembly and Chl biosynthesis; deletion of the Psb28 protein, which has a proposed role in CP47 biogenesis, yielded a mutant with disrupted Chl biosynthesis (Dobáková *et al*., 2009a). The Pitt protein has a proposed role in binding POR, localising it to sites of PSII assembly (Schottkowski *et al*., 2009). Recently, it was demonstrated that the Ycf39 protein is important for the formation of the D1/D2 reaction centre complex and that chlorophyll recycling is perturbed in a null mutant (Knoppova *et al*., 2014). Further

investigations into this area have been carried out in this thesis, linking the terminal enzyme of Chl biosynthesis with the YidC/Oxa1/Alb3 insertase which has a critical role in thylakoid biogenesis (Spence *et al*., 2004; Ossenbühl *et al*., 2006); results and discussion are presented in Chapter 3.

Vavilin and co-workers (2007) demonstrated that Chl and D1 turnover do not correlate, implying that Chl is recycled during PSII repair. This makes sense biologically, as *de novo* synthesis of Chl is an energetically expensive process involving a large biosynthetic pathway (Section 1.3.), but raises the question of where the Chl is stored during PSII repair. Current evidence suggests that the so-called high-light induced protein (HLIP) family, which are also known as small chlorophyll *a* binding proteins (Scps), are involved in Chl storage. There are four HLIP proteins encoded by *Synechocystis* genome assigned HliA (ScpC), HliB (ScpD), HliC (ScpB) and HliD (ScpE), each of which consist of a single membrane spanning helix with a highly conserved chlorophyll a binding (CAB) domain. There is a fifth Hlip which is fused to the C-terminal domain of ferrochelatase. HLIPs are found to be upregulated under various stress conditions (Bhaya *et al*., 2002), and mutants lacking all five HLIPs are photosensitive and have reduced pigment levels (Xu *et al*., 2004). Furthermore there is evidence to suggest that HliA, HliB and HliC interact with CP47 suggesting a role in photoprotection and Chl storage during repair (Promnares *et al*., 2006; Yao *et al*., 2007). The fourth non-fused HLIP, HliD, appears not to interact with PSII but instead interacts with chlorophyll synthase based on data obtained in this thesis; results and discussion are presented in Chapters 3 and 4.

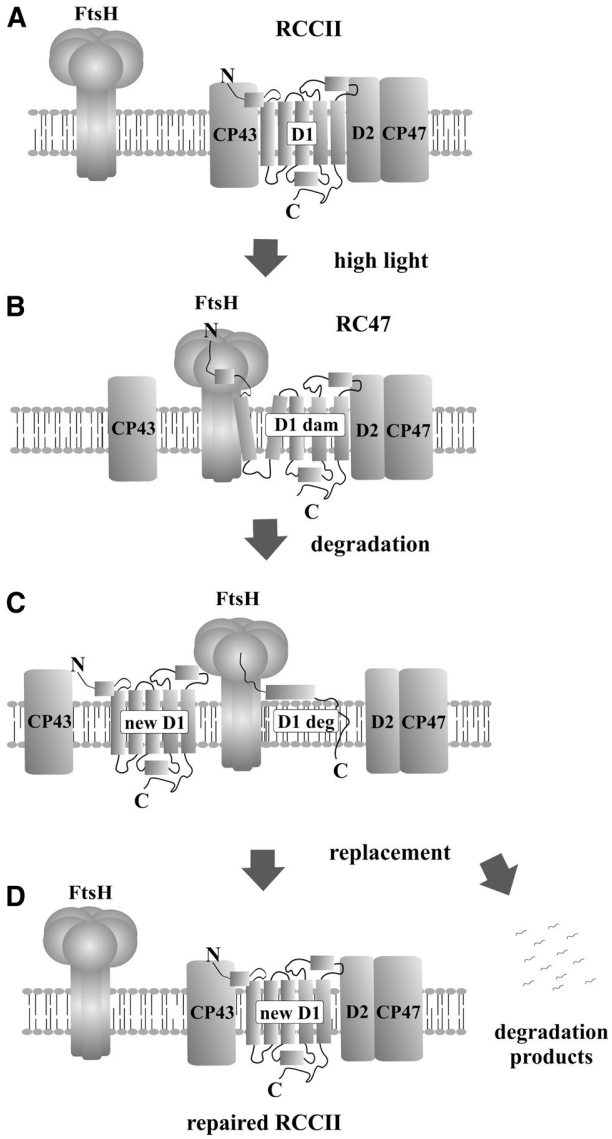

Figure 17. Proposed model for selective D1 replacement during PSII repair in *Synechocystis*

A. Intact PSII core complex with the functional and correctly folded D1 protein.

B. High light–induced inactivation of PSII is followed by the release of CP43 and extrinsic proteins. In the resulting core complex lacking CP43 (RC47), the structure of damaged D1 protein (D1 dam) is destabilized, the protein is recognized by FtsH, and its released N-terminus is caught by the protease.

C. The damaged D1 subunit is degraded (D1 deg) by FtsH from the N- to the C-terminus, releasing short oligopeptides but no distinct larger fragments.

D. Insertion of the new D1 molecule and reassembly of the active dimeric PSII core complex (RCCII). Taken from Komenda *et al*., 2007.

1.7. Photosystem I

Photosystem I is a large, multisubunit complex situated within the thylakoid membranes of oxygenic photosynthetic organisms. Whilst the structures of plant and cyanobacterial PSII complexes are almost identical, the discrepancies between the two PSI complexes are larger. The crystal structure of the cyanobacterial and plant PSI complexes have been solved to 2.5 Å and 3.4 Å respectively (Jordan *et al*., 2001; Amunts *et al*., 2007). The plant structure reveals a large monomeric core surrounded by peripheral light-harvesting complexes (LHCI) forming a PSI-LHCI supercomplex, whilst the cyanobacterial PSI is trimeric. Further discussion will be limited to the cyanobacterial PSI. The subunits of PSI are designated PsaA-P with PsaG, PsaH, PsaN, PsaO and PsaP not present in cyanobacteria.

The PsaA and PsaB proteins form a heterodimer at the core of the PSI reaction centre and bind the electron transport components P700, A_0, A_1 and Fe-S_x (PSI electron transport is discussed in 1.1.4.). The Fe-S_x and Fe-S_x electon acceptors are bound to PsaC, which in turn binds PsaD and PsaE forming the stromal ferredoxin docking site. PsaF is exposed to the lumenal side of the membrane and functions as a plastocyanin or cytochrome c_6 docking site. The PsaL protein is required for the formation of PSI trimers (Chitnis *et al*., 1993) and PsaJ appears to bind and stabilise the PsaF subunit (Fischer *et al*., 1999).

Due to its high stability and relatively low turnover rates when compared with PSII, PSI assembly and repair have not been studied as extensively. The Ycf3, Ycf4 and Ycf37 proteins have implicated roles as assembly factors (Dühring *et al*., 2007).

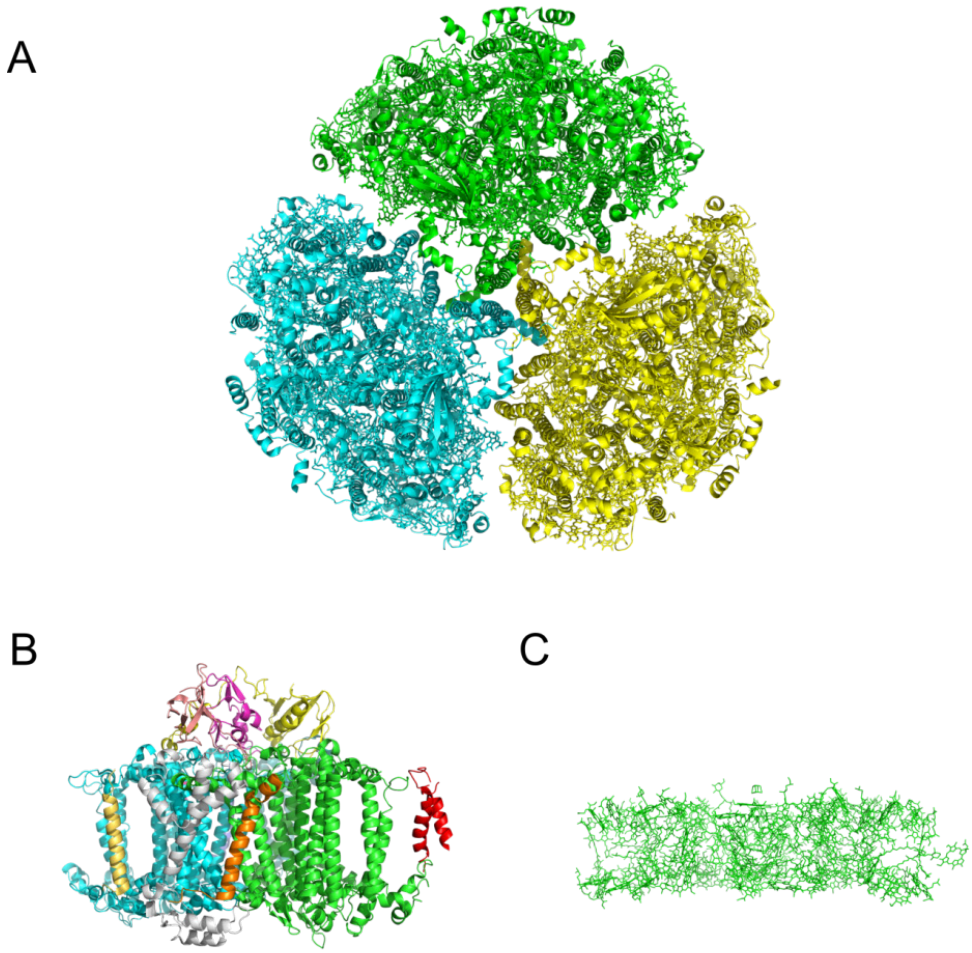

Figure 18. The crystal structure of Synechococcus elongatus PSI at 2.5 Å.

A. Stromal side of a PSII trimer. Each PSI complex is labelled with a different colour.

B. Membrane view of a PSI monomer. Colours are as follows: Green – PsaA, blue – PsaB, pink – PsaC, yellow – PsaD, salmon – PsaE, white – PsaF, orange – PsaJ, red – PsaK. The I and L subunits are situated at the back of the molecule from this angle and are therefore obscured.

C. The arrangement of the cofactors within the PSI molecule monomer. The image is taken from the same angle and is to the same scale as (**B**).

Chapter 2: Materials and Methods

2.1. Standard buffers, Reagents and Media

All buffers and culture media were prepared using Milli-Q ultra pure water. Growth media, buffers and solutions were sterilised either by autoclaving (15 p.s.i., 121°C for 20 minutes) or by filtration through 0.2 µm filters. Heat sensitive reagents such as antibiotics and vitamins were only added to growth media after the solution had cooled below 50 °C.

Growth media used in this work are listed in Table 1.

2.2. *Escherichia coli* strains, growth and plasmids

The *E. coli* strains used in this work are listed in Table 2, plasmids are listed in Table 3. All strains were grown at 37 °C in Luria-Bertani (LB) medium supplemented with the relevant antibiotic(s). The following antibiotic concentrations were used (µg ml^{-1}): Kanamycin 30; ampicillin 100; chloramphenicol 34. When grown in liquid, cells were agitated at 250 rpm. *E. coli* strains were stored at -80 °C in 20% (v/v) glycerol.

2.3. *Synechocystis* strains and growth

Synechocystis strains used in this work are listed in Table 2. Strains were grown in BG11 media supplemented with 5mM glucose (if required) and 10 mM TES. Cultures were illuminated with 40 µE light. When required antibiotics were used at the following concentrations (µg ml^{-1}): Kanamycin 30; erythromycin 15; zeocin 5; choramphenicol 34. Synechocystis stock were stored at -80 °C in 10% (v/v) DMSO BG11.

2.4. *Rhodobacter sphaeroides* strains and growth

Rhodobacter sphaeroides strains used in this work are listed in Table 2. Cells were grown semi-aerobically at 34 °C in M22 medium. When grown in liquid cells were agitated at 150 rpm. When antibiotic selection was required kanamycin was used at 30 µg ml^{-1}. Stocks were stored at -80 °C in 50% glycerol in LB medium.

2.5. Competent *E. coli* cells

2.5.1. Chemically competent E. coli cells

Chemically competent JM109 cells were purchased from Promega. All other chemically competent cells were made as follows:

A 50 ml culture of the relevant strain was grown in a 250 ml shake flask and harvested by centrifugation (4000 *xg*, 4 °C) once it had reached an OD_{600} of 0.6. Cells were washed twice by resuspension in 25 ml cold 0.1 M $MgCl_2$ solution followed by centrifugation. The washed cells were resuspended in 1 ml 0.1M $CaCl_2$ 20% (v/v) glycerol, aliquotted, flash frozen in liquid nitrogen and stored at -80 °C until required.

2.5.2. Electrocompetent *E. coli* cells

E. coli cells were grown in a 500 ml culture until an OD_{600} of 0.6 had been reached and then incubated on ice for 25 minutes with gentle agitation. Cells were then pelleted by centrifugation (4000 *xg*, 4 °C) and resuspended in 500 ml cold 10% (v/v) glycerol. Further resuspension and centrifugation steps were carried out with 250 ml, 30 ml and 1 ml 10% glycerol. Cells were then aliquotted, flash frozen in liquid nitrogen and stored at -80 °C until required.

2.6. Genetic transformation of cells

2.6.1. Chemical transformation of *E. coli*

An aliquot of chemically competent cells was thawed on ice and incubated on ice with 10-50 ng of plasmid DNA for 30 minutes. The cells were then heat shocked at 42 °C for 45 seconds followed by a further 2 minute incubation on ice. 1 ml of LB was then added to the suspension followed by a 60 minute incubation at 37 °C, 250 rpm. Cells were then pelleted by centrifugation (3000 rpm, 2 min), resuspended in 50 µl LB and plated on to a LB agar plate with the appropriate antibiotic. Colonies were grown overnight at 37 °C.

2.6.2. Electroporation of *E. coli*

An aliquot of electrocompetent cells was thawed on ice and incubated on ice with 10-50 ng of plasmid DNA for 2 minutes. The cell suspension was transferred to an electroporation cuvette and an electric current was applied. 1 ml of SOC medium was added immediately after shocking and cells were transferred to a 1.5 ml microcentrifuge tube. Cells were incubated at 37°C for 60 minutes, pelleted (3000 rpm, 2 minutes), resuspended in 50 µl LB and plated on to an agar plate with the appropriate antibiotic. Colonies were grown overnight at 37 °C.

2.6.3. Transformation of *Synechocystis*

100 µl of a liquid culture or scraping of cells from a BG11 plate resuspended in 100 µl QH_2O of the recipient *Synechocystis* strain was transferred to a 500 µl microcentrifuge tube. 10-50 ng of linear or plasmid DNA was then added and cells were incubated at 30 °C with 40 µE light for 60 minutes. Cells were then transferred on to a BG11 plate and grown overnight. Initial selection was carried out by transferring the cell mass to a BG11 plate containing a low concentration of the appropriate selection antibiotic (µg ml^{-1}): Kanamycin 10; Erythromycin 5; Zeocin 2. Following successful growth at the initial antibiotic concentration the cell mass was transferred to an agar plate containing double the previous amount of antibiotic, this doubling process was repeated until full segregation of the construct was achieved (usually 4 doublings). Segregation was confirmed by colony PCR.

2.7. Nucleic acid manipulation

2.7.1. Preperation of plamid DNA

Mini-preps were perfomed using a plasmid mini-prep kit (QIAGEN) according to the manufacturer's instructions. DNA was eluted in 40 µl QH_2O.

2.7.2. Polymerase chain reaction

Amplification of DNA by polymerase chain reaction (PCR) was carried out using ACUZYME or BIOTAQ DNA polymerase (BIOLINE). ACUZYME reactions were carried out using 25 µl 2x ACUZYME ready mix (2.5 units ACUZYME polymerase, 2 mM dNTPs, 4 mM $MgCl_2$), 125 ng of each primer (Table 4), 10 ng template DNA, 1 µl DMSO and

made up to 50 µl with QH_2O. In the case of *Synechocystis* colony PCR a small amount of colony was resuspended in 5 µl QH_2O and 1 µl of this was used in place of template DNA, other reactants were adjusted proportionally to give a final reaction volume of 20 µl.

Rba. sphaeroides colony PCR was performed using BIOTAQ DNA polymerase. Reactions contained 0.5 units of BIOTAQ DNA polymerase, 125 ng of each primer, 16mM $(NH_4)_2SO_4$, 67 mM Tris-HCl (pH 8.8), 1 mM dNTPs, 4 mM $MgCl_2$, 1 µl DMSO. Template DNA was obtained the same way as for *Synechocystis* colony PCR (above). BIOTAQ reactions were performed in a total volume of 20 µl.

Primers were produced either by Sigma-Aldrich or Invitrogen and diluted to 125 ng μl^{-1} in QH_2O. Reactions consisted of a 3 minute initial denaturation at 95 °C followed by 30 cycles of annealing (58 °C for 30 seconds), extension (72 °C, 2 minutes kb^{-1} ACUZYME or 1 minute kb^{-1} BIOTAQ) and denaturation (95 °C, 30 seconds). A final extension of 10 minutes at 72 °C was then carried out.

PCR products were then analysed directly by agarose gel electrophoresis (2.7.4) or purified using a PCR clean up kit (QIAGEN).

2.7.3. Restriction enzyme digests

All restriction enzymes were purchased from Promega or New England Biolabs. Reaction buffers were selected based on the manufacturer's instructions. Digests were carried out in 50 µl reactions consisting of: 5 µl enzyme buffer, 5 µl BSA, 5 µl plasmid DNA or 25 µl purified PCR product, 1 µl of each enzyme and the required volume of QH_2O. Digests were incubated at 37 °C for 60 minutes.

2.7.4. Agarose gel electrophoresis of DNA

Analysis of PCR products and restriction digests was carried out by electrophoresis on 1% agarose gels made in 1x TAE (0.04 M Tris-acetate, 1 mM EDTA) containing 0.5 mg ml^{-1} ethidium bromide. DNA loading dye (0.03% bromophenol blue, 0.03% xylene cyanol, 60% glycerol, 60 mM EDTA in 10 mM Tris-HCl pH 7.6) was added to the sample prior to loading and Hyperladder I (BIOLINE) was run alongside samples to allow size estimation. Gels were visualised under UV light.

2.7.5. Recovery of DNA from agarose gels

DNA was recovered from excised agarose gel bands using a gel extraction kit (QIAGEN) according to the manufacturer's instructions. DNA was eluted in 40 µl QH_2O.

2.7.6. Ligation of DNA fragments

Ligation reactions were carried out in a final volume of 10 µl. A 7:1 molar ratio of insert to vector was generally used, although if a ligation was unsuccessful other ratios e.g. 3:1 or 1:1 were attempted. Reactions consisted of 1 µl 10x ligation buffer, 1 µl T4 DNA ligase (New England Biolabs) and appropriate amounts of insert, vector and QH_2O. Ligations were left at room temperature for 2 hours before transformation in to competent cells.

2.7.7. DNA sequencing

DNA sequencing was performed by GATC Biotech. A sample of DNA mini-prep (2.7.1) along with the relevant primers was sent for analysis. Upon electronic delivery of sequence data CodonCode Aligner ver3.7.1 was used to analyse sequence files.

2.8. Mutagenesis

2.8.1. 3xFLAG-tagging of *Synechocystis* genes

A gene of interest was cloned in to the pPD-FLAG vector between DNA regions homologous to up- and downstream regions of the *psbAII* gene encoding a redundant copy of a PSII subunit. This vector was then transformed in to WT *Synechocystis* as described in (2.6.3.). Resultant strains contained an N-terminally tagged gene of interest in place of *psbAII.* C-terminal 3x FLAG-tagging was achieved in the same way using the pPD-CFLAG in place of the pPD-FLAG vector.

2.8.2. Deletion of *Synechocystis* genes

Deletion of *Synechocystis* genes was achieved by replacement of the native gene of interest with an antibiotic resistance cassette using a modified version of the megaprimer method (Ke and Madison, 1997). Approximately 500 bp regions up- and downstream of the gene of interest were amplified in order to give primary

megaprimers. The upstream reverse and downstream forward primers contained overhang regions which themselves acted as primers for amplification of a resistance cassette. The megaprimer containing the upstream region of the gene, and therefore the forward resistance cassette primer was used in a PCR reaction in conjunction with a reverse primer to amplify half of the resistance cassette. The other half of the resistance cassette was amplified in a similar way using a forward primer situated within the resistance cassette gene and the megaprimer containing the downstream region of the gene of interest. The megaprimer-resistance cassette DNA fragments were then used in a final reaction with the original upstream forward and downstream reverse primers to create the finished construct. Knock out constructs were transformed into the relevant strain.

2.8.3. Mutagenesis of Rhodobacter sphaeroides

Rba. sphaeroides mutagenesis was carried out using the pK18mobsacB plasmid containing both a kanamycin resistance cassette and the *sacB* gene, the product of which catalyses the polymerisation of sucrose. Up- and downstream regions of the target gene were cloned in to the multiple cloning site and the resultant vector was transformed into electrocompetent S17-1 *E. coli* cells. These cells were then conjugated with the recipient *Rba. sphaeroides* strain:

50 ml of the recipient *Rba. sphaeroides* strain was grown, pelleted and resuspended in 200 µl LB medium. A loop of S17-1 *E. coli* colonies was then resuspended in the 200 µl *Rhodobacter sphaeroides* cell suspension. After gentle mixing, the resultant cell mixture was pippetted on to an LB plate in 50 µl droplets and left overnight at 34 °C. The dried cell mass was transferred to an M22 agar plate containing kanamycin and incubated at 34 °C until transconjugant colonies appeared. These were grown in liquid M22 containing kanamycin and, following serial dilution, plated on to M22 agarose plates containing 10% (w/v) sucrose. Resultant colonies were the screened for kanamycin sensitivity by replica plating on to gridded M22 agar plates of which one contained both sucrose and kanamycin and one contained only sucrose. Kanamycin sensitive colonies were screened by colony PCR (2.7.2.).

2.9. Protein Analysis

2.9.1. Determination of protein concentration

Protein concentration was determined by either Bradford assay (Biorad) or absorbance at 280 nm (A_{280}).

The Bradford assay was carried out as per the manufacturer's instructions. A_{280} readings were converted in to an estimate of protein concentration using the following equation (Gill and Von Hippel, 1989):

$$A_{280} = \frac{(5960n_{Trp} + 1280n_{Tyr} + 120n_{Cys})}{Mr}$$

Where n_{Trp}, n_{Tyr} and n_{Cys} are the numbers of tryptophan, tyrosine and cystine residues respectively and Mr is the predicted molecular weight of the protein.

2.9.2. SDS-polyacrylamide gel electrophoresis (PAGE)

SDS-PAGE was carried out either on self-poured or precast polyacrylamide gels. Self-poured gels were made using the Laemmli (1970) buffer system and the protocol from Sambrook *et al*. (1989). A 5% stacking gel was used in conjunction with a 12% resolving gel. Precast 12% polyacrylamide gels were purchased from Invitrogen and used as per the manufacturer's instructions. Biorad precision plus standards were run concomitantly with samples to allow molecular weight estimation. Proteins were visualised by staining with Coomassie Brilliant Blue. If higher sensitivity was required gels were silver stained using a kit (Biorad).

2.9.3. Clear Native (CN)-PAGE

CN-PAGE was carried out on a 4-16% gradient gel following the protocol of Wittig *et al*. (2007). Gels were made using 16 x 20 cm glass plates with 1 mm spacers. Up to 8 µg of chlorophyll was loaded per lane. Gels were run at a constant temperature of 4 °C.

2.9.4. 2D-gel electrophoresis

CN-PAGE was run as described above. Lanes of interest were excised from the gel, incubated in denaturing buffer (1 % SDS (w/v), 1% dithiothreitol (DTT) (w/v), 25 mM

Tris/HCl, pH 7.5) for 20 minutes and placed horizontally on to a SDS-gel (5% stacking, 12-20% gradient resolving ; 16 x 20 cm, 1.5 mm) containing 7 M urea. Gels were run at a constant temperature of 23 °C and visualised either by staining or immunoblot.

2.9.5. Immunoblot analysis of proteins: Blotting procedure

SDS-PAGE was carried out as described in 2.9.2. (with the exception of the staining step). The gel was then equilibrated in transfer buffer (10 mM $NaHCO_3$, 3 mM $NaCO_3$, 10% Methanol) for 5 minutes. A transfer 'sandwich' consisting of two porous pads, two sheets of filter paper, the gel and nitrocellulose membrane was created under saturation of transfer buffer with the gel and nitrocellulose membrane in direct contact. This was then placed in blotting apparatus and transferred at 30 mA overnight or 350 mA for 60 minutes.

2.9.6. Immunoblot analysis of proteins: Immunodetection

Upon completion of blotting, the nitrocellulose membrane incubated in blocking buffer (5% milk powder, 50 mM Tris/HCl pH 7.6 150 mM NaCl) for 60 minutes. After blocking, the membrane was incubated with the relevant primary antibody diluted to the appropriate concentration (generally 1:1000 – 1:10,000) in antibody buffer (50 mM Tris/HCl pH 7.6 150 mM NaCl, 0.05% Tween 20) for 4 hours at room temperature or overnight at 4 °C. The membrane was then washed for 3 x 5 minutes in antibody buffer before application of the relevant peroxidase-conjugated secondary antibody for 60 minutes. The membrane was washed a futher 3 x 5 minutes and then imaged by application of luminal/peroxide solution (cyanagen) in conjunction with a ChemiDoc-It imaging dock (UVP).

2.9.7. Preparation of samples for mass spectrometry (in-solution)

Samples to be analysed by mass spectrometry were prepared as follows: samples were denatured and reduced by addition of 1% SDS and 5 mM DTT followed by s-alkylation by 10 mM idoacetamide. Denatured proteins were digested with trypsin overnight at 37 °C, dried in a vacuum centrifuge and re-dissolved in 200 µl 25% acetonitrile (ACN), 10 mM K_2HPO_4 pH 3.0. The samples were cleaned using 20 µl POROS 20 SP (PerSeptive Biosystems) cation exchange columns according to the manufacturer's instructions and eluted in 25% ACN, 10 mM K_2HPO_4, 0.5 M KCl.

Samples were dried once again in a vacuum centrifuge and desalted using C_{18} SpinTip columns (Proteobio). Peptides were dried in a vacuum centrifuge and stored at -20 °C.

2.9.8. Perpetration of samples for mass spectrometry (in-gel)

SDS-PAGE gel samples were prepared for mass spectrometry using a modified version of Pandey *et al*. (2000). Gel bands were excised, cut into small pieces and incubated in 100 µl 50 mM ammonium bicarbonate (ABC) for 5 minutes before addition of 100 µl ACN and further incubation for 10 minutes. The solvent was discarded and the process of ABC followed by ACN incubation was repeated until no Coomassie stain was visible. 50 µl 10 mM dithiothreitol (DTT) was added and samples were incubated at 56 °C for 30 minutes followed by removal of the liquid. Samples were then incubated in 50 µl 55 mM idoacetamide (IAA) 50 mM ABC in the dark at room temperature for 20 minutes followed removal of excess liquid. Samples were then incubated in 100 µl 50 µl ABC for 10 minutes. 100 µl ACN was then added and the samples incubated for a further 10 minutes after which the excess reagents were discarded. The gel pieces were then dried in a vacuum centrifuge and rehydrated with digestion buffer (12.5 ng μl^{-1} trypsin, 5 mM $CaCl_2$, 50 mM ABC) and incubated overnight at 37 °C. Peptides which had diffused out of the gel were removed to a LoBind microcentrifuge tube and the gel pieces were treated with 100 µl ACN (37 °C, 15 minutes), 50 µl 5% formic acid and 100 µl ACN. Excess reagent was removed and added to the microcentrifuge tube after each treatment. The peptide solution was then dried in a vacuum centrifuge and the peptides stored at -20 °C.

2.9.9. Mass spectrometry

Peptides were re-dissolved in 7 µl 0.1% (v/v) trifluoroacetic acid, 3% (v/v) ACN. This solution was analysed by LC-MS/MS using an Ultimate 3000 RSLCnano liquid chromatography system (Dionex) with 5 mm x 300 µm trapping and 7 µm x 15 cm analytical PepMap C_{18} reverse phase columns. Elution of tryptic peptides was by a 60 minute linear gradient from 94% 0.1% (v/v) formic acid to 40% 0.1% (v/v) formic acid, 80% (v/v) ACN at a flow rate of 300 nl $minute^{-1}$. Mass spectra were acquired onluine using a Maxis UHR-TOF instrument (Bruker Daltonics) operating with in line format with automated dependent MS/MS scans. Peak lists for database search in the

Mascot Generic Files format were created from the datafiles and submitted for database searching using Mascot Daemon v.2.2.0 running with Mascot Server v.2.2.01 (Matrix Science) against the *Synechocystis* sp. PCC 6803 complete proteome database (www.uniprot.org) Parameters were set to permit one missed cleavage with S-carboxymethyl cysteine as a fixed modificationand oxidised methionine as a variable modification. Tolerences for both peptide (MS) and product (MS/MS) were ±0.5 Da. Mass spectrometry was kindly performed by Dr. Phillip Jackson (University of Sheffield, UK).

2.9.10. Quantitative mass spectrometry

Whole cell lysate was prepared by bead beating in the presence of protease inhibitor in lysis buffer (0.1 M Tris-HCl, 0.1 M DTT, pH 7.6) (10x 1 min), unbroken cells were removed by centrifugation (5000 xg, 10 min). To the lysate (0.5 mL in lysis buffer) 10 µL 10% SDS (final concentration 0.2%) and 2 µL ^{15}N-labelled QconCAT internal standard at 15 µM was added, followed by incubation at 56°C for 30 min. The proteins contained in the cell lysate were solubilised and digested with a combination of endoproteinase LysC and trypsin according to Wisniewski *et al*. (2009).

After drying by vacuum centrifugation, the tryptic peptides were dissolved in 18 µL 0.1% TFA, 3% acetonitrile with sonication for 5 min, and any insoluble material was removed by centrifugation at 16,000 x *g* for 5 min. 15 µL (equivalent to approximately 167 µg of peptides) was injected onto a porous graphitic carbon column (Hypercarb, 5 µm, 2.1 x 50 mm, Thermo Scientific, Loughborough, UK) maintained at 30°C. Solvents were (A) 0.1% TFA, 3% acetonitrile and (B) 0.1% TFA, 97% acetonitrile, delivered by an Ultimate 3000 chromatography system (Dionex, Camberley, UK) at 0.2 mL/min. Peptides were separated with a 110 min gradient from 2-70% solvent B, monitoring absorbance at 214 nm and collecting fractions at 1 min intervals from 25-110 min. Collected fractions were dried by vacuum centrifugation.

Analysis of the hypercarb fractions was carried out as in (Qian *et al*., 2013).

2.9.11. Analysis of kinetic data

Assays were analysed using Igor Pro 6.34A software (WaveMetrics Inc, USA). Data was fitted to the Michaelis–Menten equation:

$$v_{ss} = \frac{V_{max} \cdot [S]}{K_m + [S]}$$

Where v_{ss} is the steady state rate, V_{max} is the theoretical maximum rate achieved by the system, K_m is the substrate concentration at which the rate is half V_{max} and [*S*] is the substrate concentration.

2.10. Protein Purification

2.10.1. Purification of His_6-tagged proteins

3 L of BL21 *E. coli* cells containing the relevant pET14b plasmid were cultured at 37 °C in baffled flasks. At an A_{600} of 0.6, protein synthesis was induced by addition of isopropyl β-D-1-thiogalactopyranoside (IPTG) to a final concentration of 0.4 mM. Cells were transferred to a 20 °C incubator, left overnight and harvested by centrifugation (4000 rpm, 20 minutes). Cells were resuspended in binding buffer (25 mM Tris-HCl pH 7.4, 0.5 M NaCl, 5 mM imidazole) containing DNAase and broken by sonication. Cell lysate was centrifuged (50,000 *xg*, 20 minutes) in order to obtain soluble and insoluble fractions. The soluble fraction was stored on ice whilst the insoluble fraction was resuspended in binding buffer containing 8 M urea, sonicated and incubated at 4 °C for 1 hour with gentle agtation. The insoluble fraction was then centrifuged again (50,000 *xg*, 20 minutes). The supernatants from both the soluble and insoluble fractions were passed through 0.2 µm filters and then applied to separate chelating Sepharose (GE Heathcare) columns pre-equilibrated with $NiSO_4$. After binding, columns were washed with wash buffer 1 (25 mM Tris-HCl pH 7.4, 0.5 M NaCl, 50 mM imidazole) followed by wash buffer 2 (25 mM Tris-HCl pH 7.4, 0.5 M NaCl, 100 mM imidazole). Protein was then eluted using elution buffer (25 mM Tris-HCl pH 7.4, 0.5 M NaCl, 500 mM imidazole). All buffers used in conjunction with the solubilised membrane fraction contained 8 M urea. Urea was removed from the final sample by dialysis.

2.10.2. Purification of FLAG-tagged proteins from *Synechocystis*

4L of the relevant *Synechocystis* strain was cultured and harvested by centrifugation (8000 rpm, 20 minutes), and resuspended in FLAG-buffer (25 mM sodium phosphate buffer, 10 mM $MgCl_2$, 0.05 M NaCl, 10% (v/v) glycerol) containing protease inhibitor (BioCompare). From this stage onwards all steps were carried out under dim green light.

Cells were lysed by bead beating, using 0.1 mm glass beads, for eight cycles of 55 seconds. The cell-bead suspension was cooled on ice between cycles. After breakage, cell lysate was transferred to a centrifuge tube and separated by centrifugation (60,000 *xg*, 30 minutes), yielding soluble and insoluble fractions.

The insoluble membrane fraction was resuspended in FLAG-buffer to give a final volume of 10 ml and solublised by addition of β-DDM to a final concentration of 1.5%. Solubilisation was carried out at 4 °C with gentle agitation. Solubilised membranes were centrifuged (60,000 *xg*, 30 minutes) in order to remove any unsolubilised material. All further processing of solubilised material was carried out in the presence of 0.04% β-DDM in order to maintain the critical micelle concentration.

Solubilised membranes were applied to a pre-equilibrated gravity flow column containing 300 µl ANTI-FLAG-M2-Agarose (Sigma). The flow through was collected and reapplied to the column twice more, for a total of three bindings. Columns were then washed with 6 ml FLAG buffer. Elution was carried out by resuspension of the resin in 300 µl FLAG buffer containing 75 µg 3x FLAG peptide, gentle agitation at 4 °C for 1 hour and filtration through a 0.22 µm spin column to remove resin.

2.11. HPLC gel filtration of protein complexes

In order to analyse FLAG column eluate, gel filtration HPLC was carried out. β-DDM was added to the sample to a final concentration of 1%. The sample was then run at 0.2 ml $minute^{-1}$ on a BioSep-SEC-S 3000 (Phenomenex) gel filtration column in conjunction with an Agilent 1200 HPLC system set to monitor absorbance at 280 nm and 440 nm. The running buffer used was 20 mM HEPES, 0.25% β-DDM. If necessary sample fractions were collected and stored at -20 °C.

2.12. FPLC gel filtration

Recombinant protein purified from *E. coli* was further purified by size exclusion chromatography on an ÄKTA FPLC (GE Healthcare). Gel filtration buffer was 50 mM Tris, 100 mM NaCl, 3% (v/v) glycerol. The UV absorbance profile of the eluate was monitored at 280 nm.

2.13. Pigment analysis

2.13.1. Extraction of pigments from whole cells or protein preparations

Pigment extractions were carried out using a 9:1 ratio of methanol to sample. After addition of methanol samples were vigorously mixed using a vortex, incubated on ice for 20 minutes and then centrifuged (15,000 rpm, 20 min) to remove all insoluble material. If necessary extracted pigments were concentrated under a stream of nitrogen gas.

2.13.2. Extraction of pigments from growth media

Pigment producing strains were cultured in the presence of 0.2% (v/v) Tween 80, facilitating diffusion of pigments in to the growth medium. The medium was then treated with diethyl ether and acetonitrile in a 3:2:1 ratio (medium : diethyl ether : acetonitrile). After vigorous agitation the mixture was left to settle, allowing the formation of a distinct upper and lower phase. The mixture was separated using a separating flask and the lower phase discarded. The upper, pigment containing, phase was collected and dried using a rotary evaporator.

2.13.3. HPLC analysis of pigments

Extracted pigments were loaded on to an Agilent-1200 series HPLC system in conjunction with a reverse phase column (Analytical: Nova-Pak C18, 4 µm particle size, 3.9 x 150mm; Waters. Preparative: UniverSil C18, 5 µm particle size, 10 x 150 mm; Fortis).

2.13.4. Separation of chlorophyll precursors

Reverse phase HPLC was carried out using 350mM ammonium acetate 30% methanol as solvent A and 100% methanol as solvent B. Pigments were eluted with a linear

gradient of solvent B (65%-75% 35 min) followed by 100% solvent B at a flow rate of 0.9 ml minute^{-1} at 40°C. Pigment content was monitored by absorbance (433 nm, 440 nm, 632 nm, 663 nm) and fluorometry (440 nm excitation, 670 nm emission).

2.13.5. Separation of chlorophyllide and chlorophyll

Reverse phase HPLC was carried out using 350mM ammonium acetate 30% methanol as solvent A and 100% methanol as solvent B. Pigments were eluted with a linear gradient of solvent B (65%-100% 15 min) followed by 100% solvent B at a flow rate of 0.9 mL minute^{-1} at 40°C. Pigment content was monitored by absorbance (440 nm, 663 nm) and fluorometry (440 nm excitation, 670 nm emission). If high throughput was required, flow rate was increased to 1.8 ml minute and all timings were halved.

2.14. Spectroscopy

2.14.1. Absorbance spectroscopy

Absorbance spectroscopy was carried out using a Cary 50 UV-Vis stectrophotometer set to measure the desired wavelengths.

2.14.2. Low temperature fluorescence spectroscopy

Emission spectra were recorded in a cryo-stable buffer comprising of 20 mM HEPES, 55 % glycerol (v/v) 25% sucrose (w/v). Samples were cooled to 77K in an Optistat DN-V optical cryostat (Oxford Instruments). Measurements were recoreded on a SPEX FluoroLog spectrofluorimeter. Excitiation was provided from a tungsten light source in the visible-IR region of the spectrum. Excitation slit widths were 5 mm and emission widths were 2.5 mm. Multiple scans were averaged in order to attain high quality spectra.

Growth Media	Reagents
LB/LB agar	Ready mixed from FORMEDIUM, prepared according to manufacturer's instructions
SOC	40% yeast extract, 20% tryptone, 5% NaClv
Bg11	<u>Stock solutions</u> **Trace Minerals (1 L)**: 2.86 g boric acid 1.81 g manganese chloride 0.22 g zinc sulphate 0.39 g sodium molybdate 0.079 g copper sulphate, 0.049 g cobaltus nitrate **100x Bg11 (1 L)**: 149.6 g sodium nitrate 7.49 g magnesium sulphate 3.60 g calcium chloride 0.6 g citric acid 0.10 g EDTA (0.56 ml of 0.5 M pH 8.0 stock) 100 ml trace minerals stock **1000x Iron (1 L)**: 6 g ferric ammonium citrate **1000x Phosphate (1 L)**: 30.5 g dipotassium hydrophosphate **1000x Carbonate(1 L)**: 20 g sodium carbonate **1 M TES/KOH pH 8.2** **1 M Glucose** <u>1x Bg11 liquid medium (1 L)</u> 10 ml 100x Bg11 1 ml each 1000x stock. After autoclaving TES and glucose (if required) added to a final concentration of 10 mM and 5 mM respectively <u>Bg11 agar (1 L)</u> 1x Bg11 15 g bacto-agar TES and glucose (if required) added after melting

Table 1. Growth media

Growth Media	Reagents
M22	<u>Stock solutions</u> **Solution C:** 40 g nitriloacetic acid 96 g magnesium chloride 13.36 g calcium chloride 0.5 g EDTA 1.044 g zinc chloride 1.0 g ferrous chloride 0.36 g manganese chloride 0.037 g ammonium heptamolybdate 0.031 g cupric chloride 0.0496 g cobaltus nitrate 0.0228 g boric acid **10x M22 (4L)**: 122.4 g potassium dihydrogen orthophosphate 120.0 g dipotassium hydrogen orthophosphate 100.0 g lactic acid 20 g ammonium sulphate 20 g sodium chloride 173.7 g sodium succinate 10.8 g sodium glutamate 1.6 g aspartic acid 800 ml solution C **10,000x Vitamins (100 ml)**: 1 g Nicotimic acid 0.5 g Thiamine 0.1 g 4- aminobenzoic acid 10 mg biotin **Casamino acids (1 L)**: 50 g Casein Hydrosylate <u>1x M22 (1 L)</u> 100 ml 10x M22 20 ml casamino acids Vitamins added after autoclaving <u>1x M22 agar (1 L)</u> 100 ml 10x M22 15 g bacto-agar Vitamins added after cooling

***E. coli* strains**

Strain	Abbreviation	Properties	Source
S17-1	-	RP4-2 (Tc::Mu, Nm::TN7) integrated into the chromosome: *thi pro hsdR hsdM*$^{+}$ *recA* Tp^{R} (Sm^{R})	Simon *et al*. (1983)
JM109	-	*end*A1 *gln*V44 *thi*-1 relA1 *gyr*A96 recA1 *mcr*B^{+} Δ(*lac-pro*AB) e14-[F' traD36 *pro*AB^{+} *lac*I^{q} lacZΔM15] *hsd*R17 ($r_{K}^{-}m_{K}^{-}$)	Promega
BL21 (DE3)	BL21	(F^{-} *ompT* $r_{B}^{-}m_{B}^{-}$) + bacteriophage DE3	Studier and Moffat (1986)

***Rba. sphaeroides* strains**

Strain	Abbreviation	Properties	Source
2.4.1	-	Wild-type	S. Kaplan, university of Texas
Δ*bchC*/*bchX*	-	In frame deletion of the *bchC* and *bchX* genes	This study
Δ*bchC*/*bchX*/ *bchF*	Δ*CXF*	In frame deletion of the *bchC*, *bchX* and *bchF* genes	This study

***Synechocystis* strains**

Strain	Abbreviation	Properties	Source
Synechocystis sp PCC 6803	*Synechocystis*	Wild-type	Dr R. Sobotka, Institute of microbiology, Třeboň
FLAG-*chlG*	-	N-terminally FLAG-tagged copy of *Synechocystis chlG* in place of the *psbAII* gene	This study
FLAG-*chlG*/Δ*chlG*	FG/ΔG	FLAG-*chlG* strain in which the native *chlG* gene has been replaced with a zeocin resistance cassette	This study
yidC-FLAG	-	C-terminally FLAG-tagged copy of *Synechocystis yidC* in place of the *psbAII* gene	This study
yidC-FLAG/Δ*yidC*	-	*yidC*-FLAG strain in which the native *yidC* gene has been replaced with an erythromycin resistance cassette	This study
FLAG-*ycf39*/Δ*ycf*39	-	N-terminally FLAG-tagged copy of Synechocystis *ycf39* in place of the *psbAII* gene; native *ycf39* gene replced with an erythromycin resistance cassette	Dr R. Sobotka, Institute of microbiology, Třeboň

Table 2. Strains

Empty vectors

Plasmid	Properties	Source
pPD-FLAG	pBluescript II KS+ based vector containing a 3xFLAG encoding sequence. Km^R	Dr P. Davison and Dr D. Canniffe, University of Sheffield
pPD-CFLAG	A modified version of the pPD-FLAG vector enabelling C-terminal tagging of inserts. Km^R	Dr R. Sobotka, Institute of microbiology, Třeboň
pK18mobsacB	An allelic exchange suicide vector mobilised by E. coli S17-1. Allows blue white screening for inserts. Km^R	Novagen
pET14b	pBR322-based expression vector with the T7 promoter and terimator, His_6-tag and thrombin linker. Km^R	Novagen

Modified vectors

Plasmid	Properties	Source
pPD-FLAG-*chlG*	pPD-FLAG vector containing a N-terminally 3xFLAG-tagged *chlG* gene flanked by *psaAII* up- and downstream regions	This study
pPD-CFLAG-*yidC*	pPD-CFLAG vector containing a C-terminally tagged 3xFLAG-tagged *yidC* gene flanked by *psaAII* up- and downstream regions	This study
pK18mobsacB-Δ*bchC*/Δ*bchX*	*bchC* and *bchX* knock out construct containing regions up- and downstream of the the two genes.	This study
pK18mobsacB-Δ*bchF*	*bchF* knock out construct containing regions up- and downstream of the the gene.	This study
pET14b-*Gloop*	Expression vector containing His_6-tagged *Gloop*	This study

Table 3. Plasmids

Primers (in order of appearance)

Primer	Sequence (5' - 3')	Restriction site
chlG Forward	GCGCTCTAGACATATGGTGAGCAAGGGCGAGGAGCTGTTCAC	NdeI
chlG Reverse	GCGCTCTAGAGCGGCCGCCTTGTACAGCTCGTCCATGCCGAGAGTGAT	NotI
chlG-upstream Forward	TCGTTGAGCGGGAGAGTTTG	-
chlG-upstream Reverse	ACATTAATTGCGTTGCGCTCACTGCGGCTTCATCAACTGAAGACG	-
chlG-downstream Forward	CAACTTAATCGCCTTGCAGCACATCAAGTCCTTGCCGGTGATGT	-
chlG-downstream Reverse	AATTGACCAACCATTTCTCC	-
Zeo internal forward	CGGGTCGCGCAGGGCGAAC	-
Zeo internal reverse	CAACTTAATCGCCTTGCAGCACATCAAGTCCTTGCCGGTGATGT	-
yidC Forward	TCTAGACATATGGATTTTGGTATCGGTTTTATTTCGACAAATATC	NdeI
yidC Reverse	ACGGCTAGCCGAGGTTTTTTCCTTCTTTTTACTGCTTTTCT	NheI
yidC-upstream Forward	GCGAAAATGATTAAAATGCCTAGGGGGA	-
yidC-upstream Reverse	CTGCAATCGGATGCGATTATTGAATATGGCGCTCTTTCATCAGGGGCT	-
yidC-downstream Forward	GCATCCCTTAACTTGTTTTTCGTGTGGATGTACATTGTCATGGCCAACGTCT	-
yidC-downstream Reverse	ACCGCTCAATCTGGCTTGAGGATAGAT	-
Ery internal forward	TTGTTGATCACGATAATTTC	-
Ery internal reverse	CTGATAAGTGAGCTATTCAC	-
bchC/*bchX*-upstream forward	CCGGAATTCGCTCCTGCACCGGGTGCGCG	EcoRI
bchC/*bchX*-upstream reverse	GCGCTCTAGAAGCGTTTTCCCCCGCGCTCTTC	XbaI
bchC/*bchX*-downstream forward	GCGCTCTAGATCTCGATACCCTCGCGCGGC	XbaI
bchC/*bchX*-downstream reverse	CCCCAAGCTTGTCCTCGAACAGCTTGCCCGTG	HindIII
bchC/*bchX* conformation forward	GACGATCCACTGCCGCTCGG	-
bchC/*bchX* conformation reverse	GCGCTCTAGATCTCGATACCCTCGCGCGGC	-

bchF upstream forward	CCGGAATTCGCTCCTGCACCGGGTGCGCG	EcoRI
bchF upstream reverse	GCGCTCTAGAAGCGTTTTCCCCCGCGCTCTTC	XbaI
bchF downstream forward	GCGCTCTAGATCTCGATACCCTCGCGCGGC	XbaI
bchF downstream reverse	CCCCAAGCTTGTCCTCGAACAGCTTGCCCGTG	HindIII
bchF conformation forward	GACGGCCACCGGGCCCTC	-
bchF conformation reverse	GAGGCGAGGCAGGCATCCTC	-
Gloop Forward	CCGCATATGTCTGACACCCAGAACACCGGTCAG	NdeI
Gloop Reverse	CGCGGATCCTTAAGCCTGGTATTTAACGTCGTTTTCC	EcoRI

Table 4. Primers

Chapter 3: A Cyanobacterial Chlorophyll Synthase-HliD complex associates with the Ycf39 Protein and the YidC/Alb3 insertase

3.1. Summary

In order to investigate the delivery of chlorophyll to nascent chlorophyll binding proteins the terminal enzyme of Chl biosynthesis of *Synechocystis* was FLAG-tagged and subjected to immunoprecipitation assays. An enzymatically active protein-pigment complex containing the high-light-inducible protein HliD, membrane insertase YidC and putative PSII assembly factor Ycf39 was retrieved. 'Reciprocal' pull-down experiments with FLAG-tagged YidC and Ycf39 both yielded eluates containing CS. Further analysis by CN-PAGE and size exclusion chromatography revealed that the FLAG-CS eluate consists of a tightly associated CS-HliD core which contains Chl, Chlide and carotenoids, with YidC and Ycf39 more loosely attached.

The data presented in this chapter provide the first evidence for a link between Chl biosynthesis and YidC-dependent co-translational insertion of nascent photosystem polypeptides into membranes. This close physical linkage is likely to coordinate the arrival of pigments and nascent apoproteins to produce photosynthetic protein-pigment complexes with minimal risk of accumulating phototoxic unbound Chls.

3.2. Introduction

Chlorophyll synthase (CS) catalyses the terminal stage of chlorophyll biosynthesis, the conversion of Chlide to chlorophyll (Chl). The enzyme is discussed at length in (1.3.11.).

The structures of photosystems I and II (Jordan *et al*., 2001; Umena *et al*., 2011) show how Chl molecules are arranged within these complexes allowing for highly efficient light harvesting and energy transfer. Thus, the biogenesis of PSI and PSII must involve close interplay between the chlorophyll biosynthesis pathway and the PSI and PSII assembly apparatus. Numerous studies provide circumstantial evidence for such a linkage suggesting that Chl is inserted into these complexes cotranslationally and is likely to be a prerequisite for correct folding and membrane incorporation of chl-proteins (Chua *et al*., 1976; Eichacker *et al*., 1996; Müller and Eichacker, 1999). It has been shown using a Δ*chlL* deletion mutant of *Synechocystis*, which is unable to synthesise Chl in the dark that *de novo* synthesis of Chl is essential for the synthesis of all cyanobacterial Chl proteins (Kopečná *et al*., 2013). Channelling of Chl from the Chl biosynthesis pathway to nascent Chl-binding proteins would also serve to prevent the occurrence of free, phototoxic Chls with give rise to reactive oxygen species (Apel and Hirt, 2004).

Whilst there are reports of putative protein factors connecting Chl biosynthesis and PSII biogenesis (Dobáková *et al*., 2009; Schottkowski *et al*., 2009), the mechanisms of Chl delivery to nascent Chl binding proteins remain unclear. The enzymes involved with the latter stages of Chl biosynthesis are known to be membrane associated (Masuda and Fujita, 2008), whilst CS is an integral membrane protein (Addlesee *et al*., 2000). Given that the major Chl binding components of PSI (PsaA and PsaB) and PSII (D1, D2, CP43 and CP47) are relatively large, hydrophobic, integral membrane proteins believed to be synthesised by membrane associated ribosomes, the use of CS in pull-down assays is a promising strategy to test the idea that the terminal enzyme of Chl biosynthesis is closely associated with the protein synthesis/insertion machinery for the cotranslational insertion of Chl in to nascent photosystem apoproteins.

3.3. Results

3.3.1. FLAG-tagging of the *chlG* gene

In order to identify putative interaction partners of CS, a mutant strain was created. Firstly a FLAG-tagged version of the CS gene (*chlG*) was added to the *Synechocystis* genome in place of the *psbAII* gene (Figure 1), which is one of three genes encoding the D1 protein of PSII and removal of which does not result in a mutant phenotype (Dr. Roman Sobotka, personal communication). This was achieved using the pPD-FLAG vector: the *chlG* gene was cloned from *Synechocystis* genomic DNA using primers with the appropriate overhang to allow restriction digest and ligation in to the cloning site of pPD-FLAG, placing the *chlG* gene directly 5' of the 3x FLAG tag situated upstream of the cloning site and maintaining the correct reading frame. WT *Synechocystis* was then transformed with the pPD-FLAG-*chlG* plasmid and recombination was initiated by selection on kanamycin. Transformants were grown on increasing antibiotic concentrations until full segregation was achieved, which was confirmed by PCR (Figure 1) yielding the FLAG-*chlG* strain expressing N-terminally tagged CS.

3.3.2. Deletion of native *chlG* from the FLAG-*chlG* strain

In order to confirm that the FLAG-tagged CS produced by the FLAG-*chlG* strain was functional and to ensure that all copies of CS produced by the cell were FLAG-tagged, the original *chlG* gene was deleted in the FLAG-*chlG* background. This was achieved using the megaprimer method (Ke and Madison, 1997), summarised in Figure 2. Segregation was carried out as described previously and checked using PCR (Figure 2).

The resultant FLAG-*chlG*/Δ*chlG* strain (henceforth FGΔG) exhibits no noticeable phenotype when compared with WT; the whole cell spectra (Figure 3A) and growth rate (Figure 3B) are almost identical implying that the FLAG-tagged version of the protein is capable of adequately replacing the native protein with minimal impact on cell viability, albeit with seemingly less CS expression than in WT (Figure 3C).

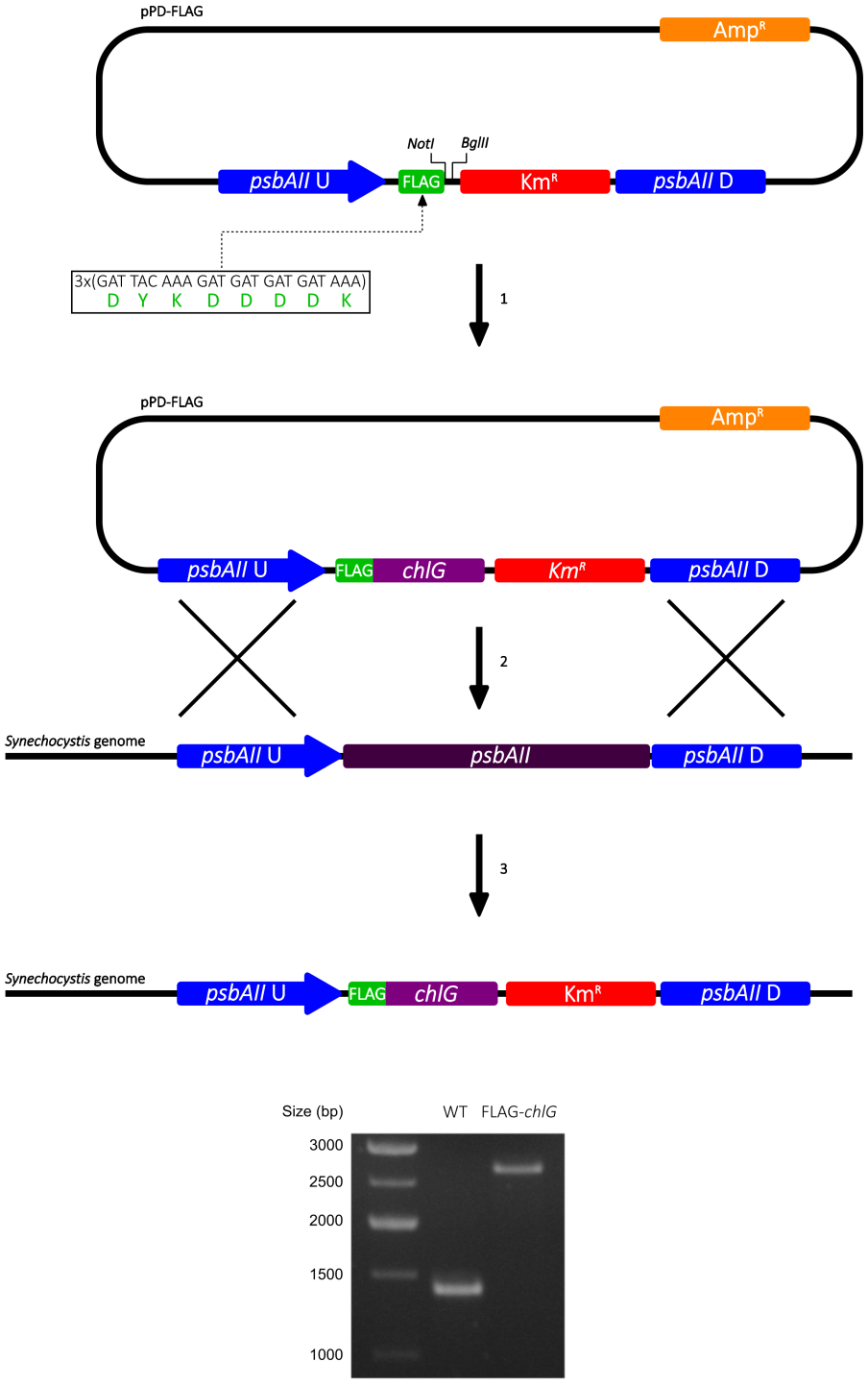

Figure 1. 3x FLAG-tagging of the *chlG* gene in *Synechocystis*. 1. Ligation of the *chlG* gene directly 3' of the FLAG-tag into the pPD-FLAG vector. **2**. Transformation of WT *Synechocystis* with the resulting plasmid and antibiotic-induced recombination. **3**. Full segregation of the mutant construct yielding 3x FLAG-tagged *chlG* in place of the *psbAII* gene. The agarose gel shows the colony-PCR products yielded using primers situated up- and downstream of *psbAII*. U - upstream, D - downstream, Amp^R - ampilcillin resistance cassette, Km^R - kanamycin resistance cassette.

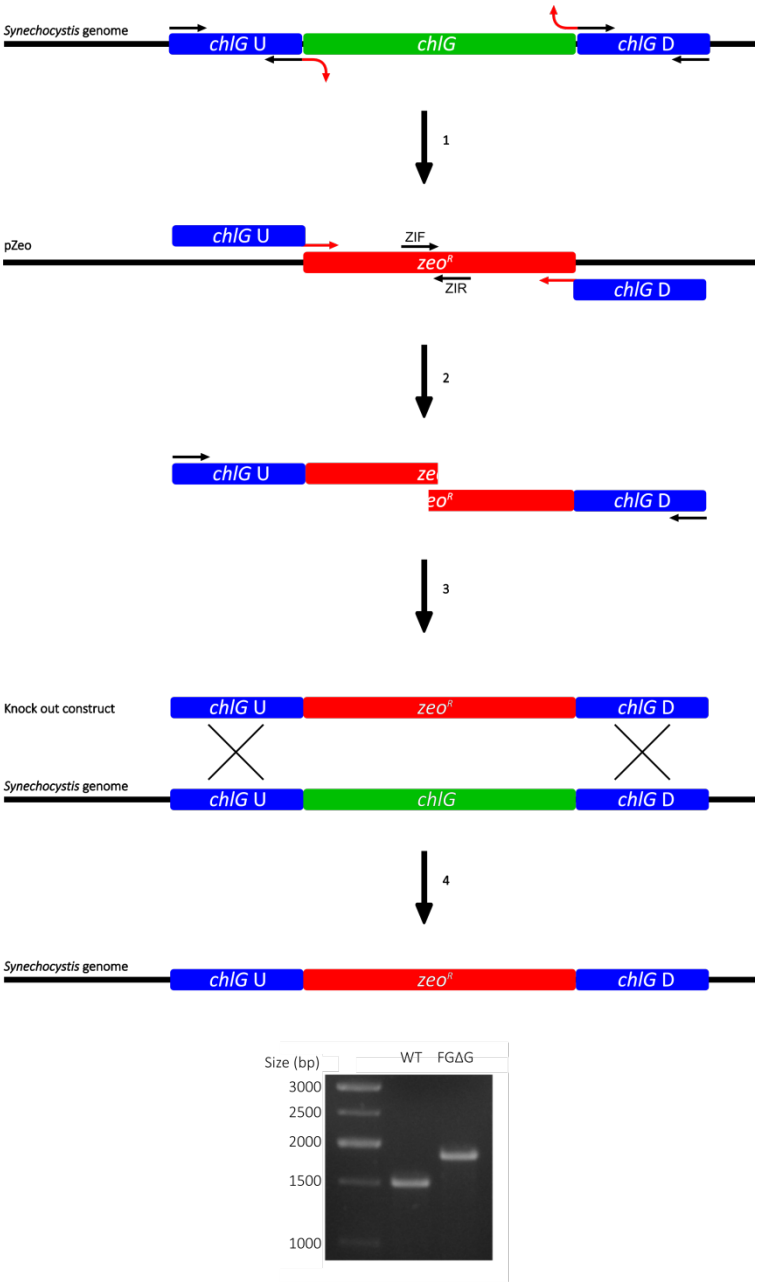

Figure 2. Deletion of the native *chlG* gene from the FLAG-*chlG* strain using the megaprimer method. 1. Cloning of regions up- and downstream of the *chlG* gene, the upstream reverse and downstream forward primers have overhangs complimentary to the start and end, respectively, of a zeocin resistance cassette. **2.** Cloning of a zeocin cassette using the 'megaprimers' created in the previous step in conjunction with primers complementary to sites inside the resistance gene. ZIF (zeocin internal forward); ZIR (zeocin internal reverse). **3.** Overlap extension PCR using the original upstream forward and downstream reverse primers yielding the *chlG* knock out construct, transformation into the FLAG-*chlG* genome and antibiotic induced recombination. **4.** Full segregation of the knock out construct yielding the FLAG-*chlG*/Δ*chlG* strain (FGΔG). U - upstream, D - downstream, Zeo^R - zeocin resistance cassette.

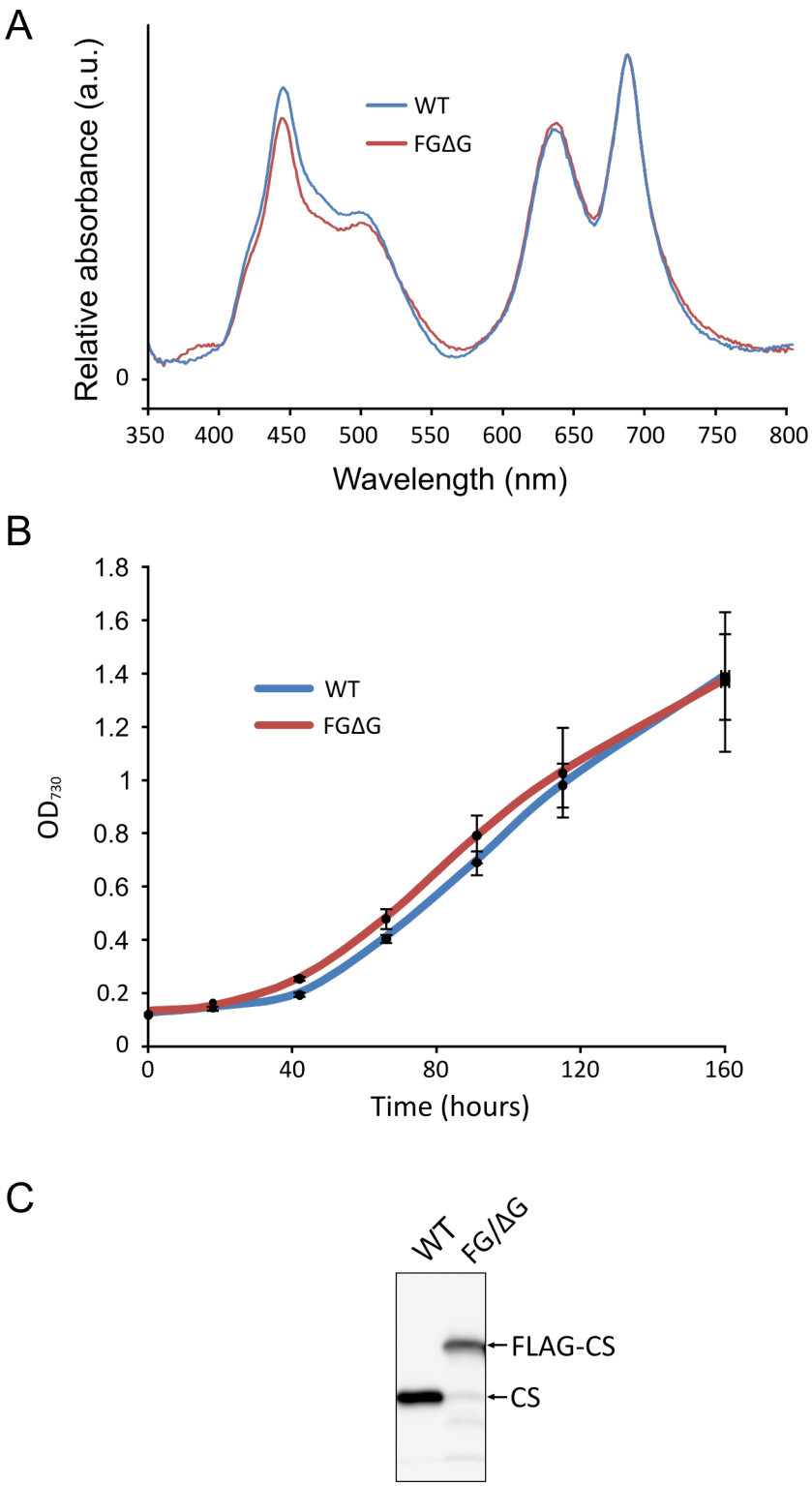

Figure 3. Analysis of the FGΔG strain. A. Whole cell spectra of WT (blue) and FGΔG (red). Spectra are corrected for light scatter at 750 nm. a.u. - arbitrary units. **B.** Growth curve of photoautotrophically grown WT and FGΔG cells. **C.** Immunoblot of membrane preparations using a CS specific antibody, samples were standardised by protein level. The production of the primary antibody used is detatiled in Chapter 6.

3.3.3. Purification of chlorophyll synthase and putative interaction partners using FLAG-affinity chromatography

A membrane fraction was prepared from a large culture (4 L) of the FGΔG strain and, after solubilisation with 1.5% β-DDM, applied to an anti-FLAG affinity column. After thorough washing, specifically bound proteins were eluted with excess FLAG peptide.

The FLAG-eluate was analysed by SDS-PAGE (Figure 4); visible bands were excised and, after in-gel tryptic digestion, analysed by LC-MS/MS (Figure 4C). The Ycf39 homologue Slr0399, the Slr1471 protein belonging to the YidC/Oxa1/Alb3 family of membrane insertases (henceforth YidC), the high-light-inducible protein (Hlip) HliD, the Sll1167 protein belonging to the AmpH family and the PSI subunits PsaA and PsaB were identified. Of these, only weak PsaA and PsaB bands were observable in the WT control pull-down (Figure 4A), indicating that the PSI subunits within the FGΔG eluate are likely to be a result of non-specific binding to the column. The presence of YidC, HliD and Ycf39 was confirmed using specific antibodies (Figure 4B) and in solution tryptic digest followed by MS (not shown).

3.3.4. Construction of a *Synechocystis* mutant strain expressing FLAG-tagged YidC.

In order to further reinforce the results presented above, 'reciprocal' pull-down experiments were attempted. To this end a FLAG-tagged YidC mutant strain was created.

A pPD-FLAG construct similar to that described in Section 3.3.1. was created with the *yidC* gene ligated directly 3' of the 3x FLAG tag. Although this construct segregated into the *Synechocystis* genome successfully, a preliminary FLAG-purification with the resultant FLAG-*yidC* strain yielded no protein. Attempts to fully segregate a *yidC* knock-out construct in this background proved impossible, implying that the N-terminal tag was impairing the function of the tagged protein.

In order to circumvent the problems arising from an N-terminal tag, a C-terminal tag was attempted. The *yidC* gene was ligated into a modified version of the pPD-FLAG vector, pPD-CFLAG, directly 5' of the FLAG tag (Figure 5). Segregation of this construct yielded the *yidC*-FLAG strain.

The native *yidC* gene was deleted from the *yidC*-FLAG strain using the megaprimer method described in Figure 2 (with erythromycin in place of zeocin) yielding a *yidC*-FLAG/Δ*yidC* strain with no noticeable mutant phenotype indicating that the FLAG-tagged version of the gene is fully active and capable of adequately replacing the native protein.

A

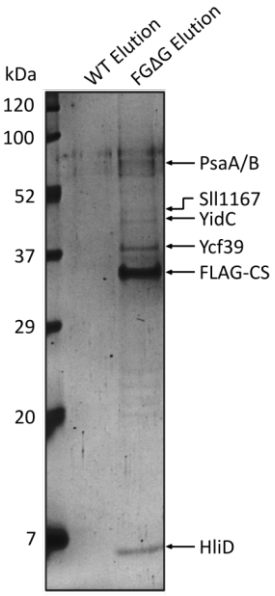

B

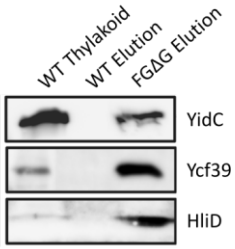

C

Protein	Uniprot Identifier Gene Name	Mass (Da)	Coverage (%)	Peptides
Photosystem I P700 chlorophyll a apoprotein A1	P29254 PsaA	83124	8	R.ALSIIQGR.A K.LLDAGVAPK.D K.NVNNLLDR.M K.LNVAPAIQPR.A K.VSVDNNPVPTSFEK.W K.DIPLPHEFILEPSK.M
Photosystem I P700 chlorophyll a apoprotein A2	P29255 PsaB	81354	6	R.TPLANLVR.W K.FSQDLAQDPTTR.R K.DFGYSFPCDGPGR.G R.DYDPVANKDNVLAR.M
Penicillin-binding protein 4	P74200 Sll1167	44532	8	K.DVAFGEPR.G R.ASLNQYLIDR.L R.VNPETGNGIVLLLSGNR.S
Membrane protein insertase	P74155 YidC (Oxa1, Alb3)	42656	20	R.TGFLFIK.A R.YKDDPAK.Q R.ITQPLMK.E R.ESLPFEK.K K.LLDEQQK.A K.AFNQVIPEK.N R.EPLPENLQK.L K.TQLEIQSTEGK.A K.NSQILTPTYSVTK.G
Ycf39 gene product	P74429 Ycf39	36724	51	R.AAEYPK.V K.VPLMDIK.N R.QVDWEGK.L R.ATDSLTIR.Q R.AVELDSVAR.K K.FVFFSILR.A R.ISQVPMAVLR.F R.LAFSEVLASGK.A R.VLVVGGTGTLGR.Q R.FFQWTYNASDR.L R.QAIDQGHTVVCLVR.S K.ELDYEVNPTQTEGK.K K.ETTTLESYLQEYFGR.I K.LKELDYEVNPTQTEGK.K K.ALTADMAPVYEQFGLDPK.E
Chlorophyll a synthase	Q55145 ChlG	35357	7	R.QLGLK.S R.NPLENDVK.Y K.GAAPGESSIWK.I
High light inducible protein	P72932 HliD	6468	44	K.FGFNNYAEK.L M.SEELQPNQTPVQEDPK.F

Figure 4. Analysis of the protein components of the FGΔG eluate. A. SDS-PAGE of the FGΔG and WT control eluates, labelled bands were excised and identified by MS (Figure 4C). **B.** Immunoblot of the FGΔG and WT control eluates using specific antibodies. **C.** Following SDS-PAGE (Figure 4A) protein bands were identified by nanoLC-MS/MS and database searching. Peptides are shown with their flanking amino acid residues separated by dots.

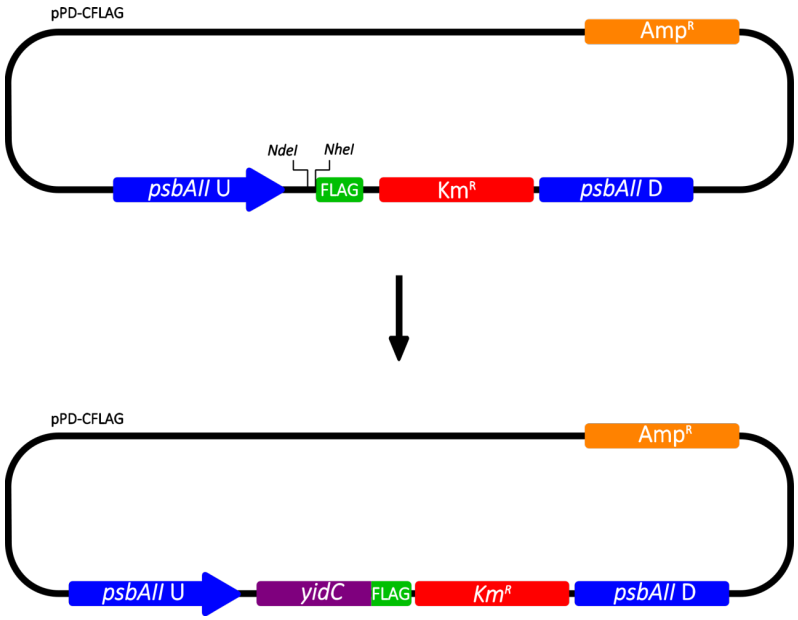

Figure 5. C-terminal 3x FLAG-tagging of the *yidC* gene in *Synechocystis*. The *yidC* gene was ligated directly 5' of the 3x FLAG tag in a modified version of the pPD-FLAG vector (pPD-CFLAG). The remaining cloning steps are identical to those shown in Figure 1 (steps 2 and 3).

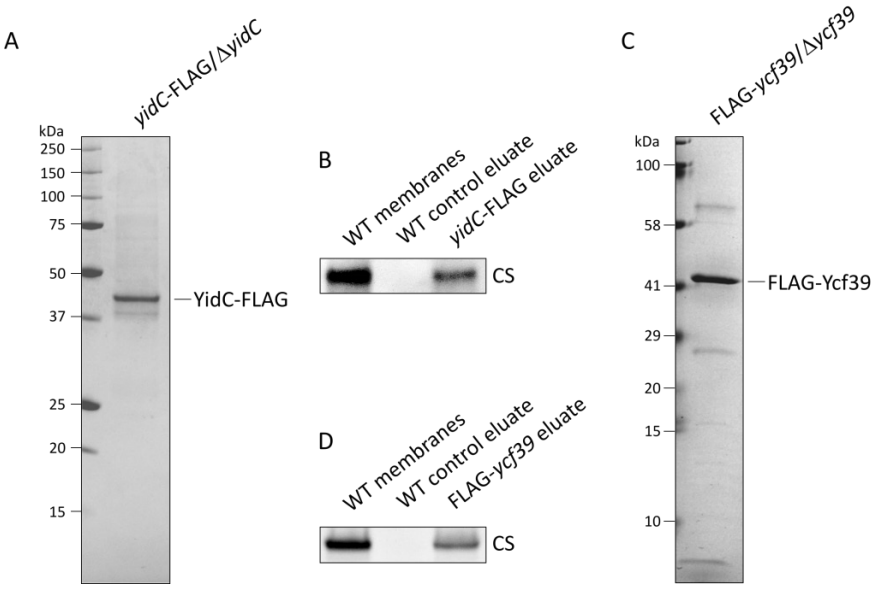

Figure 6. Reciprocal pull-down experiments using FLAG-tagged YidC and Ycf39. A. SDS-PAGE of the elution obtained from FLAG pull-down experiments using the *yidC*-FLAG mutant. B. Immunoblot of the *yidC*-FLAG/Δ*yidC* and WT control eluates using a CS specific antibody. C. SDS-PAGE of the elution obtained from FLAG pull-down experiments using the FLAG-*ycf39*/Δ*ycf39* mutant. D. Immunoblot of the *yidC*-FLAG/Δ*yidC* and WT control eluates using a CS specific antibody.

3.3.5. 'Reciprocal' pull-downs using FLAG-tagged chlorophyll synthase interaction partners

FLAG-immunoprecipitiation was carried out as described in Section 3.3.3., using membranes prepared from the *yidC*-FLAG/Δ*yidC* strain and a FLAG-*ycf39*/Δ*ycf39* mutant made in the same way as described previously (Section 3.3.1/2.) (kindly provided by Dr. Roman Sobotka, Institute of microbiology, Třeboň, Czech Republic). The eluates from both experiments, along with a WT control, were analysed by SDS-PAGE and immunoblot (Figure 6). In both cases CS was detected in the FLAG-eluate but not in the WT control, indicating a specific interaction with CS in both cases.

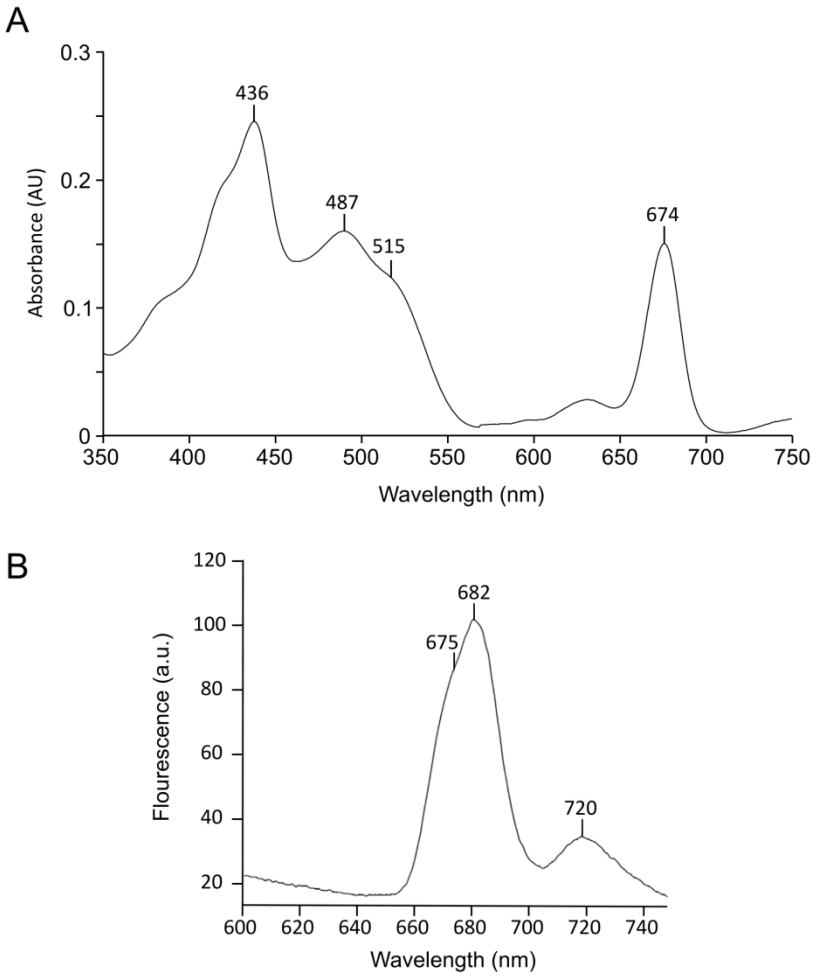

Figure 7. Spectral analysis of the FGΔG eluate. **A.** Absorption spectra of the FGΔG pull-down eluate. AU - absorbance units. **B.** Low temperature (77K) Chl emission spectra of the FGΔG pull-down eluate. a.u. - arbitrary units.

3.3.6. Spectral analysis of the FGΔG eluate

The FGΔG eluate was visibly green-orange, implying the presence of pigments. The absorption spectrum shows maxima at 674 and 436 indicative of Chl and/or Chlide and at 487 and 515 implying the presence of carotenoids (Figure 7A). The fluorescence emission spectrum (Figure 7B) resolves two emitting components; a major peak at 682 nm with a 675 nm shoulder (likely to arise from free Chl) and a small 720 nm peak characteristic of PSI. This 682 nm peak is indicative of a novel pigment-protein complex containing CS.

3.3.7. Analysis of the FGΔG eluate by CN-PAGE and size exclusion chromatography

In order to examine the association of the various eluate components, a sample of the FGΔG eluate was concentrated and run on CN-PAGE. Two orange bands with predicted masses of <100 kDa were resolved (denoted CN1 and CN2) along with PSI (Figure 8). These complexes were further resolved by a second, denaturing, gel. Sypro Orange staining followed by MS of excised bands revealed that the major protein components of the CN1 and CN2 bands are CS and HliD, providing clear evidence that these two proteins form a protein-pigment complex. Immunodetection using specific antibodies reveals that Ycf39, YidC and Sll1167 form a higher molecular weight complex that is not visible without the aid of stain and therefore unlikely to contain pigments.

HPLC size exclusion chromatography was used to further characterise the composition, molecular masses and spectral properties of the components of the FGΔG elution. Several complexes were resolved (Figure 9) with the largest eluting in the void volume, peak GF1; the red shift of the Chl in this peak and that of GF2 is indicative of PSI. The column fractions corresponding to peaks GF1-4 were analysed by immunoblot showing that most of the YidC and Ycf39 eluted slightly later than peak GF1 (~5.7 ml), whereas most of the HliD eluted either in the GF3 peak containing FLAG-CS, or in the GF4 peak containing neither FLAG-CS nor Ycf39 (Figure 9). This analysis showed that YidC and Ycf39 tend to become detached from ChlG but remain in large complexes with molecular masses higher than 400 kDa, although small amounts of YidC and Ycf39 retain an association with CS. HliD associated preferentially with CS forming a complex with an apparent molecular mass of

approximately 70 kDa. Given the molecular masses of FLAG-CS and HliD, at 38.5 and 6.5 kDa respectively, the complex is likely to be CS(HliD)$_4$. A substantial proportion of the HliD in the eluate became detached from FLAG-CS and migrated as a ~40 kDa aggregate probably consisting of several copies of the protein. As the HliD mass is about 6.5 kDa and if associated lipids, detergents and pigments are also taken into consideration, the number of HliD copies could be close to four. In conclusion, gel filtration yielded a pattern of complexes somewhat different from the CN-PAGE analysis, as the FLAG-CS-HliD interaction was apparently less stable during this separation method resulting in an abundant free HliD peak (GF4). Moreover, YidC and Ycf39 remained assembled within a high-molecular-mass complex that was not observed on CN-PAGE. On the other hand, this approach validated the conclusion derived from the 2D-electrophoresis (Figure 8) showing that the FLAG-CS eluate consists of an abundant CS-HliD 'core' and less tightly attached Ycf39/YidC components.

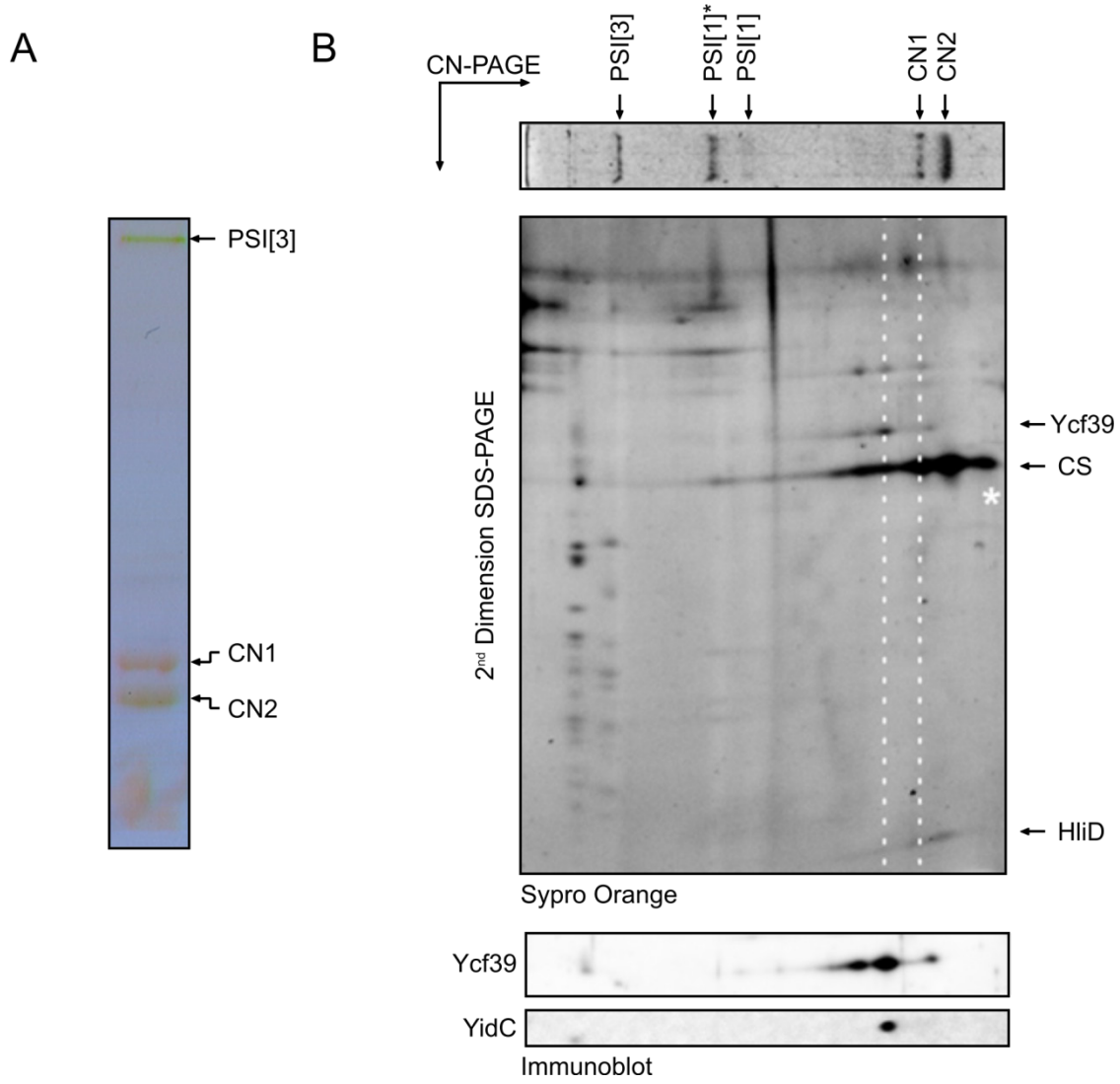

Figure 8. Clear native and 2D electrophoresis of the FGΔG eluate. A. Colour scan of a CN-PAGE of the FGΔG eluate. PSI[3] - photosystem I trimer. **B.** The gel strip from CN-PAGE with separated FGΔG eluate components was further separated in a second dimension by SDS-PAGE. The gel was stained by Sypro Orange and then blotted onto a nitrocellulose membrane. The identities of designated spots on the stained gel was assigned by MS and further verified using specific antibodies.

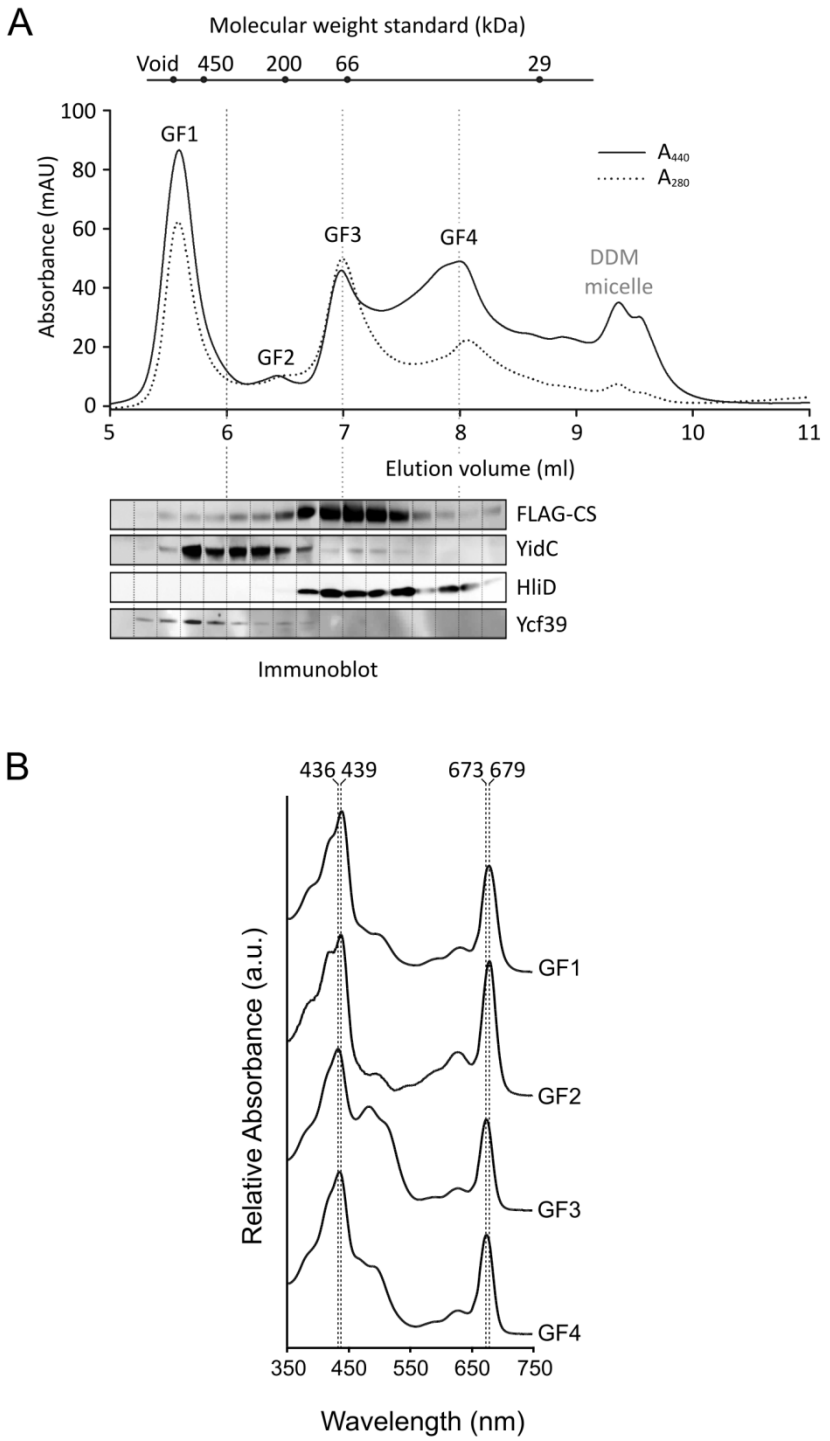

Figure 9. HPLC gel filtration of the FGΔG eluate and immunodetection of eluted proteins. **A.** FGΔG eluate was loaded on a BioSep 3000 column and eluted protein complexes were monitored by absorbance at 440 and 280 nm (A_{440} and A_{280}). Eluted fractions were collected and subjected to immunoblot analysis; each band corresponds to the 0.2 ml fraction of the column elution with which it is aligned. **B.** Absorption spectra of the corresponding gel filtration peaks as collected by the HPLC diode array detector; maxima are indicated by dashed lines.

3.3.8. Analysis of the pigments associated with FLAG-chlorophyll synthase

The spectral analysis of the eluate (Figure 7) and the CS-HliD 'core' complex (Figure 9B, GF3) indicate the presence of Chl and/or Chlide and carotenoids forming a protein-pigment complex. In order to further analyse the pigment content of the FGΔG eluate, reverse-phase chromatography was carried out revealing the major pigment components of the eluate as: Chlide, Chl, myxoxanthophyll, zeaxanthin and β-carotene.

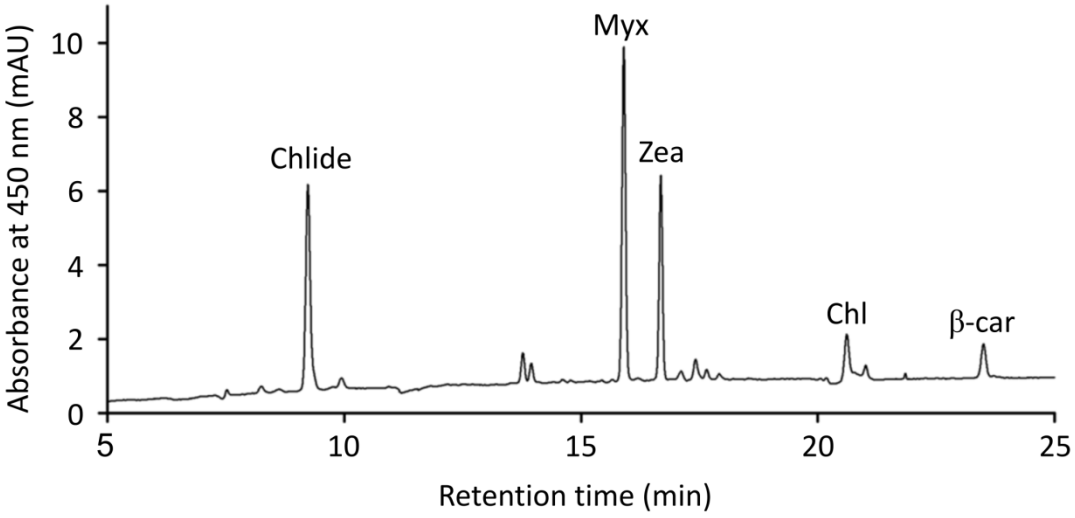

Figure 10. Pigment analysis of the FGΔG eluate by reverse phase chromatography. Myx - myxoxanthophyll, Zea - zeaxanthin β-car - β-carotene.

3.3.9. Chlorophyll synthase activity of the purified FLAG-CS complex

Oster *et al*, (1997) showed that an *E. coli* cell extract containing recombinant CS from *Synechocystis* catalyses the attachment of geranylgeraniol or phytol tails to the Chlide macrocycle. The CS activity of the purified CS preparation was investigated initially by assaying the capacity of the FGΔG eluate to use the endogenous Chlide pool (Figure 10) as a source of substrate. Geranylgeranyl-diphosphate (GGPP) was added to the FGΔG eluate, the stopped assay was terminated at various times during the 32-minute time period, then the geranylgeranyl-Chl product was quantified using HPLC (Figure 11A). The data showed the concomitant increase in geranylgeranyl-Chl (Chl_{GG}), and the decrease in Chlide, indicating that the FLAG-CS-HliD-Ycf39-YidC complex possesses Chl synthase activity and the co-eluting Chlide is accessible to the CS. Furthermore the subsequent addition of exogenous geranylgeranyl-diphosphate and Chlide stimulated continued Chl synthase activity (Figure 11C).

3.4. Discussion

Given that photosystem formation requires a supply of chlorophylls, which must be tightly synchronised with synthesis of nascent apoproteins to avoid accumulation of unused pigments it was reasonable to hypothesise that (bacterio)chlorophyll synthases are in close proximity to the protein synthesis/insertion/assembly apparatus for photosystem biogenesis. Such close connection would minimise the time for pigment transfer from the synthase to the translocon channel containing nascent polypeptides and therefore the risk of photoxidative damage to Chls and their surroundings. One way to establish a fully concerted biosynthetic/assembly mechanism would involve a protein supercomplex comprising CS and translocon components, as recently suggested (Sobotka, 2014).

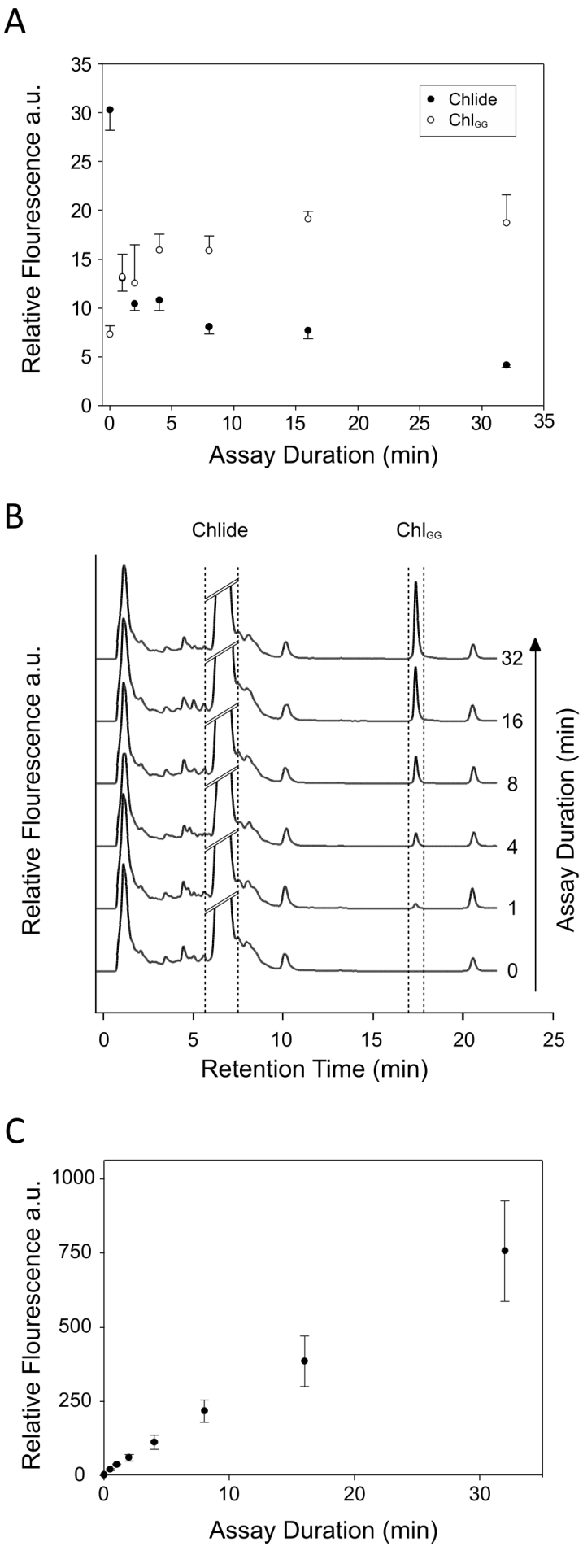

Figure 11. Activity of the FLAG-purified chlorophyll synthase complex. Stopped assays were performed in the presence of 20 µM geranylgeranyl diphosphate, assays were performed in triplicate and each time point was analysed by reverse-phase HPLC. **A.** Coversion of the endogenous Chlide pool to geranyl-geranyl-chlorophyll (Chl$_{GG}$). **B.** Utilisation of exogenously added Chlide, assays were carried out as in A, but with the addition of 20 mM Chlide, each chromatography trace is representative of one of three replicates. **C.** Evolution of GG-Chl in the exogenous assays in **B**.

In this chapter FLAG-tagged CS was used as bait in pull-down experiments. Additional work been carried out in this area is presented in Chidgey *et al*., 2014 which contains additional experimental data and discussion relating to the topic.

The results in this chapter show that CS forms a relatively stable, active, pigment-protein complex primarily with HliD a member of the CAB-like protein family. More loosely attached are Ycf39 a member of the short chain dehydrogenases (Kallberg *et al*., 2002) and the YidC insertase. Nevertheless, both proteins remain attached to CS-HliD during cell breakage, membrane solubilisation, extensive washing on the FLAG-affinity column and CN-PAGE (Figure 8). The only experimental technique that 'seperated' the CS-HliD core from the Ycf39 and YidC components of the FGΔG eluate was gel filtration (Figure 9) and this involved an incubation with 1% β-DDM prior to injection of the sample, which was required to allow high resolution chromatography of the eluate. Moreover, 'reciprocal' pull-down experiments using mutant *Synechocystis* strains expressing FLAG-tagged Ycf39 and YidC yielded eluates that both contained CS, providing further evidence for specific interactions (Figure 6).

As a general membrane protein insertase, it is likely that YidC is involved with the synthesis of CS. This could lead to suggestions that the observed interaction between YidC and CS is due to 'capturing' nascent CS as it is being inserted into the membrane. It is however very unlikely that the miniscule amounts of nascent FLAG-CS would pull down enough YidC to be visible by coomassie blue staining (Figure 4). As further circumstantial evidence, multiple similar FLAG-pull-down experiments have been carried out on various *Synechocystis* membrane proteins and YidC has not been detectable by LC-MS/MS of the whole elution, let alone as a Coomassie stained band on SDS-PAGE (data not shown).

These results show a direct interaction of CS-HliD with YidC and therefore provide the first evidence for the long proposed direct link between Chl biosynthsis and protein synthesis.

3.11.1 The HliD Compontent

HliD is a small, one helix protein and shows it significant similarity with plant chlorophyll *a*/*b* binding proteins and possesses a highly conserved chlorophyll binding

domain (CAB) motif. Genes encoding Hlips are common in cyanobacterial genomes and are generally upregulated under various stress conditions (Bhaya *et al*., 2002). The *Synechocysis* genome encodes four small Hlips designated HliA-D and a fifth fused to the C-terminal of ferrochelatase. Individual Hlips appear to have distinct yet overlapping roles, which is reflected in their different patterns of regulation (He *et al*., 2001). HliA, HliB and HliC have been found to interact with the PSII subunit CP47, and are likely to photoprotect the PSII assembly machinery and stabilise chlorophylls released during the process of PSII repair (Promnares *et al*., 2006; Yao *et al*., 2007). HliD however does not co-localise with PSII (Yao *et al*., 2007) but, as demonstrated in this work, instead interacts with CS (Figure 4). The data presented in this chapter indicate that the CS-HliD complex binds carotenoids, Chl and Chlide. The CS-HliD complex is able to convert this endogenous Chlide pool, as well as exogenous Chlide, in the presence of GGPP (Figure 11). The endogenous Chlide pool could arise due to arrested *de novo* synthesis of Chl during cell breakage and immunoprecipitation. However, Chl biosynthesis is a tightly regulated, concerted process leaving the notion of accumulation of an intermediate to high levels in a fully functioning strain (Figure 3) unlikely. Furthermore de-esterification and subsequent recycling of Chl has been demonstrated in *Synechocystis* (Vavilin and Vermaas, 2007). It is therefore suggested that the Chlide interacting with CS could be channelled to CS-HliD from degraded Chl-binding proteins (perhaps via other Hlips) where it is phytylated and loaded into nascent apoproteins. The associated carotenoids are likely to play a role in photoprotection, acting as scavengers for potentially harmful energy absorbed by Chlide/Chls whilst in contact with CS-HliD. The CS-HliD complex contains relatively high levels of carotenoid compared with free HliD (Figure 9B; peaks GF3 and GF4), indicating that some of the carotenoid binding potential of CS-HliD could come from CS, perhaps at the CS-HliD interface.

3.11.2. The YidC component

YidC belongs to the evolutionarily conserved YidC/Oxa1/Alb3 protein family involved in biogenesis of membrane proteins in bacteria, mitochondria and chloroplasts. It is thought to be involved in assisting partitioning of transmembrane segments into the lipid bilayer and folding of nascent membrane proteins (Beck *et al*., 2001; Nagamori *et al*., 2004). In *E. coli*, YidC binds to the SecY component of the SecYEG protein

conducting channel, where nascent transmembrane segments laterally escape the translocon (Sachelaru *et al*., 2013). The critical role of YidC/Alb3 for biogenesis of cyanobacterial and plant thylakoid membranes is well documented (Spence *et al*., 2004; Göhre *et al*., 2006; Ossenbühl *et al*., 2006). Like the bacterial YidC, chloroplast Alb3 associates with the SecY translocase (Klostermann *et al*., 2002) and in the current model the core photosystem subunits are synthesised on the Sec translocon associated with YidC (Sobotka, 2014). Various techniques have demonstrated an interaction between Alb3 and chlorophyll binding proteins (Pasch *et al*., 2005; Göhre *et al*., 2006).

It is likely that YidC assists loading of Chl into nascent apoproteins. Interestingly, ribosomal pausing occurs at distinct sites during the elongation of the D1 subunit of PSI, and this pausing seems to be intimately associated with Chl binding (Kim *et al*., 1994). Thus, it is tempting to speculate that YidC fixes nascent polypeptides in positions favourable for Chl insertion and that ribosome pausing allows time for attachment of Chl provided by bound CS. This hypothesis is in line with evidence that the translocon machinery can be extended by various factors involved in processing of the translocated polypeptide. In the endoplasmic reticulum, oligosaccharyl transferase and signal peptidase are components of the translocon (Rapoport, 2007). The bacterial translocon was shown to interact with chaperones such as PpiD (Antonoaea *et al*., 2008) and with FtsH proteases ensuring quality control of translated proteins or the integrity of the translocon itself (van Bloois *et al*., 2008). It appears that, in addition to its role for protein in translocation, the SecYEG/YidC core serves as a platform for accessory proteins devoted to nascent protein modification, cofactor binding, or early steps of complex assembly.

3.11.3. The Ycf39 component

Ycf39 belongs to a family of atypical short-chain dehydrogenases/reductases, which have an NAD(P)H binding motif near the N-terminus but lack the canonical Tyr residue critical for activity of typical short-chain dehydrogenase/reducatses (Kallberg *et al*., 2002). The function of Ycf39 is yet to be fully established; deletion of the cognate *slr0399* gene had no effect on cell viability, but it did complement mutations near to the Q_A quinone acceptor of PSII (Ermakova-Gerdes and Vermaas, 1999). This

observation led to speculation that Ycf39 is a chaperone-like protein involved in quinone insertion into the PSII complex. Inactivation of the *Arabidopsis* Ycf39 homolog Hcf244 greatly decreased accumulation of PSII core proteins, and although the mechanism of Hcf244 action was not explained, it appears to be connected to the synthesis of the D1 protein (Link *et al*., 2012). The association of the cyanobacterial Ycf39 with CS and HliD suggests its role in pigment insertion or modification. This is supported by recent data which confirm the involvement of Ycf39 in the delivery of chlorophyll to the newly synthesized D1 protein and stabilization of the PSII reaction centre complex (Knoppová *et al*., 2014).

3.11.4. The Sll1167 component

The Sll1167 protein is related to the AmpH family of bacterial enzymes expected to assist in remodeling of peptidoglycan layer (González-Leiza *et al*., 2011); its enigmatic occurrence in the vicinity of chlorophyll-protein biosynthesis components raises the possibility that Sll1167 plays a structural or functional role in photosystem biogenesis.

3.11.5. Future work

Given that association of CS with HliD YidC and Ycf39 demonstrated in this chapter, the next step is to investigate the effects of high light on the composition of this complex. This could yield information as to whether the complex composition changes as the focus of the cells shifts from thylakoid biogenesis to photosystem repair. This is investigated in the next chapter.

Chapter 4: Analysis of the effects of light shock on chlorophyll synthase and its interaction partners

4.1. Summary

In order to analyse the effects of high light stress on chlorophyll synthase (CS) and its interaction partners, an experiment was designed in which early log-phase *Synechcocystis* cells were subjected to a light shock involving abrupt transfer from moderate (40 photon m^{-2} s^{-1}) to high (800 photon m^{-2} s^{-1}) light conditions. Analysis of pull-down experiments carried out on cells before and after light shock revealed that CS continues to interact with the HliD and YidC proteins during light shock whilst the interaction of CS with Ycf39 is abolished by high light. The light shock appears to cause a rearrangement of the remaining FLAG-CS eluate components. Further experiments carried out on WT cells reveal that under light shock CS moves from lower molecular weight complexes with Ycf39 to higher molecular weight complexes without. The cellular levels of CS interaction partners were analysed by mass spectrometry and display no clear evidence of changes in abundance.

4.2. Introduction

The Earth's rotation and various meteorological factors mean that terrestrial light levels are constantly fluctuating between almost complete darkness and intense sunlight. Photosynthetic organisms have to constantly adapt to these changing light conditions: if light is at a premium the focus is on efficient energy capture whereas in high-light conditions the focus shifts to dissipation of excess energy and repair of damaged light-harvesting apparatus.

Photosynthetic organisms have evolved numerous ways to deal with fluctuating light intensities including: changes to the size and number of light-harvesting antenna (Anderson *et al*., 1995; Walters, 2005), non-photochemical quenching (El Bissati *et al*., 2000; Müller *et al*., 2001) and state transitions, in which the distribution of energy between photosystems is altered (Fujimori *et al*., 2005; Mullineaux and Emlyn-Jones, 2005). Although these preventative systems are in place, photodamage is an inevitable fact of life for phototrophs. Repair mechanisms are in place that allow damaged subunits of light harvesting protein complexes to be removed and replaced by newly synthesised subunits circumventing the necessity for *de novo* synthesis of all components of a photosynthetic complex. Damage occurs most frequently to Chl-binding proteins as a result of singlet oxygen species arising after energy is accepted by pigment molecules but cannot be utilised or dissipated safely (photoinhibition). The D1 subunit of PSII is the most well studied example of this, with high turnover rates even in low and moderate light conditions (Ohad *et al*., 1984; Komenda *et al*., 2000). The requirement of newly synthesised Chl-binding photosystem subunits during repair in turn leads to a requirement for Chl. Vavilin and Vermaas (2007) demonstrated that Chl is removed from damaged Chl binding proteins and recycled into nascent light harvesting polypeptides; this proceeds via the removal of the tail moiety to create Chlide, which is re-esterified prior to insertion into the new Chl-binding protein.

The previous chapter presented data implicating CS, in concert with the HliD, Ycf39 and YidC proteins, in a role in Chl handover during thylakoid membrane biogenesis. In order to investigate whether the same complex is involved in Chl handover during the repair process a light shock experiment was carried out in which log phase

Synechocystis cells were irradiated with extreme light conditions in order to induce repair.

4.3. Results

4.3.1. Light shock of FGΔG *Synechocystis* cells

An experiment was designed in which an 8 L culture of *Synechocystis* FG/ΔG cells (see Section 3.3.) under moderate light conditions (ML; 40 µmol photon m^{-2} s^{-1}) was grown to log phase, in which cells undergo rapid division and therefore carry out high levels of thylakoid biogenesis. 4 L of the culture was harvested and frozen whilst the remaining 4 L was diluted two-fold with fresh BG11 medium, in order to reduce cell shading, and irradiated with a very high light level (800 µmol photon m^{-2} s^{-1}) for 80 minutes. These light shocked cells (LS) were then harvested. The experiment therefore yielded two cell pellets, ML and LS, which having come from the same initial 8 L culture have had identical conditions up until the point of the light shock treatment. The culture vessel contained a temperature coil connected to a thermostat controlled water bath set to 30 °C. This was monitored periodically to ensure that excess heat from the additional light bulbs did not increase the culture temperature. Thus, any differences observed between the ML and LS cells should be a direct result of the increased light conditions.

Absorbance and fluorescence spectroscopy were carried out on the two sets of cells (Figure 1). The results show a decrease in the overall amount of pigment in the cells. The fluorescence emission spectra show that emission from the phycobilisomes remains relatively constant (Figure 1B) and that Chl emission decreases overall, particularly from the CP47 subunit of PSII (Figure 1E; 685 nm) after light shock relative to the pre light shock sample.

4.3.2. FLAG-CS pull-downs from pre- and post-light shock cells

In order to investigate the impact of light shock on CS and its interaction partners FLAG-pulldowns were carried out using the pre- and post-light shock material described above. Pull-downs were carried out as described in Section 3.3. The two eluates were analysed by SDS-PAGE, immunoblot and mass spectrometry which indicate that HliD and YidC remain in complexes with CS under light shock conditions.

However, it appears that the interaction of CS with Ycf39 is abolished after light shock; the Ycf39 band is not observable in the SDS-gel and no detectable specific signal was observed during immunoblot. Small amounts of Ycf39 were detectable in the LS eluate by mass spectrometry but at greatly reduced levels (Figure 2C). Comparison of the ML and LS samples using both SDS-PAGE gel and mass spectrometry revealed no novel CS interaction partners in the light shocked FLAG-CS eluate. The representative peptides observed for each of the detected proteins are the same as those found in Chapter 3: Figure 4.

4.3.3. Further analysis of the composition of the pre- and post-light shock FLAG-CS eluates by size exclusion chromatography.

In order to further characterise the protein composition of the two eluates, size exclusion chromatography was carried out as in Section 3.8. The data obtained yield traces similar to those observed in Section 3.8. (albeit with much higher 'GF2' peaks) with PSI eluting in the void volume (GF1), three other pigment containing peaks (GF2, GF3 and GF4) and free β-DDM micelles. Comparison of the two traces after normalisation to the β-DDM micelle peak reveals differing elution profiles, indicating a change in composition of the FLAG-CS eluate after light shock treatment (Figure 3). The levels of PSI in the LS elution are much lower than that of the ML, and it that appears the GF2 and GF3 peaks 'swap' after light shock with GF2 being dominant in the ML elution and GF3 in the LS. The GF4 peak appears to shift from a double peak in ML to favouring the latter of the two peaks in LS.

Fractions collected from the size exclusion chromatography experiments were run on SDS-PAGE and interrogated with specific antibodies (Figure 4), the immunoblot signals obtained were analysed using ImageJ software (Schneider *et al*., 2012) yielding density values allowing relative quantification of fractions, plotted as histograms and overlaid with the size exclusion chromatography HPLC traces to allow visualisation of the relative distribution of the eluate components (Figure 5). These reveal that light shock has an effect on the distribution of each of the components of the FLAG-CS eluate.

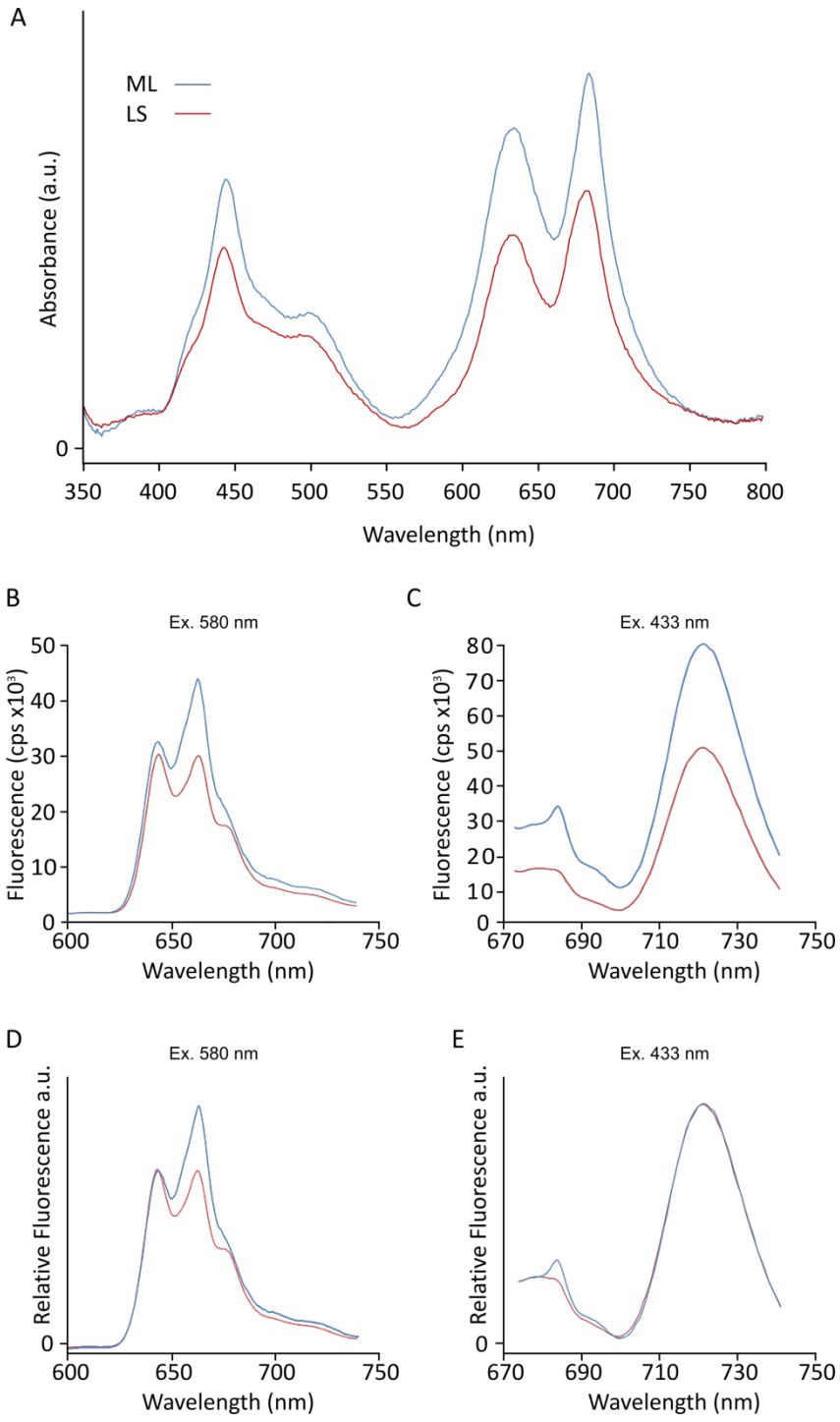

Figure 1. Spectroscopic analysis of the FG/ΔG strain before (ML) and after (LS) light shock treatment. A. Absorbance spectra of whole cells. Traces were normalised at 750 nm and adjusted for cell scatter. **B**. 77 K fluorescence excitation spectra of whole cells before (blue) and after (red) light shock, excitation wavelength was 580 nm for phycobilisomes. cps – counts per second **C**. 77 K fluorescence spectra carried out in the same way as (**B**) with an excitation wavelength of 433 nm for Chl. **D.** The traces shown in (**B**) normalised to phycobilisome emission (642 nm). E. The traces carried out in (**C**) normalised to CP43 emission (678 nm).

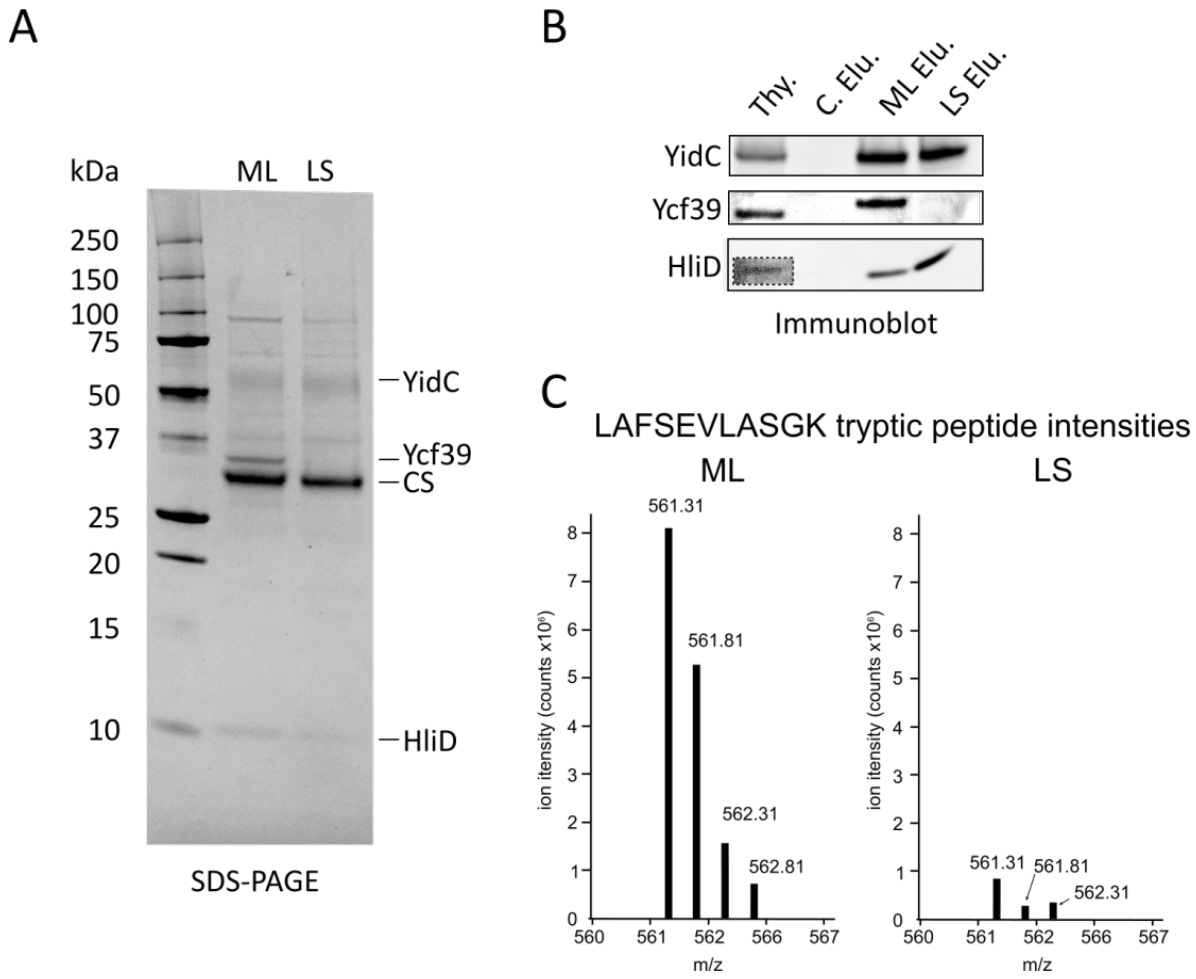

Figure 2. Analysis of pre- and post-light shock FLAG-CS eluates. A. SDS-PAGE. **B**. Immunoblot analysis. Dashed box indicates an area in which the exposure has been artificially increased. Thy. – WT membranes; C. Elu. – WT control elution; ML Elu. – moderate light elution; LS elu. - light shock elution. **C**. Relative intensities of the LAFSEVLASGK tryptic peptide representative of Ycf39 as observed by mass spectrometry after tryptic digest of the eluates.

In the ML sample YidC appears to be mainly associated with the GF2 peak, with large amounts also associated with the GF3 peak, and very small amounts still detectable up to the 8 ml elution volume corresponding to GF4. The majority of the YidC in the LS sample appears to be within a high molecular weight complex with seemingly much less associated with the GF3 peak. No detectable levels were observed beyond 7.6 ml.

HliD is very clearly associated with the GF2 and GF3 peaks in the ML trace with the immunoblot signals mirroring the latter half of the trace. In the LS sample the distribution less well ordered and indicates the presence of HliD in roughly equal amounts from 7.0 ml to 8.2 ml, with the exception of the 7.4 – 7.6 ml fraction which has a substantially higher signal.

As would be expected, the bait protein is detectable in the most fractions in both the ML (11) and LS (9) samples. Overall the CS in the LS sample tends towards higher molecular weights. No CS is observed in the LS sample beyond 8 ml.

Ycf39 appears to be mainly associated with the GF2 peak in the ML sample, and is once again undetectable in the LS sample.

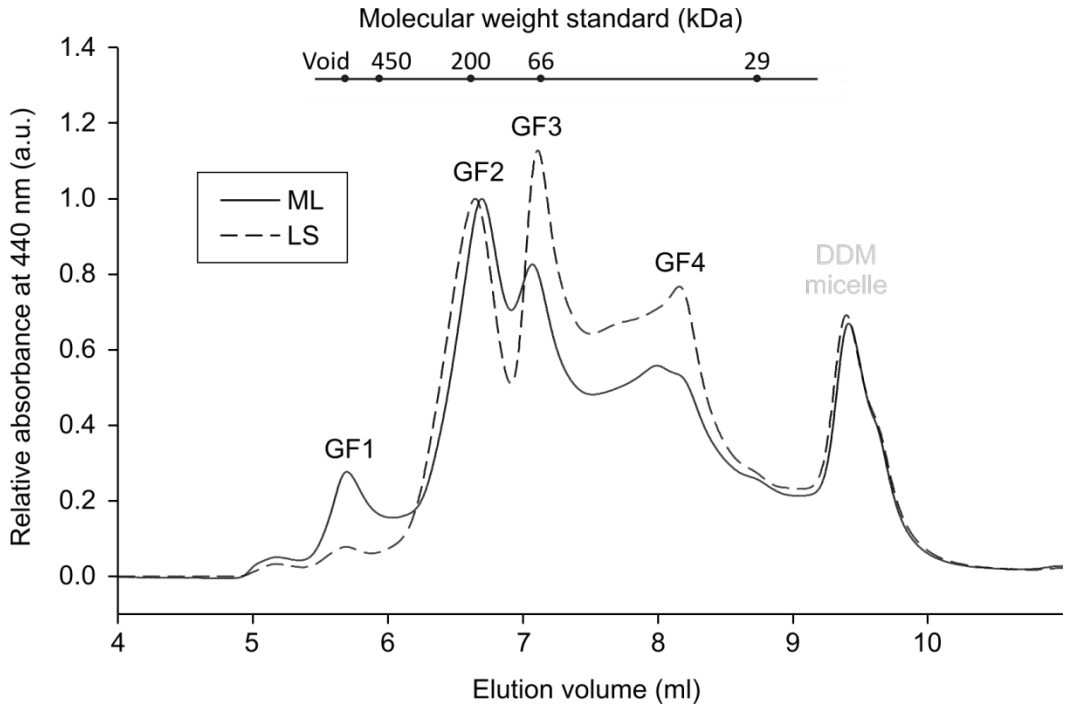

Figure 3. Size exclusion chromatography of the ML and LS FLAG-CS eluates. ML and LS eluates were loaded on a BioSep 3000 column and eluted protein complexes were monitored by absorbance at 440 nm. Traces were normalised to the DDM micelle peak to allow comparison of the two traces.

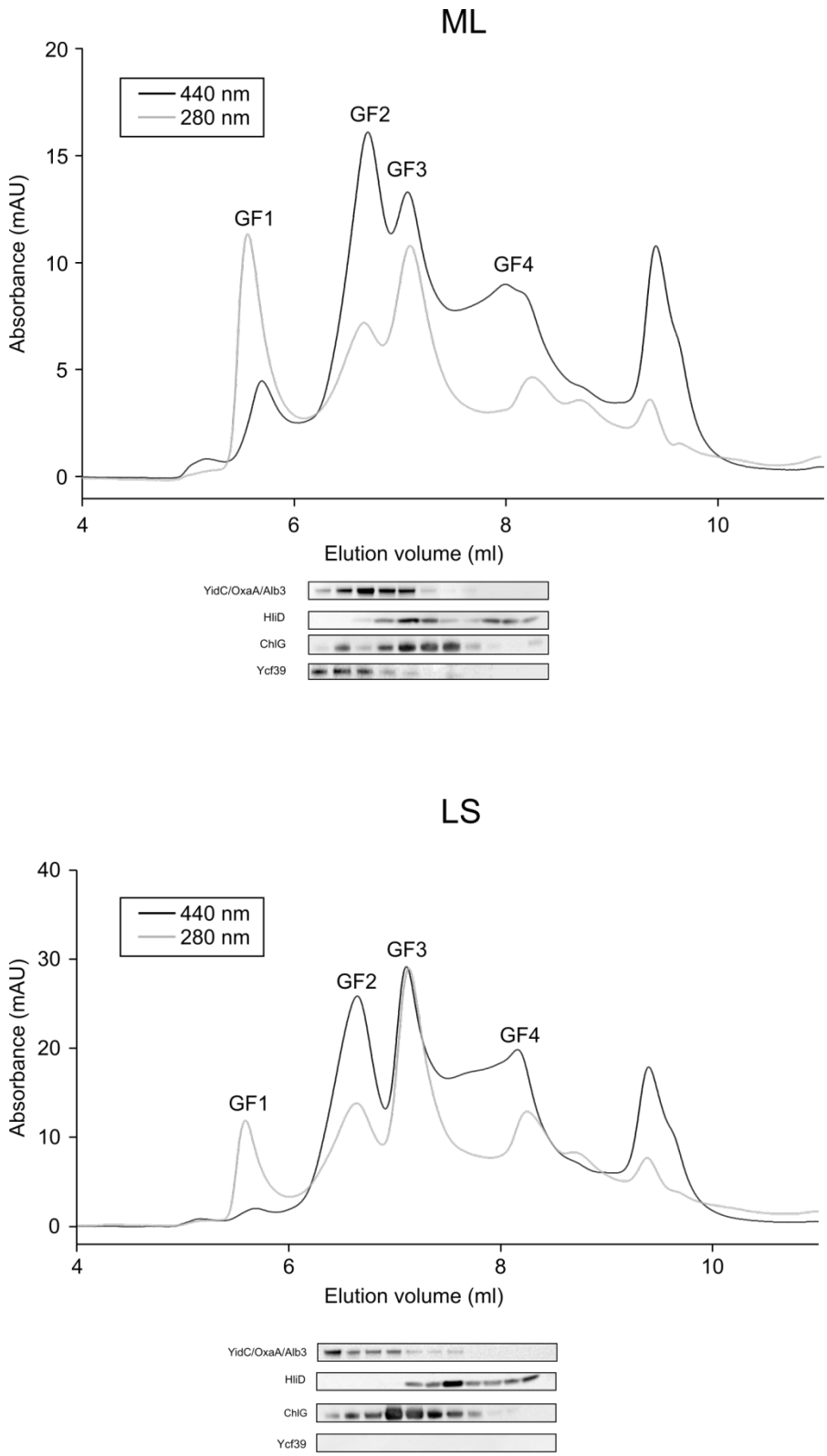

Figure 4. Size exclusion chromatography of the ML and LS FLAG-CS eluates. ML and LS eluates were loaded on a BioSep 3000 column and eluted protein complexes were monitored by absorbance at 440 nm and 280 nm. Collected fractions were run on SDS-PAGE and subjected to immunoblot; each band represents the 0.2 ml fraction with which it is aligned in the accompanying trace.

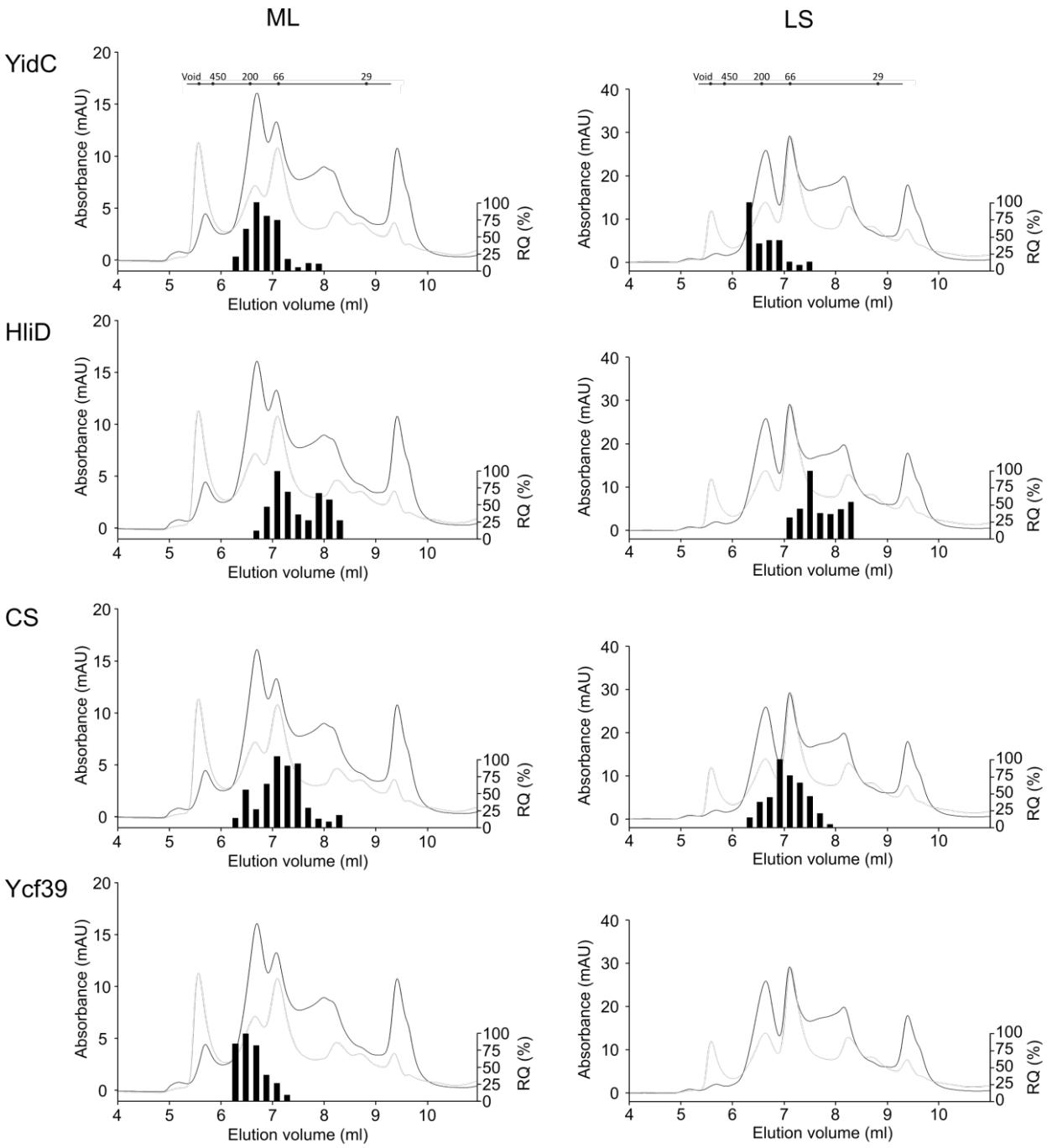

Figure 5. Relative distribution of the components of the ML and LS FLAG-CS eluates during size exclusion chromatography. Immunoblot bands from Figure 4 were analysed yielding relative quantification values, these values are expressed in histogram form as a percentage of the highest value in that blot (i.e. the highest immunoblot signal is expressed as 100 %). Each bar represents the 0.2 ml fraction with which it is aligned. RQ – relative quantity.

4.3.4. Analysis of the distribution of CS and its interaction partners in WT membranes before and after light shock.

In order to investigate the effects of light shock on the distribution of CS and its interaction partners without the bias of a pull-down assay, the light shock experiment was repeated using WT *Synechocystis* cells. These cells were broken and the solubilised membrane fraction was run on CN-PAGE (Figure 6). The results show that the light shock treatment has had a profound effect of the various light harvesting components of the *Synechocystis* thylakoid membrane. The levels of PSI trimer (PSI[3]) are heavily reduced after light shock treatment, as are PSII dimers (PSII[2]). In place of the previously well defined PSI and PSII monomer bands (PSI[1] and PSII[1]) in the ML sample is an indistinguishable green smear in the LS. The CN lanes representing the ML and LS samples were excised from the gel and run on a 12-20 % polyacrylamide denaturing gel. The resulting second dimension gels were analysed by Coomassie staining and immunoblot.

The immunoblots reveal that under moderate light conditions CS is associated with Ycf39 in relatively low molecular weight complexes similar to those described in Chapter 3: Figure 8B (Figure 6; ML, dotted lines) with a very small CS signal situated at a higher molecular weight (Figure 6; ML, black arrow). After light shock treatment it appears that whilst a small proportion of CS remains in a similar complex (with Ycf39 just detectable) the majority has shifted to higher molecular weight complexes in which no Ycf39 is detectable (Figure 6; LS, dotted lines). The YidC signals indicate that it is plausible that YidC is involved in any of the complexes described above, however because YidC is a highly abundant membrane protein the signal obtained is very high making it impossible to determine whether or not this is truly the case. The light shock treatment does seem to have an impact on the distribution of YidC throughout the membranes although whether or not that is in part due to an interaction with CS is unclear. The membrane was probed with the anti-HliD antibody but no specific signals were observed.

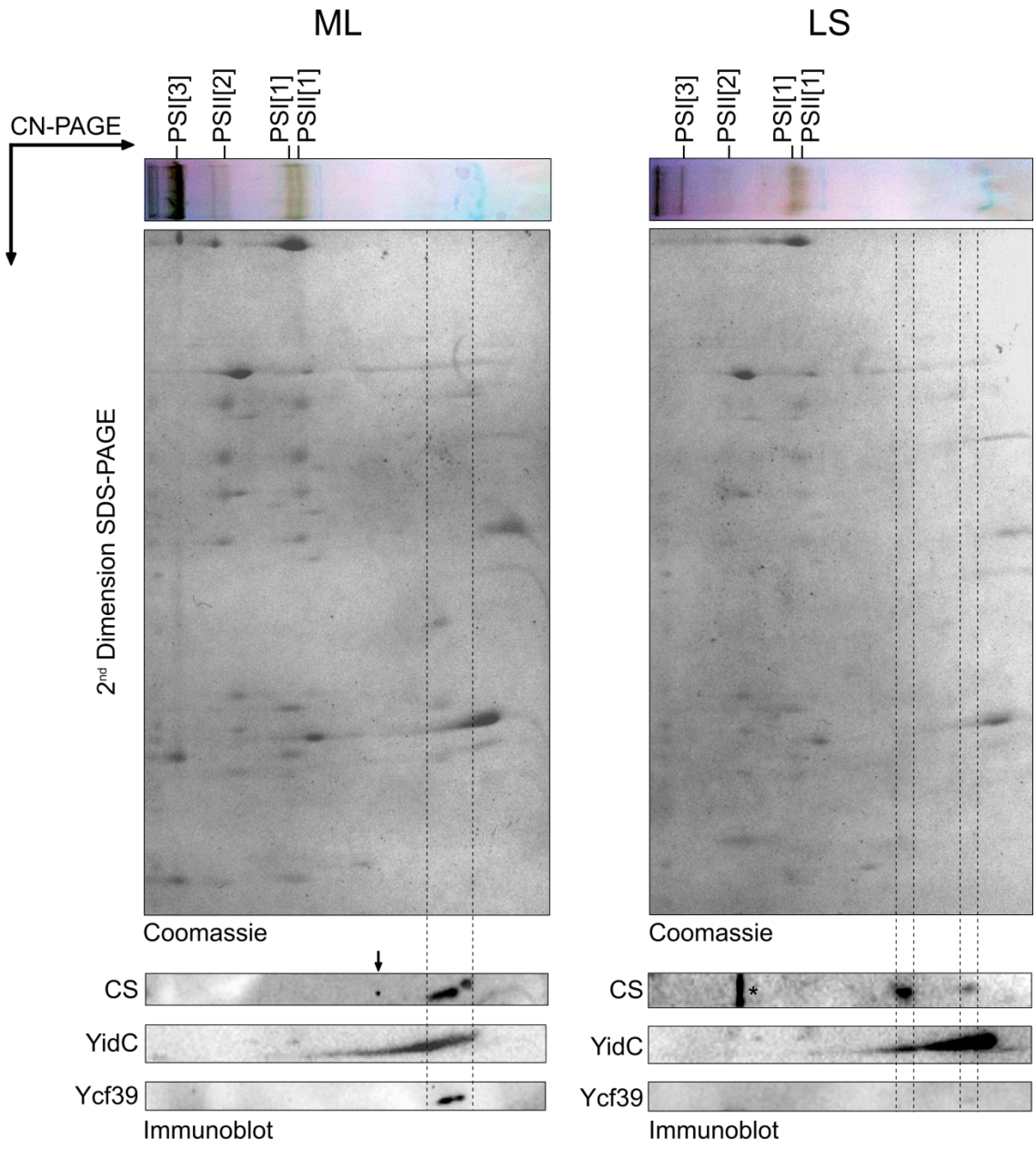

Figure 6. Two dimensional gel electrophoresis of WT membranes before and after light shock. Membranes were run in the first dimension on a clear native gel. The first dimensions were excised from the initial gel and run on a 12-20 % denaturing gel. Two gels were run in parallel, with one being stained using Coomassie brilliant blue and the other transferred to nitrocellulose membrane and interrogated with antibodies. Asterisk indicates a non-specific signal. The arrow is discussed in Section 4.3.4.

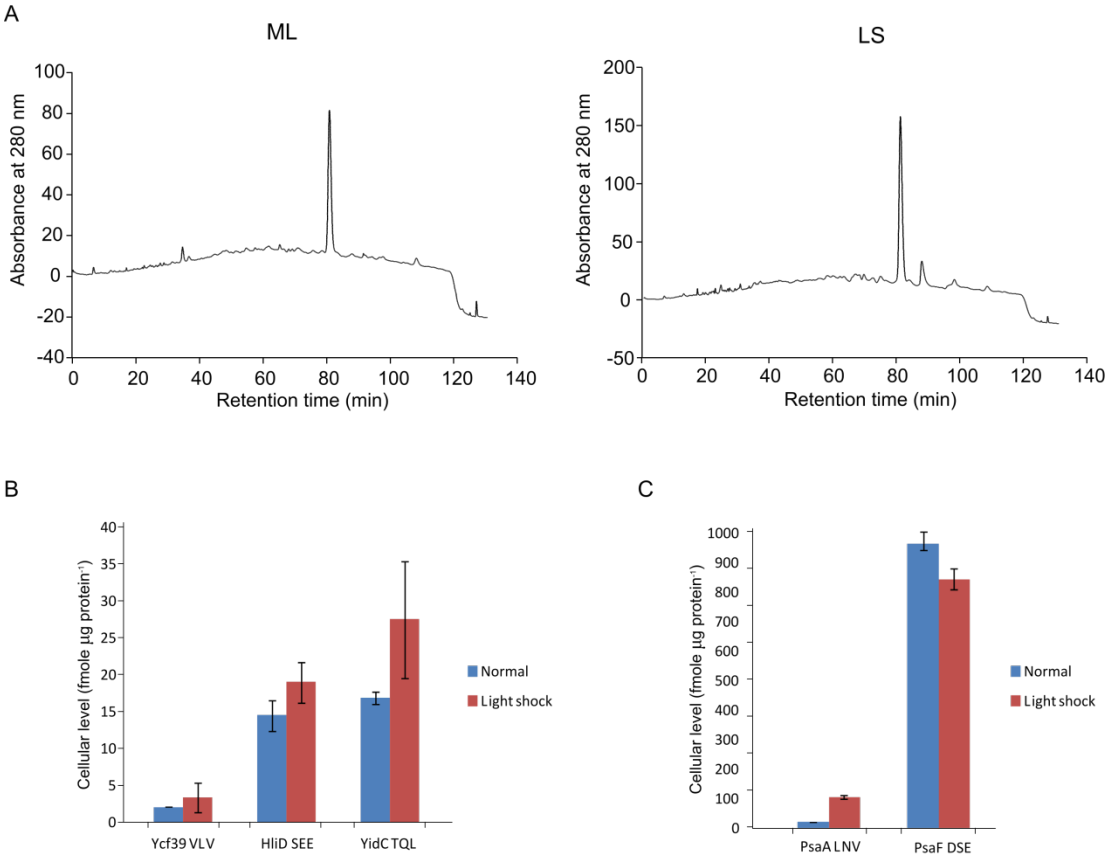

Figure 7. Quantification of CS interaction partners in WT membranes before and after light shock by mass spectrometry. A. Whole cell lysate was solublised, treated with trypsin and separated on a 'hypercarb' porous graphitic column. Fractions from these chromatography runs were collected and analysed by mass spectrometry. Peptide amounts were compared against ^{15}N standards added to the samples prior to digestion and quantities of each peptide were calculated in fmole µg protein^{-1}. **B**. Quantities of CS interaction partners before and after light shock. Letters after protein names are the first three letters of the representative tryptic peptide used for calculations which are the same as those described in Section 3; Figure 4. **C.** Quantities of PsaA and PsaF peptides before and after light shock. Representative peptides were: PsaA – LNVAPAIQPR, PsaF – DSEIPTSPR.

4.3.5. Quantification of CS interaction partners in WT membranes before and after light shock by mass spectrometry

In order to investigate the effect of light shock on the cellular abundance of CS interaction partners a portion of the cells discussed in Section 4.3.1. was disrupted and solublised. The whole cell lysates were 'spiked' with a known amount of ^{15}N-labelled QconCAT polypeptide containing representative tryptic peptides from CS, HliD, Ycf39 and YidC as well as the PSI subunits PsaA and PsaF. This mixture was then subjected to tryptic digest and run by HPLC using a 'hypercarb' porous graphitic column. The fractions collected during HPLC were analysed by mass spectroscopy yielding intensities for representative peptides, these intensities were compared with the intensities obtained for the ^{15}N labelled peptides yielding quantitative values for each of the peptides (Figure 7).

The results show that whilst all of the protein quantities appear to change slightly between moderate light and light shock, the only statistically significant change observed is an increase in the levels of the PsaA protein which is elevated roughly 5-fold after light shock treatment. Neither of the peptides which represent CS was observed meaning that no values could be obtained for CS.

4.4. Discussion

Synechocystis cells must adapt to varying light conditions based on environmental factors. In this chapter early log phase cells under moderate light conditions (40 photon m^{-2} s^{-1}) were irradiated with very high light conditions (800 photon m^{-2} s^{-1}) with the intention of taking cells from a state where they are rapidly dividing and therefore thylakoid biogenesis levels are high to a state where the absolute focus of the cells is photoprotection and repair of damaged light-harvesting apparatus. The impact of this treatment on CS and its interaction partners was investigated.

The high light treatment undoubtedly had an effect on the cells; the absorbance and fluorescence spectra altered (Figure 1) as did the thylakoid profile when analysed by CN-PAGE (Figure 6) indicating large scale changes to thylakoid components which is in agreement with previous similar studies in cyanobacteria and plants (Herbstová *et al*., 2012; Kopečná *et al*., 2012). In order to specifically analyse the effects of high light

shock on CS and its interaction partners, FLAG-CS pull-downs were carried out from FGΔG cells before and after light shock treatment. The results indicate that HliD and YidC maintain their interactions with CS under light shock conditions, whereas the CS-Ycf39 interaction is almost completely abolished with the protein no longer visible by SDS-PAGE or by immunoblot and with only a small amount detected by mass spectrometry.

Further investigation of the pre- and post-light shock FLAG-CS eluates by size exclusion chromatography indicated that the remaining FLAG-CS eluate components YidC and HliD, as well as CS itself are differently distributed during the chromatography in the ML and LS samples implying that the components have formed different complexes after light shock.

A similar experiment was carried out on WT cells, a portion of which was broken and the membrane fraction was analysed by 2D-gel electrophoresis. Immunoblot of the resulting gels indicated that under moderate light conditions CS and Ycf39 formed a complex similar to that observed in Chapter 3 which, under light shock, is down regulated. Whilst the amount of CS in this complex diminished after light shock a large signal was observed in higher molecular weight complexes after light shock where there was previously a very small signal. Quantitative mass spectrometry was carried out on the ML and LS membrane preparations using ^{15}N labelled peptides as standards to observe changes in the levels of CS and its interaction partners. The results show that there are no significant changes in the levels of Ycf39, HliD and YidC after light shock, although the levels of PSI chlorophyll binding protein PsaA increase 5 fold.

4.4.1. Interaction of CS with YidC and HliD is not dependent on the presence of Ycf39

In the previous chapter it was found that CS formed a complex with HliD, which is associated with YidC and Ycf39. However questions remain as to the exact nature of the complex. The data presented here indicate an interaction of CS with HliD and YidC in the absence of Ycf39, demonstrating that Ycf39 is not required for the formation of CS-YidC complexes. This could explain why no YidC was observed in the FLAG-Ycf39

pulldown eluate (Section 3.3.5.) and means that if there is interaction of Ycf39 with YidC it could be mediated by CS-HliD.

4.4.2. Light shock causes a rearrangement of CS containing complexes

In addition to the loss of Ycf39 from CS containing complexes under light shock it appears that the components that remain after light shock are rearranged into different complexes to those observed in the pre-light shock sample. The distribution of all three remaining proteins after light shock during size exclusion chromatography is altered (Figure 5). The rearrangement of CS into larger complexes under light shock is particularly pronounced in the 2D gel immunoblot (Figure 6) which demonstrates that the majority of the protein is associated with a higher molecular weight complex whilst a small amount is observable in the 'original' position. It is tempting to speculate that these two different CS complexes carry out different functions e.g. the lower molecular weight complex with Ycf39 which is observed under moderate light conditions is involved with thylakoid biogenesis, whilst the higher molecular weight complex which dominates during light-induced stress is involved with delivery of recycled Chl to light harvesting proteins during repair. Further research would be required to confirm this.

Whilst Ycf39 is no longer in complexes with CS, the mass spectrometry data obtained in this chapter indicates that the light shock does not change the levels of Ycf39 in the membrane fraction significantly. This indicates that Ycf39 may still have a role to play under extreme light conditions, which agrees with Knoppová and coworkers (2014) who implicate Ycf39 in a role with Chl recycling. It is also interesting to note that cellular levels of HliD do not appear to increase notably between ML and LS, further reinforcing the notion that its role is likely to be more as a constitutively expressed pigment binding protein than a 'high light induced' protein. The levels of the PsaA subunit of PSI are increased five-fold under light shock conditions but remain much lower than those of the PsaF subunit. Whilst this result is potentially interesting it is outside of the scope of the current chapter. The QconCAT polypeptide utilised in this work was designed primarily for a large scale proteomics project hence the inclusion of PSI.

4.4.3. Future work

Although the results obtained from the experiments carried out in a WT background agree with the findings obtained from the FGΔG strain, the fact remains that the CS produced by the FGΔG strain is done so under the influence of the *psbAII* promoter rather than the native *chlG* promoter. There is evidence that the *psbAII* promoter is unaffected by varying light intensity (Kulkarni and Golden, 1997), however, if it were possible to repeat the experiments carried out using a FLAG-CS *Synechocystis* strain in which the CS was produced under the influence of the native promoter this would improve the experiment. Attempts were made to create such a strain throughout the course of the project, but segregation of the genetic construct proved impossible.

In plants and algae photosystem assembly and repair occur in different locations within the thylakoid membrane (Aro *et al*., 1993; Uniacke and Zerges, 2007). It would be interesting to see if the two different CS complexes observed in Figure 6 were differently distributed throughout the thylakoids; this may offer further insight into the roles of CS in thylakoid biogenesis and repair. This could be achieved using imaging techniques such as super-resolution fluorescence microscopy in conjunction with labelled CS using either dye labelled specific antibody or a CS-fluorophore fusion protein. Alternatively CS could potentially mapped within the thylakoids using atomic force microscopy in conjunction with specific antibodies attached to the atomic force microscope probe in a process known as affinity mapping (Johnson *et al*., 2014).

Initially when these experiments were designed it was hoped that FLAG-CS purified after light shock might have novel interaction partners, particularly the ever-enigmatic chlorophyllase which is present in plants and algae but for which no homologue or prospective candidate has been identified in *Synechocystis* (Vavilin and Vermaas, 2007). Chl recycling is an essential part of photosystem repair, and therefore mechanisms for the controlled degradation of Chlide must be removing the tail from Chlide. Now that a successful CS assay protocol has been developed (Chapter 5) it should be tested whether or not CS is capable of catalyzing the reverse reaction in the presence of excess Chl levels.

Chapter 5: Chlorophyll synthase assays: substrate production, experimental design and preliminary characterisation of purified chlorophyll synthase

5.1. Summary

A *Rba. sphaeroides* strain was created that accumulates the Chl precursor Chlide, to provide the porphyrin substrate for characterisation of chlorophyll synthase. Large-scale culture of this strain yielded sufficient quantities of Chlide to perform CS assays using FLAG-purified CS and commercially available GGPP. The assays performed demonstrated a pre-steady state 'burst phase' followed by a steady state phase. Further analysis of this steady state phase yielded K_m values of 25.7 μM ± 19.2 and 66.8 ± 33.1 μM for Chlide and GGPP respectively.

5.2. Introduction

CS catalyses the terminal step of Chl biosynthesis, the addition of the tetraprenyl (phytyl or geranylgeranyl) tail to Chlide (Figure 1). The enzyme is discussed at length in section 1.3.11.

The activity of CS was first discovered in the etioplast membranes of oat (*Avena sativa*) (Rüdiger *et al*., 1980) and multiple subsequent studies have been carried out on the this enzyme (Benz *et al*., 1980; Schoch *et al*., 1980; Helfrich and Rüdiger, 1992) as well as on recombinant CS from Oat, *Rba. sphaeroides* and *Synechocystis* (Oster *et al*., 1997; Schmid *et al*., 2001, 2002; Kim and Lee, 2010). These studies show that the CS reaction proceeds via a ping-pong mechanism in which the tail molecule (GGPP or PPP) binds the enzyme first followed by Chlide and that CS in inhibited by bacteriochlorophyllide the bacterial Bchl precursor.

Previous studies have been carried out on either thylakoid membrane fractions or *E. coli* lysate containing recombinant CS protein (Rüdiger *et al*., 1980; Soll *et al*., 1983; Oster and Rüdiger, 1997; Oster *et al*., 1997). Given that CS appears to have an important role in thylakoid biogenesis (Chapter 3) and that it appears to be involved in feedback control of the entire Chl biosynthesis pathway including synthesis of Chl binding proteins (Shalygo *et al*., 2009), further kinetic studies of the enzyme using purified material could yield valuable information about the wider role of the enzyme.

5.3. Results

Previous studies (Oster and Rüdiger, 1997; Oster *et al*., 1997; Kim and Lee, 2010) have demonstrated the requirement of three components for successful CS assays: enzyme, Chlide and activated tetraprenyl tail; either phytyl pyrophosphate or geranylgeranyl pyrophosphate (GGPP). Of these, the former can be purified from *Synechocystis* as described in Chapter 1 and GGPP is available commercially (Sigma-Aldrich). The third component, Chlide, is not commercially available. Thus, a reliable source of Chlide is required to allow assays to be carried out.

5.3.1. Construction of a Chlorophyllide-producing *Rba. sphaeroides* mutant

Purple bacteria with interrupted Bchl biosynthesis pathways are known to excrete Bchl biosynthesis intermediates into their growth medium. Therefore, a mutant in which Bchl biosynthesis was arrested at a point where Chlide were accumulated would provide a source of Chlide for use in assays.

Bchl *a* biosynthesis proceeds via the same intermediates as Chl biosynthesis up to Chlide, at which point Bchl specific modifications are made to the molecule prior to the addition of the tail moiety (Figure 2) (see section 1.3.12. for further discussion of (B)Chl biosynthesis). A mutant in which the genes encoding the enzymes responsible for the Bchl-specific modifications are deleted should accumulate Chlide, which could then be purified for use in assays.

Figure 2A shows the Bchl-specific reactions of Bchl biosynthesis: Chlide is either reduced at the C7=C8 position by COR, a three subunit enzyme encoded by the *bchX*, *bchY* and *bchZ* genes or the C3-vinyl group is hydrated by 3-vinyl bacteriochlorophyll hydratase encoded by the bchF gene. These reactions can occur in either order (Pudek and Richards, 1975). The final Bchl-specific step is the oxidation of the hydroxyl group to an acetyl catalysed by BchF. reaction to an acetyl group. Therefore a *Rba. sphaeroides* mutant in which *bchF* and one of *bchX*, *bchY* and *bchZ* are interrupted should have its Bchl synthesis pathway arrested at a point where it accumulates Chlide.

Figure 2B shows the photosynthetic gene cluster of *Rba. sphaeroides*, a region of the genome which contains the vast majority of all genes related to photosynthesis (Naylor *et al.*, 1999). Within this cluster four of the five genes responsible for the Bchl specific reactions are situated next to each other, *bchCXYZ*, with *bchF* separated by ~23 kb. Thus, a strategy to delete all components would only involve two mutagenesis steps: removal of *bchC* and *bchX* together, followed by deletion of *bchF*.

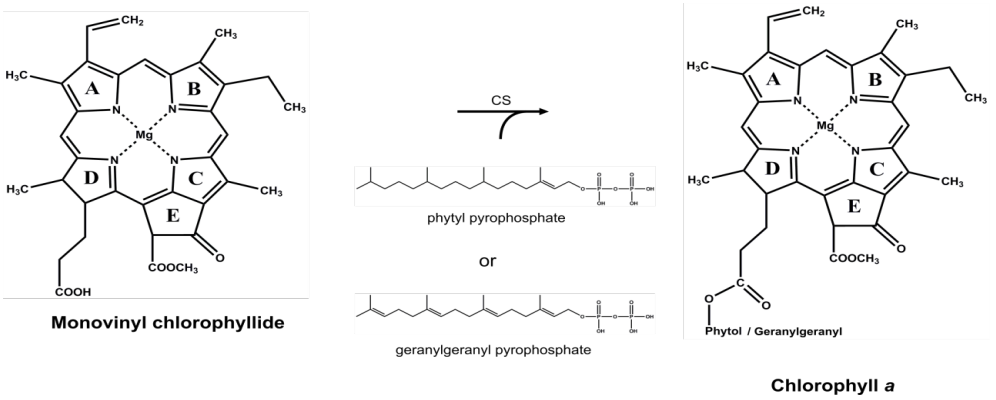

Figure 1. The reaction catalysed by CS.

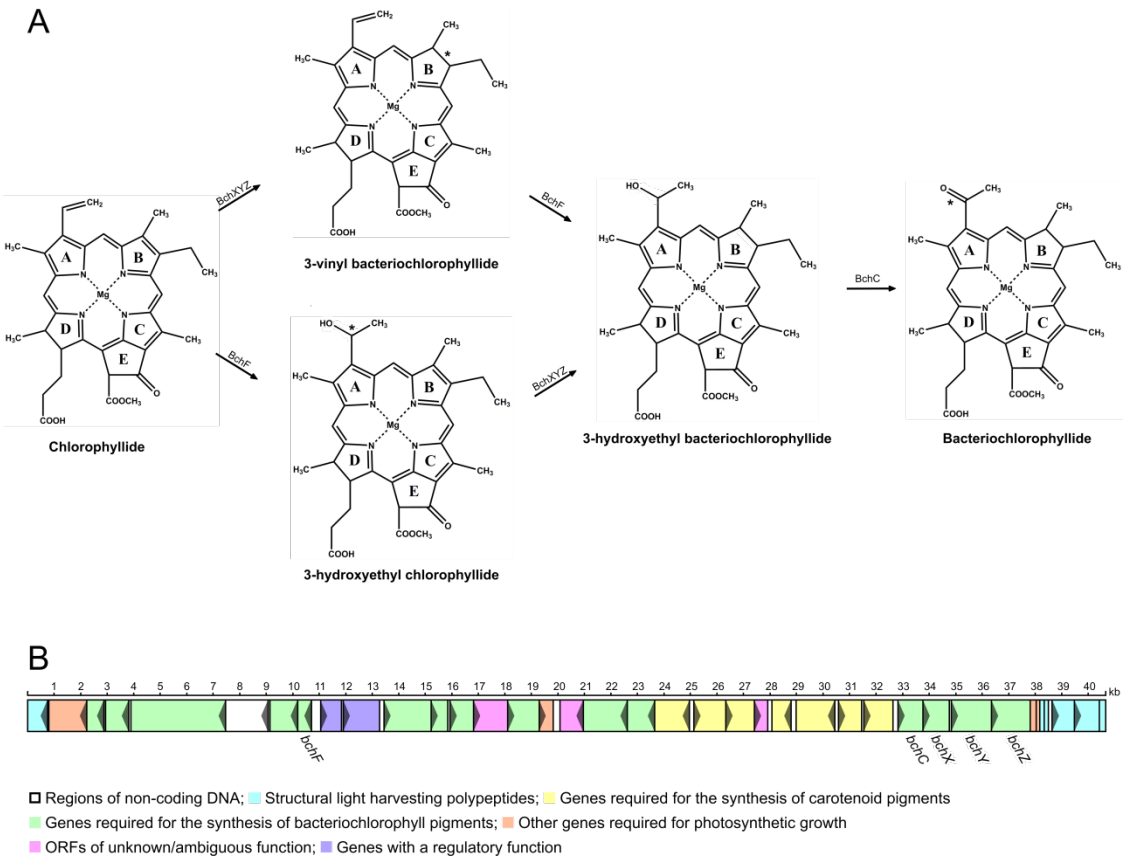

Figure 2. A. The Bchl-specific steps of Bchl biosynthesis. BchF - 3-vinyl bacteriochlorophyll hydratase; BchXYZ - the three subunits of COR; BchC - 3-hydroxyethyl bacteriochlorophyllide dehydrogenase. **B.** The photosynthetic gene cluster of *Rhodobacter sphaeroides*; genes involved with the Bchl-specific steps of Bchl-biosynthesis are annotated.

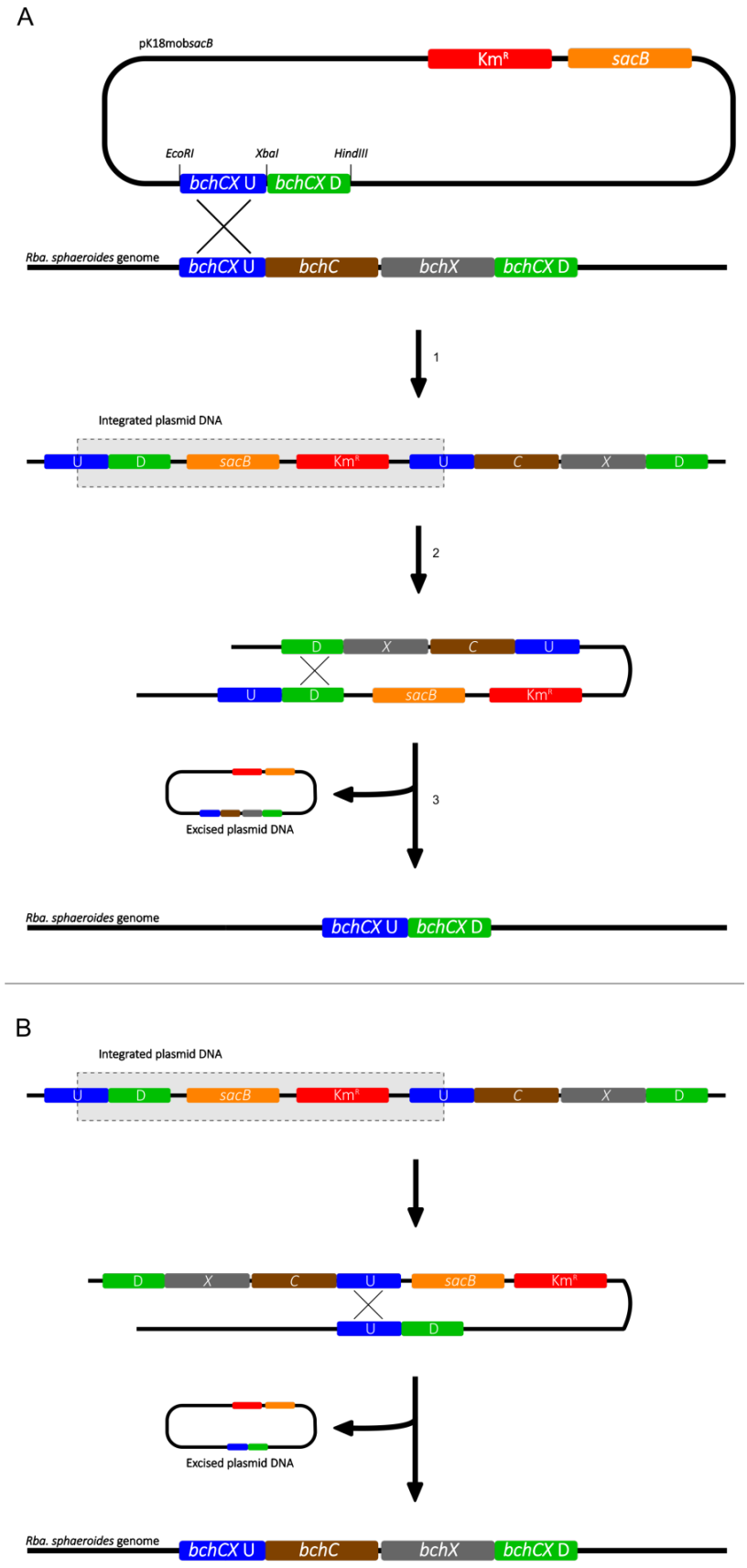

Figure 3. Deletion of bchX and bchC from Rba. sphaeroides using the pK18mobsacB suicide vector.

A. 1. Ligation of Up- (U) and downstream (D) regions of the *bchC* and *bchX* genes into the multiple cloning site of the vector, transformation into S17-1 *E. coli*, transfer to WT *Rba. sphaeroides* and first recombination event induced by kanamycin **2.** Sucrose induced recombination. **3.** Excision of plasmid DNA inculuding deleted genes.

B. Reversion to WT due to the second recombination event occurring at the same location as the first.

C. Agarose gel electrophoresis of successful knock-out strains.

5.3.2. Deletion of *bchC* and *bchX*

Mutagenesis was achieved using the pK18mobsacB suicide vector system. The plasmid contains both an antibiotic resistance cassette and the *sacB* gene, which converts sucrose to toxic fructooligosaccharides, allowing it to be used as a secondary selection marker. The process is outlined in Figure 3.

Regions up- and downstream of the genes to be deleted were cloned from the *Rba. sphaeroides* genome and ligated in to the multiple cloning site of the plasmid. The plasmid was then transformed in to the S17-1 *E. coli* strain which has chromosomally integrated conjugal transfer functions allowing transfer of the vector via bacterial conjugation. The vector was transferred to the WT *Rba. sphaeroides* recipient by overnight incubation with the donor S17-1 strain. Conjugants were cultured in the presence of kanamycin inducing a first homologous recombination event and incorporating the vector into the host genome. Successful conjugants were then cultured in the presence of sucrose (and no kanamycin) promoting a second homologous recombination event to remove the foreign DNA from the host genome. This second recombination can occur at either the same site as the first (the upstream fragment in the schematic shown in Figure 3), reverting the strain back to WT (Figure 3B) or at the other site (the downstream fragment in Figure 3) leading to a Δ*bchC*/Δ*bchX* deletion mutant.

5.3.3. Deletion of *bchF* from the Δ*bchC*/Δ*bchX* mutant

Regions up- and downstream of the *bchF* gene were ligated into the pK18mobsacB vector and the vector was conjugated into the Δ*bchC*/Δ*bchX* strain. Mutagenesis was carried out as described previously generating a Δ*bchC*/Δ*bchX*/Δ*bchF* knock-out mutant (henceforth Δ*CXF*) (Figure 3C).

5.3.4. Preliminary analysis of the Δ*CXF* mutant

The cells of the Δ*CXF* mutant are orange in colour and when pelleted from liquid culture yield a faintly green supernatant (Figure 4) indicating that the mutant has arrested Bchl biosynthesis. HPLC pigment analysis of the whole cells confirmed this and indicated that the main pigments accumulated by the mutant are Chlide and its immediate precursor, Pchlide (Figure 5). The same analysis was also carried out on

the Δ*bchC*/Δ*bchX* strain demonstrating that the majority of Chlide in these cells was further modified to 3-hydroxyethyl chlorophyllide. The absorbance spectrum of the supernatant indicates the presence of pigment (Figure 6; blue line) although neither of the absorption maxima (387 nm and 688 nm) is representative of Chlide, indicating that the Chlide within the cells is unable to escape the cell.

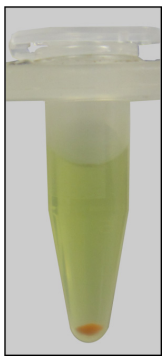

Figure 4. The Δ*CXF* mutant is orange in colour and excretes chlorophyll precursors into the growth medium. Cells were grown in liquid culture, centrifuged and photographed. Photo background has been removed for clarity.

5.3.5. Supplementing the growth medium of the Δ*CXF* mutant with Tween 80

Whilst it would be possible to purify Chlide for assays from whole cells, the yield is unfavourable as the cells make a certain amount of the desired intermediate and then stop. A well established technique for pigment purification from purple bacteria is to supplement the growth medium with Tween 80 which acts as a mild detergent allowing pigment to escape the cell (Lascelles, 1966; Richards and Lascelles, 1969; Müller *et al*., 2011). This release of pigment to the medium allows continuous synthesis of Bchl intermediates within the cell and also acts as a preliminary purification step, as harvesting the cells removes the majority of suspended matter within the culture.

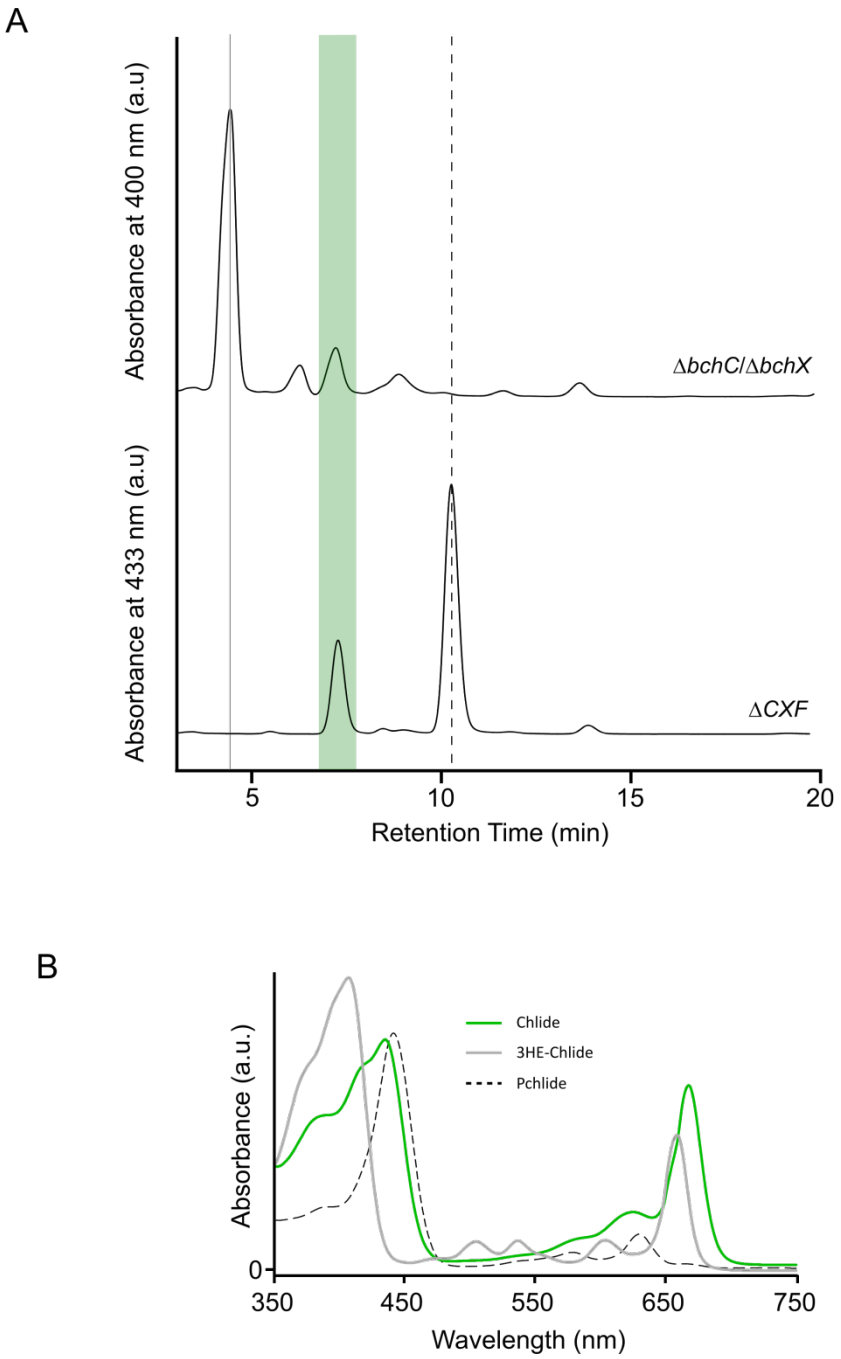

Figure 5. HPLC pigment analysis of the Δ*bchC*/Δ*bchX* and Δ*CXF* strains. **A.** Cell pellets from liquid cultures were treated with methanol and extracted pigments were loaded on to a HPLC system equipped with a C18 reverse phase column. Grey line represents 3-hydroxyethyl chlorophyllide, green area represents Chlide, dotted line represents Pchlide **B.** Absorbance spectra were recorded continuously and the relevant spectra are shown. Line style/colour is equivalent to those in (A). 3HE-Chlide – 3 hydroxyethyl chlorophyllide.

In order to test whether this technique was viable in this instance the Δ*CXF* strain was cultured in four separate flasks containing 0, 0.01%, 0.02% and 0.04% (all w/v) Tween 80, the results are shown in Figure 6. The Tween supplemented supernatants all contained significantly more pigment than the negative control, this was immediately observable using the naked eye; the supernatant went from a dull yellow-green colour to a more vibrant green (Figure 6B). The absorption spectra of the supplemented supernatants show that they contain different pigments compared with the negative control, indicating that the Tween allowed pigments, previously confined within the cell, to diffuse into the medium; furthermore the 'new' maxima observed in the spectra of the Tween supplemented supernatants are indicative of Chlide. Beyond 0.01% (the lowest concentration tested) addition of further Tween seemed to have no positive effect on the quantity of pigment in the supernatant, in fact it appeared to have a slightly negative impact. Thus, supplementing the growth media of the Δ*CXF* culture medium with 0.01% Tween 80 is a viable strategy for the production of Chlide for CS assays.

5.3.6. Investigations into the Chlide : Pchlide ratio in the Δ*CXF* mutant

Although the Δ*CXF* strain clearly accumulates Chlide (Figure 5), it also accumulates the immediate precursor, Pchlide. Reducing the amount of Pchlide synthesised by the mutant could lead to increased yields of Chlide and would also serve to aid purification of Chlide from the supernatant. In order to see if the ratio of Chlide : Pchlide varied over the course of growth e.g. whether there was more Chlide compared with Pchlide at the early stages of growth or vice versa an induction experiment was carried out.

Bchl biosynthesis is repressed in purple photosynthetic bacteria by high oxygen conditions (Niederman *et al*., 1976). Thus if a strain is cultured in minimal liquid volume in baffled flasks, with high agitation it is possible to grow cells that are nearly devoid of pigment. Transfer of these cells to low oxygen conditions (no baffles, full flasks, low agitation) induces Bchl biosynthesis allowing the early stages to be observed in a way that would not be possible if cells were cultured from a small inoculum. The results of the induction experiment are shown in Figure 7 and indicate that during early growth the relative accumulation of Chlide is low when compared

with Pchlide. As cells develop further the Chlide levels increase to ~60% that of Pchlide, with a slight drop-off as cell reach stationary phase (back down to ~50%). This demonstrates that the highest levels of Chlide relative to Pchlide occur during the mid-phase of growth; however, it also shows that the cells have the capacity to secrete more than double the amount of Chlide if the culture is left to develop fully.

These data indicate that whilst harvesting cells after one day would yield a supernatant containing a higher ratio of Chlide to Pchlide, allowing an extra day's growth more than triples the amount of Chlide produced (3.4 to 10.35 AU). Therefore although it perhaps would make purification more difficult owing to increased levels of Pchlide, it was decided that in order to allow for the highest possible yield of Chlide from cultures of Δ*CXF* the cells would be allowed to grow for 48 hours after inoculation into large (1.5 L) cultures.

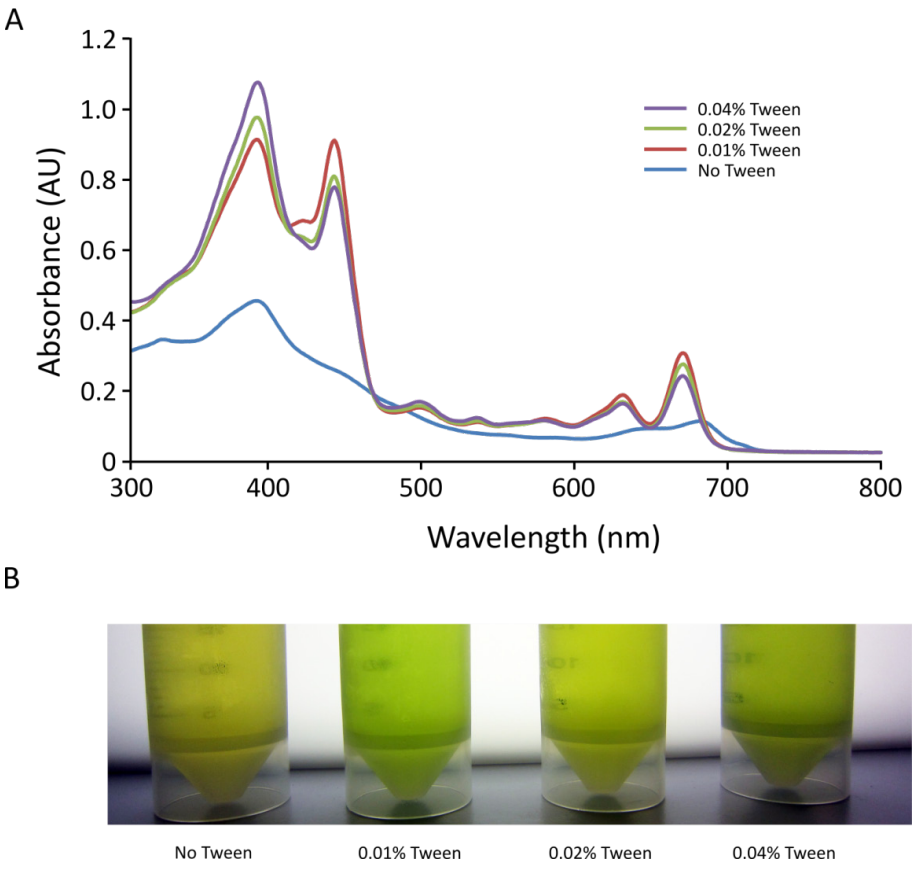

Figure 6. Analysis of the supernatant of Δ*CXF* cultures supplemented with Tween 80. **A.** Cultures were grown in media supplemented with Tween 80, cells were harvested by centrifugation and the supernatant analysed by absorption spectroscopy. **B.** Photograph of the Tween supplemented growth media.

5.3.7. Purification of Chlide from the Δ*CXF* mutant

Solvent extraction of pigments from aqueous growth media is an effective method of purification. Numerous methods were tried on a small scale to see which would prove most suitable when scaled up. The method described in Müller *et al*., (2011) in which diethyl ether and ethanol are added to form a pigment containing hypophase, failed to do so in this case, yielding a mixture of pigment, media and solvent. An alternative method (Kim and Lee, 2010) adds only diethyl ether to the aqueous media. Whilst this did successfully create a pigment-containing hypophase, this phase also contained large quantities of lipid which made further purification by evaporation difficult. A modified version of this extraction was performed in which 2 diethyl ether : 1 acetonitrile was added in a 1 : 1 ratio to the supernatant (i.e. 1.5 supernatant : 1 diethyl ether : 0.5 acetonitrile). This yielded a clear green hypophase in which could be further purified by evaporation using a rotary evaporator followed by a vacuum centrifuge.

Because the pigments purified from the Δ*CXF* supernatant were a mixture of Chlide and Pchlide further purification was required. Dried pigments were dissolved in 80 % Methanol and loaded on to an HPLC system in conjunction with a preperative C18 column. Fractions were collected and the 'Chlide' fraction from multiple runs were pooled and concentrated using a small C18 cartridge, Chlide was eluted and stored in acetone until required. The absorption spectrum of the purified Chlide is shown in Figure 3. For large scale production of Chlide four 1.5 L conical flasks were cultured yielding a total of 3 μmoles of Chlide.

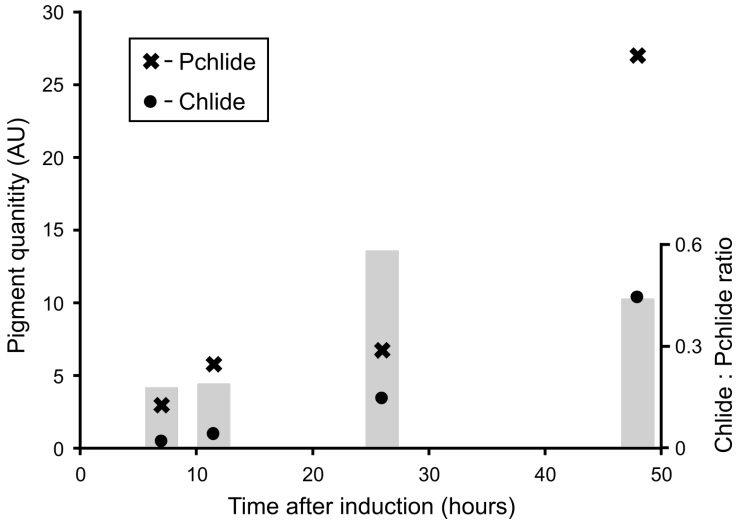

Figure 7. Induction of the Δ*CXF* strain after high oxygen culture. 200 ml of Δ*CXF* cells were cultured in 2 L capacity baffled flasks at 300 rpm; once cells reached an OD of 0.6 they were harvested in a sterile centrifuge container and transferred to a 2 L capacity non-baffled flask containing 1.8 L of growth medium supplemented with 0.01% Tween 80 with agitation at 150 rpm. 1 ml fractions were taken throughout the course of induction, then harvested by centrifugation and the supernatant analysed by reverse phase chromatography. Pigment quantity was monitored using the in-built diode array detector set to monitor the maxima of Pchlide and Chlide (632 nm and 663 nm) respectively. The scatter graph represents the amount of each pigment at each time point; bar chart represents the ratio of Chlide : Pchlide at each time point. Quantities were calculated by intergrating HPLC peaks. The relative quantity of Pchlide was calculated by multiplying the absorbance value obtained for Pchlide by 2.56 (Pchlide extinction coefficient – 30.1 mM^{-1} cm^{-1}; Chlide extinction coefficient – 77.1 mM^{-1} cm^{-1}; 77.1 / 30.1 = 2.56).

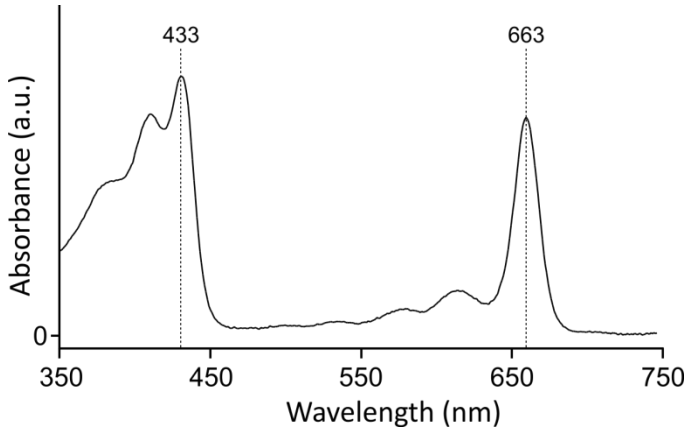

Figure 8. The absorption spectra of Chlide (in acetone) purified from the Δ*CFX* strain.

5.3.8. Development of a CS assay

Having successfully purified Chlide (see above) and CS (Section 3.4.), and with GGPP readily available commercially, it was necessary to develop an assay protocol to allow characterisation of CS. Basic assays have been carried out with FLAG-purified CS material in Section 3.3.9., but these were only used to demonstrate the activity of the enzyme and as such were not optimised for kinetic analyses. In these earlier assays, GGPP was added to FLAG-column eluate and the Chlide pool present within the eluate was esterified; further assays were carried out in which exogenous Chlide was added and shown to be utilised by the CS present in the eluate. In order to allow the relatively high throughput assay system that would be required to allow characterisation of CS to be designed some preliminary experiments were required.

5.3.9. Determination of optimum protein concentration for CS assays

Because Chlide and Chl share identical spectral properties (the function of the tail moiety being structural rather than optical) simple continuous assay systems that monitor UV-VIS absorbace or fluorescence are not possible. As such, a stopped HPLC based assay was developed. In order to optimise the number of assays that can be conducted on a given enzyme preparation it is important to know how much of the CS protein eluate was required in order to allow observable turnover. In order to test this, a set of assays were carried out at fixed GGPP and Chlide concentrations (10 µM each) for a fixed time (2 minutes) in which the protein quantity used was varied. Protein was diluted to the appropriate concentration using FLAG-buffer to yield a final volume of 30 µl per assay. Assays were quenched after 2 minutes using excess methanol (60 µl) and analysed by HPLC reverse phase chromatography (Figure 9).

The results show that the lowest quantity of protein trialed (0.15 µM; which equates to 1 µl of FLAG-CS eluate) was appropriate to allow easily observable amounts of evolved Chl_{GG}. Thus, because a FLAG-CS preparation from 4 L of *Synechocystis* cells yields ~300 µl of eluate, one preparation would be enough for ~300 assays.

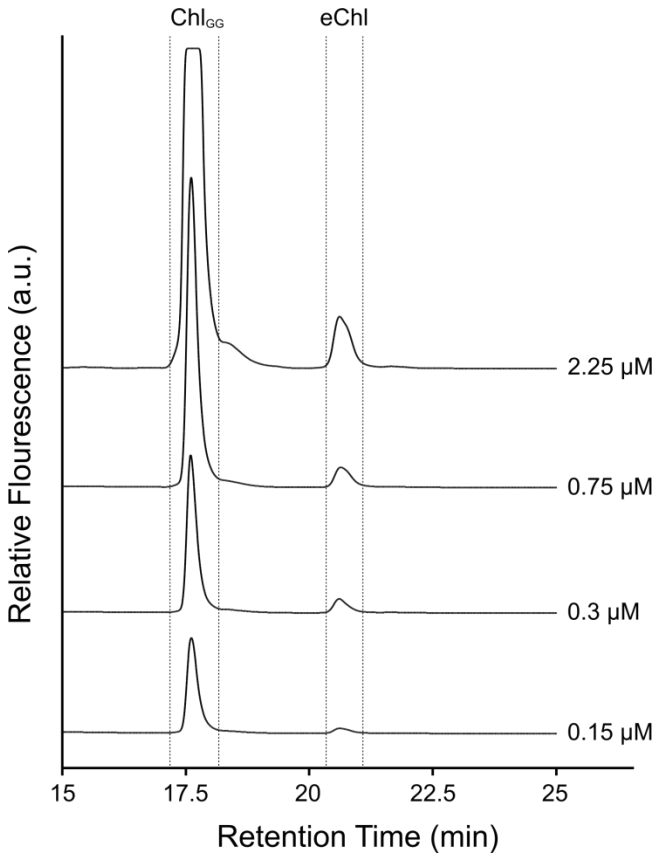

Figure 9. Variation of enzyme quantity. Reverse phase HPLC traces of assays carried out with various CS concentrations. Each trace represents a stopped assay annotated with the protein concentration used. eChl – endogenous Chl.

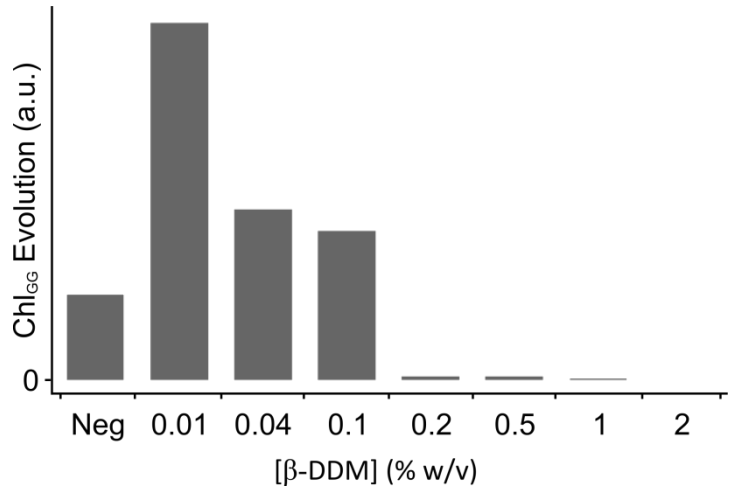

Figure 10. The effect of β-DDM variation on CS activity. Assays were carried out in FLAG buffer in the presence of 10 µM GGPP and Chlide. Neg – Negligible: no additional β-DDM was added to the assay mix, meaning that the only detergent present was from the 1 µl of CS eluate added. The concentration was therefore 0.0013% (0.04 / 30). Bars have been raised slightly from the x-axis to allow small values to be more easily observed.

5.3.10 Determination of optimum detergent concentration for the enzyme assay

Previous assays were carried out in the FLAG-purification buffer, which after solubilisation of the membrane fraction contains 0.04% β-DDM (w/v) in order to maintain the critical micelle concentration. Whilst the assays worked adequately, it was observed in another experiment that high levels of detergent compromised enzyme activity of CS (data not shown). Therefore in order to ascertain how much detergent should be present in the reactions to allow optimum activity, an experiment was carried out in which β-DDM levels were varied and Chl_{GG} evolution was observed (Figure 10).

The results show that, as would be expected, a small amount of detergent is required probably to allow efficient delivery of substrate to the active site of the enzyme, as well as to maintain CS (a membrane protein) in its optimum configuration. However, beyond this low concentration (0.01%) further detergent proves detrimental to the reaction with anything beyond 0.1% reducing Chl_{GG} evolution to negligible values. Thus, all assays were performed using 0.15 µM CS and 0.01% β-DDM.

5.3.11. Preliminary characterisation of CS

A preliminary characterisation of purified CS involved two sets of assays, one in which the GGPP concentration was varied with fixed Chlide concentrations and the other vice versa. Each assay set consisted of five substrate concentrations (6.25, 12.5, 25, 50 and 100 µM GGPP; 2.5, 5, 10, 20 and 40 µM Chlide) at five time points (15, 30, 60, 90 and 120 seconds). The enzyme concentration was kept at a constant 0.15 µM. Assays were performed in buffer conditions at pH 7.4 and 30 °C; each data point was repeated in triplicate for a total of 75 assays per dataset. Assays were set up in 96 well plates with total volumes of 30 µl, and started (by addition of enzyme) and quenched (using 60 µl methanol). Each assay was analysed by HPLC reverse phase chromatography and results were obtained using the detector which was set to monitor fluorescence continuously (excitation 440 nm, emission 670). Peaks representing the evolved Chl_{GG} and the endogenous Chl which is present in the FLAG-CS eluate (Figure 9; eChl) were integrated using Agilent Chemstation software to give relative quantities of each. Each Chl_{GG} value was divided by its respective eChl value,

which acts as an internal standard allowing direct comparison of all results. Two sample assays are shown in Figure 11.

Looking at the raw data it appears that the reaction consists of a rapid initial phase (0 – 15 seconds) followed by a steady state phase (although only two examples are shown, all assays displayed this characteristic). The early 'burst phase' is too rapid to be effectively characterised using these data. However, the subsequent steady state phase is a good candidate for further analysis.

The steady state rates of the enzyme were plotted as a function of v_{ss} and non-linear regression performed where the data were fitted to the Michelis-Menten equation (Figure 12). The resultant data imply that the enzyme obeys hyperbolic Michaelis-Menten kinetics and yielded K_m values of 25.7 µM ± 19.2 and 66.8 ± 33.1 µM for Chlide and GGPP respectively.

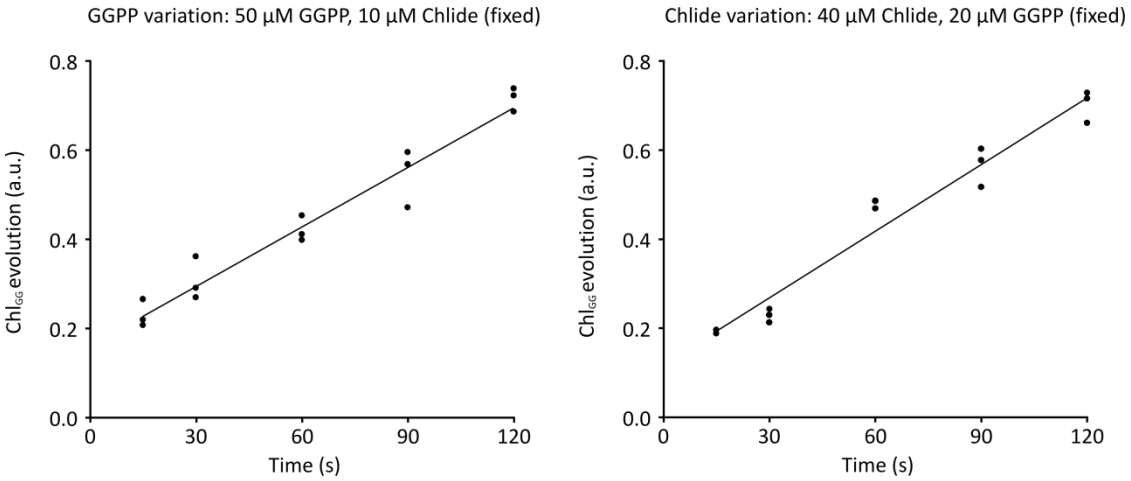

Figure 11. Sample assays from the each of the two sets of CS assays carried out. Each point represents one replicate of three. Lines are theoretical and described by the straight line equation to provide v_{ss}.

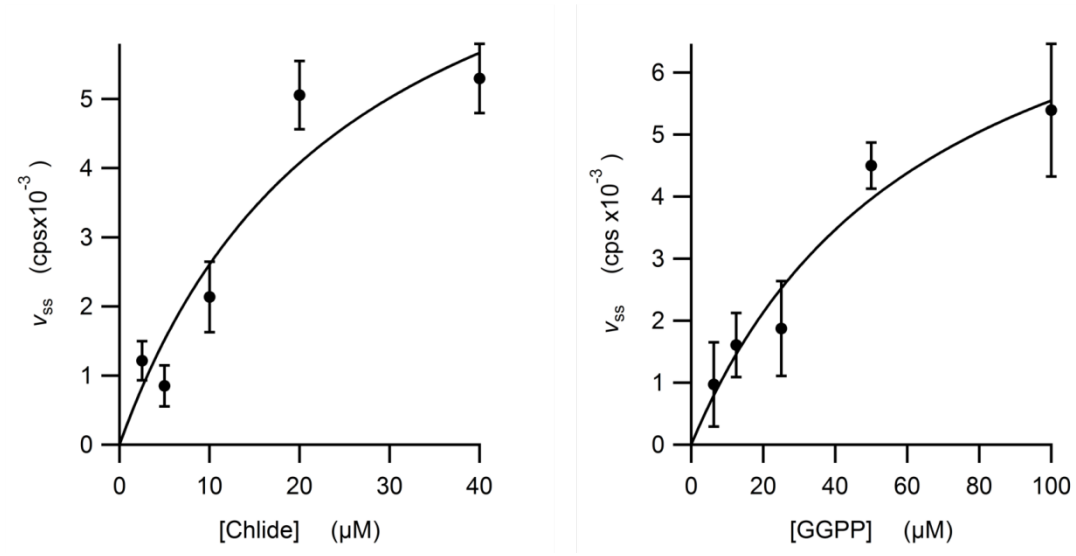

Figure 12. Secondary plots of steady state rates against substrate concentration for Chlide (left) and GGPP (Right). Steady state rates were plotted against substrate concentration to which the Michaelis-Menten model was applied.

5.4. Discussion

Multiple previous studies into CS have been carried out using a variety of systems: Oat (Rüdiger *et al*., 1980); spinach (Soll *et al*., 1983); recombinant protein heterologously expressed in *E. coli* from *Arabidopsis* (Oster and Rüdiger, 1997), *Synechocystis* and the bacterial counterpart bacteriochlorophyll synthase from *Rhodobacter capsulatus* (Oster *et al*., 1997; Addlesee and Hunter, 1999). However, all of these studies have been carried out on membrane fractions or bacterial lysate. The assays presented in this chapter are the first to be carried out on purified enzyme material, which is known to contain only a few interaction partners (Section 3.3.3.). In addition, expression of the enzyme was performed in the native host organism.

The assay data presented above imply an initial pre-steady state 'burst phase' which in this case happens in the first 15 seconds. This is consistent with the *in vivo* findings of Domanskii *et al* (2003) which demonstrate an initial rapid phase of Chlide esterification after flashing etiolated barley and oat leaves with light. Schmid *et al* (2002) report a pre-steady state burst phase, but only after preincubation of the enzyme with the GG/phytol tail moiety; in experiments where the enzyme was preincubated with Chlide or neither substrate, the burst phase was not observed. The

authors present this as part of their evidence that the reaction proceeds via a ping-pong mechanism whereby the tail binds the enzyme first, followed by Chlide. The assays presented in this chapter were initiated by addition of enzyme to an otherwise fully prepared mix, meaning that no preincubation took place, but nonetheless it displays the burst phase. It is proposed that the burst phase in this case is not dependent on preincubation with the 'first' substrate due to the fact that the enzyme preparation is much purer than that used by previous studies; allowing binding of the substrates to take place at an increased rate and therefore an almost immediate turnover. Carrying out further assays in which the enzyme concentration is greatly reduced could increase overall burst phase time, and allow further kinetic analysis.

Schmid *et al.* (2002) also observed substrate inhibition at Chlide concentrations higher than 10 µM. This was not found to be the case in the preset study, as assays were carried out at 40 µM Chlide and showed no sign of inhibition.

Previous kinetic studies (Schmid *et al*., 2002; Kim and Lee, 2010) have used linear regression, in the form of Lineweaver-Burk plots as their rate analysis tool. Whilst both studies yielded highly interesting results, this type of analysis, in which nonlinear data are transformed in order to yield a straight line to be analysed by linear regression is dated and was designed to allow 'pencil and paper' analysis of kinetic data before computers became a ubiquitous commodity. Problems arise with this system because experimental error is distorted during the transformation which can lead to misleading results when values are interpreted from the data (Greco and Hakala, 1979). Kinetic analyses of the steady state rates presented in this chapter are carried out using the Michaelis-Menten equation of nonlinear regression yielding K_m values of 25.7 µM ± 19.2 for Chlide and 66.8 ± 33.1 µM for GGPP.

There are no values in the literature to date of the K_m for GGPP making this the first reported value. The only previously published K_m value for Chlide (with GGPP as the second substrate) is 100 µM (Kim and Lee, 2010) which is fourfold the value presented in this chapter. Other enzymes of the pathway have the following K_m values for their respective porphyrins: *Synechocystis* LPOR 1.36 ± 0.34 µM for monovinyl Pchlide and 0.83 ± 0.24 µM for divinyl Pchlide (Heyes *et al*., 2006); wheat MT 36 µM for MgProto (Ellsworth and Dullaghan, 1972); MgCH H-subunit 1.22 ± 0.42

µM for deuteroporphyrin (Karger *et al*., 2001) These values are summarised in Table 1.

Enzyme	Substrate	Organism	K_m	Source
CS	Chlide	*Synechocystis*	25.7	This study
CS	Chlide	*Synechocystis*	100	Kim and Lee (2010)
LPOR	Monovinyl Pchlide	*Synechocystis*	1.36	Heyes *et al*. (2006)
MT	MgProto	Wheat	36	Ellsworth and Dullaghan (1972)
MgCH H-subunit	Deutroporphyrin	*Synechocystis*	1.22	Karger *et al*. (2001)

Table 1. K_m values of Chl biosynthesis enzymes. K_m values are in µM

5.4.1. Future work

Whilst the results presented here are a promising start, in order to carry out a full characterisation of CS, further experiments are required. As mentioned earlier, greatly reducing the amount of enzyme used per assay would potentially slow down the pre-steady state phase observed allowing it to be studied further. Extending the range of the data (i.e. more concentrations and time-points) would allow for more accurate fitting of models and should reduce the high error observed in the *K*m values obtained. The caveat to this is that each time-point of each assay must be analysed by HPLC, which, even for the data presented here required 150 HPLC runs. Thus, future experiments must be planned carefully to ensure that all data points are essential and are adding to the overall analysis.

For future assays the fluorescence detector of the HPLC used in the analysis of the assays should be calibrated to quantify the levels of products and allow true values for V_{max} and K_{cat} to be determined.

A similar experiment using PPP in place of GGPP would also greatly add to the value of the data and could perhaps shed light on the ambiguity that currently exists as to which reaction happens first; the CS or geranylgeranyl reductase. This could in turn have implications for the exact roles these enzymes play in thylakoid biogenesis.

The greatest possible improvement to this assay system would be something that allowed continuous assays as opposed to stopped. This could involve a linked assay or a modification of one of the substrates that caused a change in the optical property of the product e.g. modification of the tail with a fluorophore which is quenched on addition to the chlorin. This would mean assays could be carried out in a fraction of the time, and would potentially have greatly reduced error.

Chapter 6: Design and purification of an artificial antigen containing the extra-membranous regions of *Synechocystis* chlorophyll synthase, antibody production and subsequent immunoblot trials

6.1. Summary

An artificial protein containing predicted extra-membranous regions of CS was designed and produced with the aim of generating a specific antibody to *Synechocystis* chlorophyll synthase (CS). Immunisation of animal hosts yielded polyclonal antibodies specific to *Synechocystis* CS that also cross-react with the spinach and *Rba. sphaeroides* homologues of the protein. This antibody has been invaluable to various aspects of the projects presented in this thesis and will continue to be an important tool in investigations into chlorophyll biosynthesis and thylakoid biogenesis.

6.2. Introduction

The importance of specific antibodies in the biochemical analysis of proteins is difficult to overstate; immunoblot, along with mass spectrometry, can be considered a 'staple' technique for the identification of proteins as well their relative quantification. The biochemical applications of specific antibodies go beyond immunoblot and include immunoprecipitation and immunolabelling.

Given that specific antibodies are such a powerful tool in the biochemist's arsenal and owing to the absence of a commercially available antibody to *Synechocystis* CS, the focal point of this thesis, production of a CS specific antibody is a necessity in order to allow proper analysis of the protein.

In order to achieve this objective an artificial protein containing the extra-membranous of CS was designed, expressed and used as an antigen to produce a CS specific polyclonal antibody for use in the biochemical characterisation of CS.

6.3. Results

The initial strategy for production of an antigen was hetrologous production of the *Synechocystis* CS protein, because overexpression of members of the CS family of membrane proteins in *E. coli* has been achieved in the past (Oster *et al*., 1997; Oster and Rüdiger, 1997; Schmid *et al*., 2001; 2002). However in these instances the protein was not purified and characterisation was achieved using cell lysate. Purification of exogenous *Synechocystis* CS protein in *E. coli* was attempted using multiple different expression strategies including basic histidine tag plasmids and techniques designed to increase expression of foreign membrane proteins by adding a large soluble tag to the protein such as glutathione-*S*-transferase and the NusA protein. However, none of these techniques produced protein of sufficient quantity for antibody production (> 1 mg). Another strategy was therefore required in order to produce a suitable antigen.

In order to create a more soluble (and therefore more easily overexpressed) protein which could still provide the antigenic properties required for antibody production a strategy was devised in which the extra-membranous loops of CS are 'stitched together' to form a 'loop-only' protein.

6.3.1. Bioinformatic analysis of the secondary structure of chlorophyll synthase and design of an artificial loop-only protein

In order to estimate which regions of the CS protein are likely to be manifsted as extra-membranous loops a bioinformatic analysis was carried out using transmembrane prediction software. In order to allow for the differences in the predictions of different software, the results of four independent predictions using different programmes were compared: TMHMM (www.cbs.dtu.dk/services/TMHMM/); PRED-TMR (athina.biol.uoa.gr/PRED-TMR/); TMpred (www.ch.embnet.org/software/TMPRED_form.html); HMMTOP (www.enzim.hu/hmmtop/) (Figures 1 and 2).

The results of the transmembrane predictions were compared and regions of agreement, in which all four of the predictions predicted that the peptide sequence would be outside of the membrane, were noted (Figure 3). The nucleotide sequences corresponding to these regions were unified into a single artificial gene and codon optimised for expression in *E. coli* (https://eu.idtdna.com/CodonOpt), the resulting artificial gene was then synthesised (Bio Basic, Canada).

TMHMM

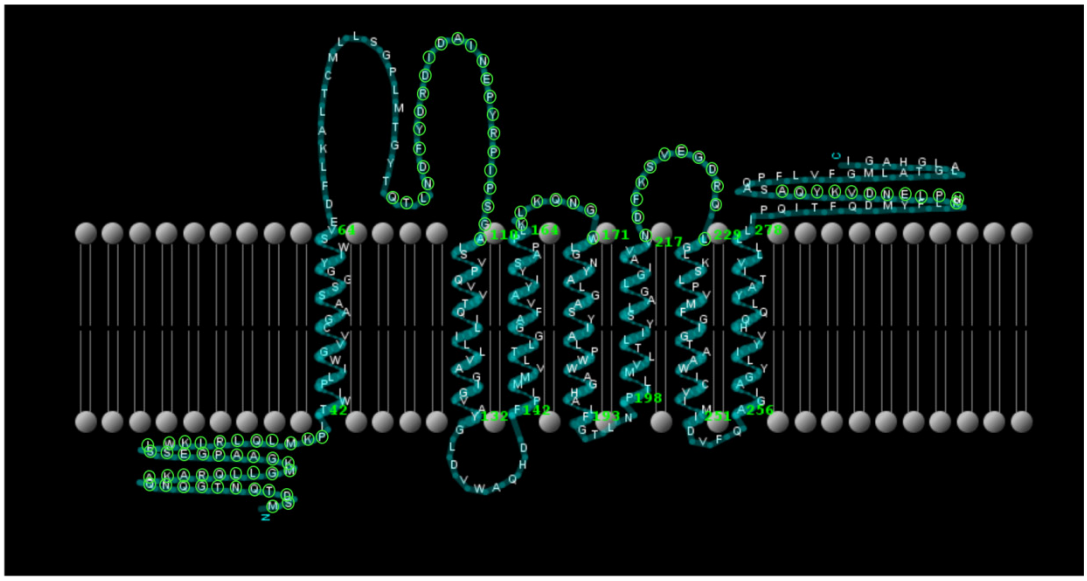

PRED-TMR

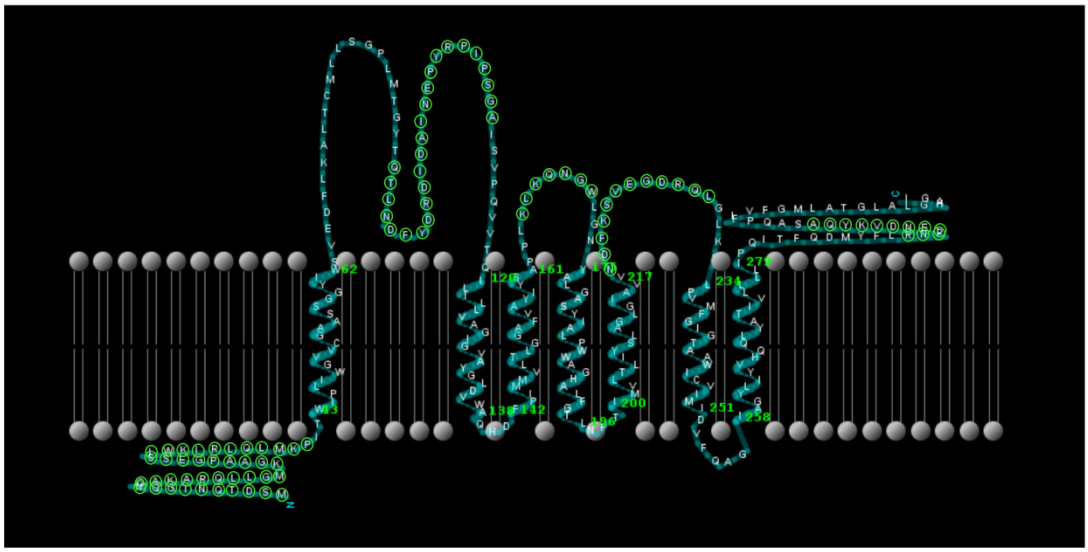

Figure 1. Secondary structure predictions of *Synechocystis* CS using TMHMM and PRED-TMR prediction software. Images were created using TMRPres2D software (Spyropoulos *et al*., 2004). Green rings represent regions of agreement shared between all four models.

TMpred

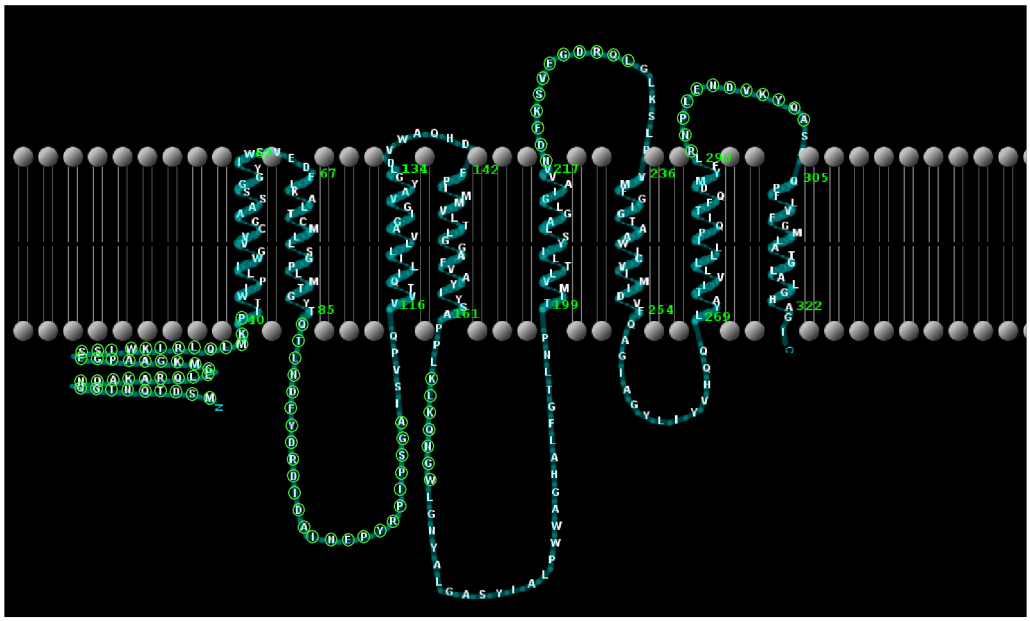

HMMTOP

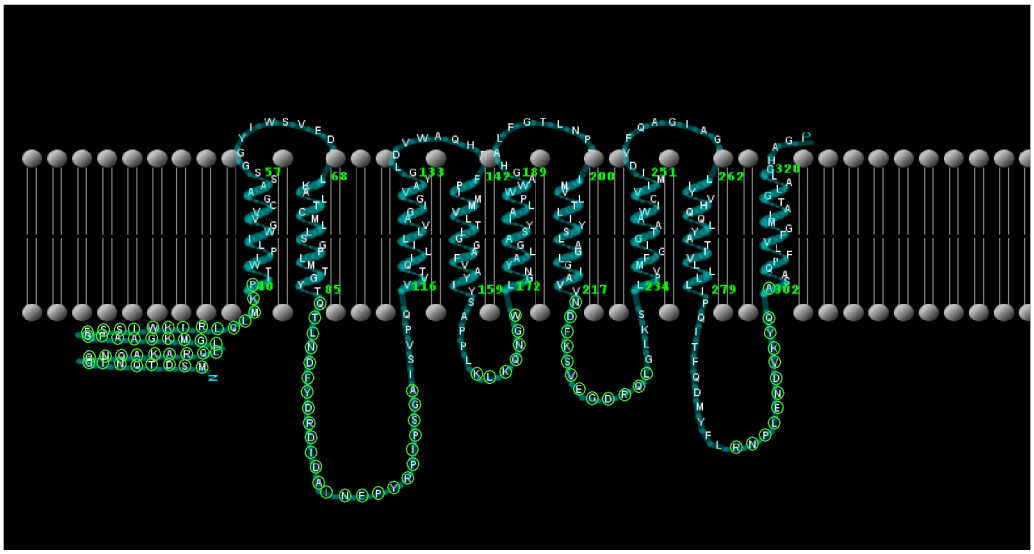

Figure 2. Secondary structure predictions of *Synechocystis* CS using TMpred and HMMTOP prediction software. Images were created using TMRPres2D software (Spyropoulos *et al*., 2004). Green rings represent regions of agreement shared between all four models.

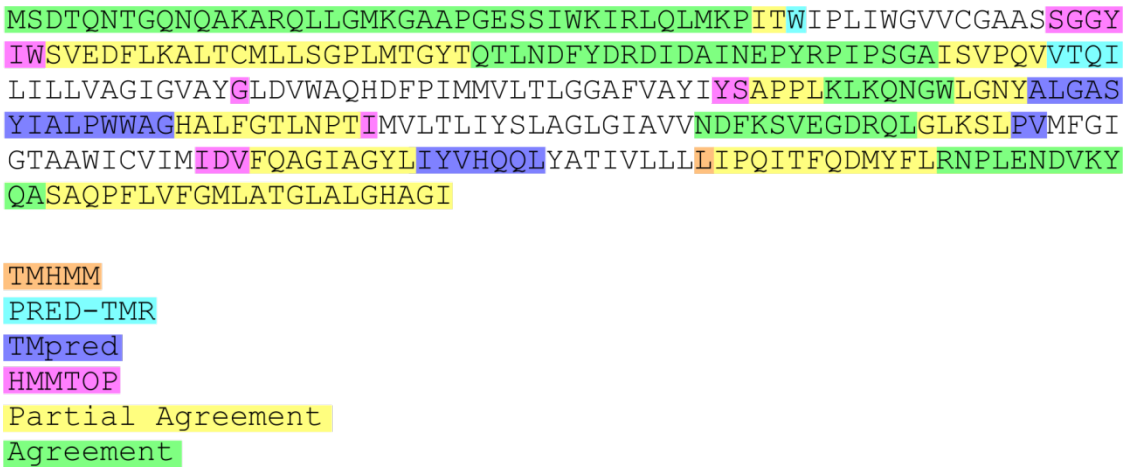

Figure 3. The chlorophyll synthase amino acid sequence annotated based on secondary structure predictions (Figures 1 and 2). Coloured areas represent extra-membranous regions as predicted by at least one programme; colours are defined in the key. Partial agreement – agreement in two or three of the four predictions; agreement – agreement in all four predictions.

6.3.2. Overexpression and purification of the artificial CS protein

The artificial gene was cloned using primers with the appropriate overhangs to allow transformation of the gene into the pET14b plasmid which has a C-terminal His_6-tag situated directly 3' of the multiple cloning site. The plasmid was transformed into BL21 cells and 3 L of the resultant strain was cultured, harvested and broken by sonication. The resultant soluble and solubilised insoluble fractions were applied to nickel-charged chelating Sepharose columns and after washing, bound material was eluted by the addition of excess imidazole. The resulting elutions were analysed by SDS-PAGE revealing high levels of a protein of the appropriate size (~13 kDa) for the artificial CS region containing protein (henceforth G-loop) in both the soluble and insoluble fractions (Figure 4).

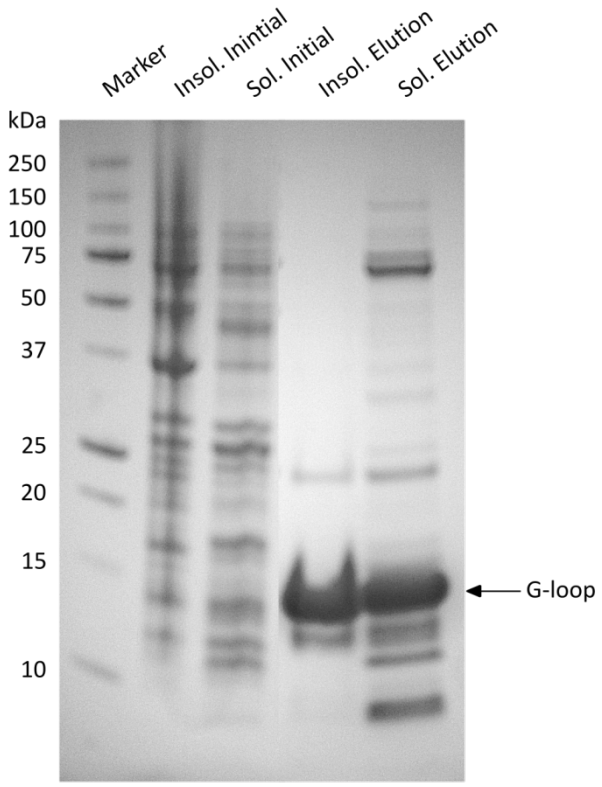

Figure 4. SDS-PAGE of purified G-loop. Insol. – purification carried out on the insoluble fraction; Sol – purification carried out on soluble fraction.

6.3.3. Further purification of G-loop by size exclusion chromatography

Although G-loop was the major protein component of the nickel column elutates from both the soluble and insoluble fractions of the G-loop expression strain, it is clear that both, particularly that of the soluble fraction, contain significant levels of contaminants (Figure 4). In order to attempt further purification of these eluates size exclusion chromatography was carried out and the resultant fractions collected and analysed by SDS-PAGE (Figure 5). These analyses show that whilst in both cases the purity of the G-loop protein was greatly enhanced by the chromatography. The material from the insoluble fraction was purified to the point where no additional contaminants were visible by coomassie staining (Figure 5B; fractions 15.0 and 15.5) whilst in the equivalent soluble material each fraction had at least two bands visible.

Thus, purification of the G-loop protein from the insoluble fraction of the overexpression strain followed by size exclusion chromatography yielded pure protein, suitable for use as an antigen for the production of antibodies.

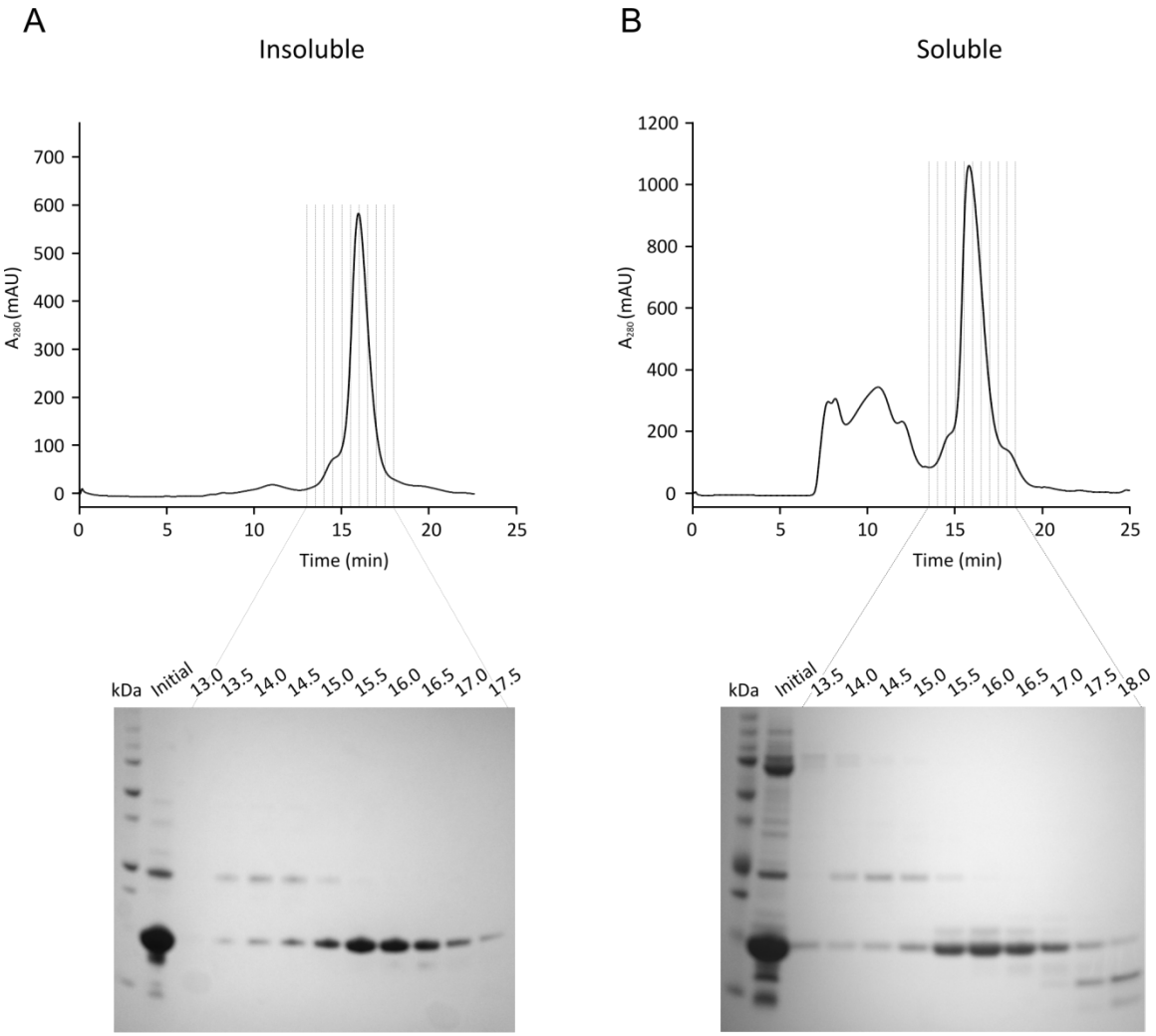

Figure 5. Size exlusion chromatography of nickel purified G-loop protein. Traces represent UV absorbance as recorded by the in-built diode array detector. Dotted lines represent 0.5 ml fractions, each fraction within the dotted lines was analysed by SDS-PAGE. Numbers correspond to the start time of fraction collection i.e. 13.0 represents the fraction collected between 13.0 minutes and 13.49 minutes. Initial – a small amount of nickel eluate was retained and run concurrently with the size exclusion fractions.

6.3.4. Antibody production and trails

Immunisation of two rats was carried out by Generon, UK and yielded sera which was then purified in-house against Protein A. The resulting antibody solution was successfully tested against FLAG-CS prepared as described in Chapter 3 (Figure 6A).

The chlorophyll synthase protein sequence is well conserved between cyanobacteria, plants and purple bacteria (Figure 7). Cross-reaction of the newly produced antibody with chlorophyll synthase proteins from other organisms would further expand the potential applications of the antibody and could allow for immunoblot, co-immunoprecipitation or immunolabelling experiments in other prokaryotes and plants. To this end, cross-reaction trials were carried out against *Arabidopsis*, spinach and *Rhodobacter sphaeroides* (Figure 6B).

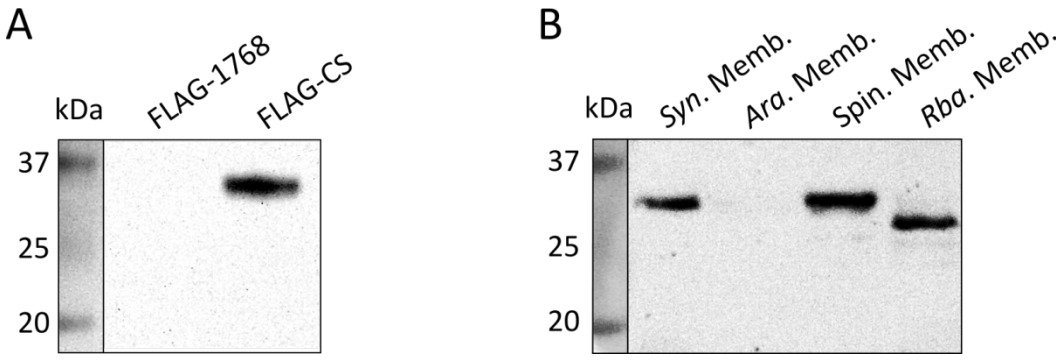

Figure 6. Immunoblot trials of the antibody raised against the G-loop protein. A. Initial trail of the antibody against FLAG-tagged chlorophyll synthase. FLAG-purified Slr1768 protein (similar in size and concentration) was run as a negative control in order to ensure that binding was specific. B. Cross-reaction trails against various other organisms. *Syn*. – *Synechocystis*; *Ara*. – *Arabidopsis*; *Rba*. – *Rba sphaeroids*; Memb. - membrane fraction. Immunoblots were imaged using chemiluminescence detection, pre-stained molecular weight markers were imaged under white light.

Figure 7. Sequence alignment of (bactrio)chlorophyll synthases from *Synechocystis*, *Arabidopsis* and *Rba. sphaeroides*. Green residues represent 100% similarity, yellow represent 66% similarity. Alignment was carried out using T-coffee software (http://www.tcoffee.org/); figure created with 'Geneious' software (Drummond *et al.*, 2011).

6.4. Discussion

In order to produce of an antibody specific to *Synechocystis* CS attempts were made to overexpress the protein in *E. coli*. After multiple failed attempts a novel strategy was designed; bioinformatic analysis was used as a tool to predict the extra-membranous segments of CS and allow design of an artificial protein which was successfully overexpressed, purified and inoculated into animal hosts. The resultant polyclonal antibodies specifically bind *Synechocystis* CS (Figure 6A) and also cross-react with the Spinach, and *Rba. sphaeroides* homologues of the protein (Figure 6B).

In terms of the initial aims of the project, this work has been successful. A specific antibody to *Synechocystis* CS has been created which has been invaluable to other projects presented in this thesis, and will continue to be useful in further studies related specifically to CS as well as the overall processes of Chl biosynthesis and thylakoid biogenesis.

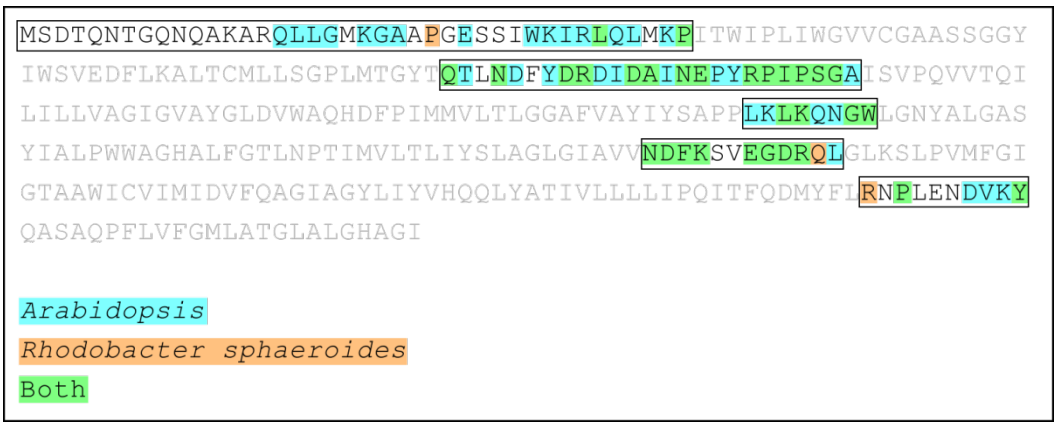

Figure 8. Identity of *Arabidopsis* and *Rba. sphaeroides* (bacterio)chlorophyll synthase to Synechocystis CS within the G-loop regions. The sequence of *Synechocystis* CS is shown with the 'G-loop' regions boxed. These regions were compared with those of the chlorophyll synthase of *Arabadopsis* and the bacteriochlorophyll synthase of *Rba. sphaeroides* using T-coffee software. Regions highlighted in blue are identical in both *Arabadopsis* and *Synechocystis*, orange regions are identical in *Rba. sphaeroides* and *Synechocystis*; whilst green regions indicate residues shared between all three organisms.

After the initial success it became apparent that the value of the antibody would be extended further if it were to successfully cross-react with other members of the CS family. To this end immunoblot trials were carried out against *Arabidopsis*, spinach and *Rba. sphaeroides* membranes (Figure 6); reactivity was observed with the latter two with *Arabadopsis* being the only negative result. This is primarily a positive result, increasing the potential uses of the antibody, but raises interesting questions regarding the lack of cross-reactivity with the *Arabidopsis* protein. Figure 8 shows the identity of the *Arabidopsis* and *Rba. sphaeroides* proteins compared with *Synechocystis* CS (unfortunately the spinach genome is yet to be published and therefore spinach CS could not be included in this analysis). It is immediately obvious that the *Arabidopsis* protein shares significantly higher identity with the *Synechocystis* version when compared with the *Rba. sphaeroides* protein (Figure 8; blue vs. orange). The only reasonable explanation based on sequence data alone is that the glutamine residue at position 228 (Q228) of the *Synechocystis* protein is an essential component of the only epitope within the G-loop protein to which an antibody was specifically raised during immunisation. Thus the *Rba. sphaeroides* protein, which shares the

same glutamate residue, is detectable whilst the *Arabidopsis* protein, which lacks it, is not. There are other potential explanations for the lack of cross-reactivity including degradation of the *Arabidopsis* CS in the thylakoid membrane sample used, rendering it undetectable or incomplete denaturation of the protein prior to immunoblot, leaving potential epitopes inaccessible to antibodies due to partial maintenance of the secondary structure.

In such cases where overexpression of a target protein proves difficult, antibodies are often raised against a single peptide chosen from the target protein. This method is somewhat of a 'gamble' as it is possible that the chosen peptide will not yield successful antibodies. The method presented in this chapter is similar to the single-peptide method, but rather than a single peptide five have been 'stitched-together' to form of an artificial protein increasing the chances success. Based on the cross-reaction trials and subsequent sequence analysis it appears that only one of the 'peptides' within the G-loop protein, the Q228 containing peptide, yielded successful antibodies indicating a success rate of 20%. This further bolsters the argument for a 'multiple-peptide' approach over a single peptide.

Chapter 7: General Discussion

The results presented in this thesis involve investigations in to the chlorophyll synthase (CS) enzyme of *Synechocystis*. It has been demonstrated that CS forms a tight, pigment containing complex with the small chlorophyll *a* binding protein HilD and that this complex associates with the YidC membrane translocase and the putative PSII assembly factor Ycf39. Further investigations revealed that the interaction of the CS-HliD 'core' with Ycf39 is almost completely abolished after light-shock and that this treatment causes a rearrangement of the remaining components. Assays were carried out on purified enzyme in the presence of chlorophyllide (Chlide) produced from a *Rba. sphaeroides* mutant and geranylgeranyl pyrophosphate (GGPP) and K_m values of 25.7 µM ± 19.2 and 66.8 ± 33.1 µM were obtained for Chlide and GGPP respectively. An antibody was produced to CS using an artificial protein containing the extramembranous loops of the CS protein.

It has long been speculated that there must be handover of chlorophyll (Chl) from the chlorophyll biosynthesis pathway to assembling light harvesting polypeptides. Eichacker and co-workers (1996) demonstrated that Chl stabilises plastid encoded Chl-binding apoproteins (P700, CP47, CP43, D2 and D1) against proteolytic degradation in barley etioplasts implying that insertion of Chl into apoproteins is necessary for correct assembly of light harvesting apparatus. Müller and Eichacker (2000) expanded on this demonstrating that in the absence of Chl the D1 precursor pD1 is continually assembled and degraded and that after initiation of Chl production PSII assembly proceeds. These studies indicate that the presence of Chl is essential for photosystem assembly to occur, and therefore a mechanism of Chl delivery to developing photosystem apoproteins is likely to exist. The results presented in this thesis provide the first direct evidence for a link between Chl biosynthesis and thylakoid biogenesis in the form of a specific interaction of CS with the YidC translocase, which is known to have a role in thylakoid biogenesis (Spence *et al*., 2004; Göhre *et al*., 2006; Ossenbühl *et al*., 2006). A specific interaction with the atypical short chain dehydrogenase Ycf39 was also observed. This protein has recently been shown to have a role in PSII assembly, adding further evidence that CS has a role in Chl handover (Knoppová *et al.,* 2014). The drastic reduction of Ycf39

associated with CS after light shock implies that the interaction of CS with Ycf39 is important for thylakoid biogenesis, but perhaps less so for photosystem repair.

The small pigment binding protein HliD was also found to be an interaction partner of CS. This single transmembrane helix shares structural similarity with the nuclear encoded plant LHCII protein. Previous studies into the Hlip family of genes to which HliD belongs have revealed that HliA, HliB and HliC interact with PSII during repair and are likely acting as pigment stores, leaving the role of HliD somewhat enigmatic (Yao *et al*., 2007). The results presented in this thesis show that HliD specifically interacts with CS forming a tightly bound protein-pigment complex containing both Chl/Chlide and carotenoids. The HliD is likely to have a pigment binding role; the carotenoids present within the complex are likely to have an energy scavenging role preventing oxidative damage. It is noteworthy that this complex was observed even under moderate light conditions and that high light treatment did not appear to increase cellular levels of HliD indicating that the protein is more constitutively expressed than the other Hlips. Although it is highly likely that the the carotenoids bound to the CS-HliD complex have a photoprotective role, there is no direct evidence. This should be addressed by carring out ultrafast pump-probe spectroscopy, with which quenching of excited Chls by the bound carotenoids could be observed.

It remains to be seen whether a CS-HliD-like complex exsits in plants and/or photosynthetic bacteria, and whether or not there is a connection with other CSs and translocase components. These questions are at the forefront of this field of study and should be addressed in the near future.

Preliminary kinetic characterisation of FLAG-purified CS was carried out using a chlorophyllide substrate produced by a *Rba. sphaeroides* mutant. K_m values of 25.7 ± 19.2 µM and 66.8 ± 33.1 µM for chlorophyllide and geranylgeranyl pyrophosphate, respectively, were obtained. The K_m value obtained for GGPP is the first to be reported. Kim and Lee (2010) published a K_m value of 100 µM for Chlide, which is fourfold higher than the one obtained in this thesis. Schmid *et al.* (2002) observed substrate inhibition at Chlide concentrations higher than 10 µM. This was not found to be the case in the preset study, as assays were carried out at 40 µM Chlide and

showed no sign of inhibition indicating that further work is required to fully understand CS as an enzyme.

In conclusion the findings of this thesis demonstrate that CS is not only an important enzyme, but an interesting one with roles as a biosynthetic enzyme as well as in thylakoid biogenesis. Further studies into CS are required in order to gain a full understanding of Chl biosynthesis as well as the Chl-dependent assembly of light harvesting complexes.

References

Acharya, K., Zazubovich, V., Reppert, M., Jankowiak, R. (2012) Primary electron donor(s) in isolated reaction center of photosystem II from *Chlamydomonas reinhardtii*. *Journal of Physical Chemistry B* **116**: 4860–4870

Adams, N.B., Reid, J.D. (2013) The allosteric role of the AAA+ domain of the ChlD Protein from the Magnesium Chelatase of *Synechocystis* Species PCC 6803. *Journal of Biological Chemistry* **288**: 28727–28732

Addlesee, H.A., Fiedor, L., Hunter, C.N. (2000) Physical Mapping of *bchG*, *orf427*, and *orf177* in the photosynthesis gene cluster of *Rhodobacter sphaeroides*: Functional Assignment of the Bacteriochlorophyll Synthetase Gene. *Journal of Bacteriology* **182:** 3175–3182

Addlesee, H.A., Gibson, L.C.D., Jensen, P.E., Hunter, C.N. (1996) Cloning, sequencing and functional assignment of the chlorophyll biosynthesis gene, *chlP*, of *Synechocystis* sp. PCC 6803. *FEBS Letters* **389:** 126–130

Addlesee, H.A., Hunter, C.N. (1999) Physical mapping and functional assignment of the geranylgeranyl-bacteriochlorophyll reductase gene, *bchP*, of Rhodobacter sphaeroides. *Journal of bacteriology* **181:** 7248–7255

Addlesee, H.A., Hunter, C.N. (2002) *Rhodospirillum rubrum* possesses a variant of the *bchP* gene, encoding geranylgeranyl-bacteriopheophytin reductase. *Journal of bacteriology* **184:** 1578–1586

Amunts, A., Drory, O., Nelson, N. (2007) The structure of a plant photosystem I supercomplex at 3.4 Å resolution. *Nature* **447:** 58–63

Anderson, J.M., Chow, W.S., Park, Y.I. (1995) The grand design of photosynthesis: Acclimation of the photosynthetic apparatus to environmental cues. *Photosynthesis Research* **46**: 129–139

Anderson, S.L., McIntosh, L. (1991) Light-activated heterotrophic growth of the cyanobacterium *Synechocystis* sp. strain PCC 6803: a blue-light-requiring process. *Journal of Bacteriology* **173:** 2761–2767

Antonoaea, R., Fürst, M., Nishiyama, K., Müller, M. (2008) The periplasmic chaperone PpiD interacts with secretory proteins exiting from the SecYEG translocon. *Biochemistry* **47:** 5649–5656

Apel, K., Hirt, H. (2004) Reactive oxygen species: metabolism, oxidative stress, and signal transduction. *Annual Review of Plant Biology* **55:** 373–399

Armbruster, U., Zühlke, J., Rengstl, B., Kreller, R., Makarenko, E., Rühle, T., Schünemann, D., Jahns, P., Weisshaar, B., Nickelsen, J., Leister, D. (2010) The *Arabidopsis* thylakoid protein PAM68 is required for efficient D1 biogenesis and photosystem II assembly. *Plant Cell* **22:** 3439–3460

Aro, E.M., Virgin, I., Andersson, B. (1993) Photoinhibition of photosystem II. Inactivation, protein damage and turnover. *Biochimica et Biophysica Acta - Bioenergetics* **1143:** 113–134

Axelsson, E., Lundqvist, J., Sawicki, A., Nilsson, S., Schröder, I., Al-Karadaghi, S., Willows, R.D., Hansson, M. (2006) Recessiveness and dominance in barley mutants deficient in Mg-Chelatase Subunit D, an AAA protein involved in chlorophyll biosynthesis. *Plant Cell* **18:** 3606–3616

Battersby, A.R. (1994) How nature builds the pigments of life: the conquest of vitamin B12. *Science* **264:** 1551–1557

Battersby, A.R., Fookes, C.J., Matcham, G.W., McDonald, E. (1979) Order of assembly of the four pyrrole rings during biosynthesis of the natural porphyrins. *Journal of the Chemical Society*, *Chemical Communications* 539–541

Beale, S.I. (2006). Biosynthesis of 5-Aminolevulinic Acid, in: Grimm, B., Porra, R.J., Rüdiger, W., Scheer, H. (Eds.), Chlorophylls and Bacteriochlorophylls, Advances in Photosynthesis and Respiration. Springer Netherlands, pp. 147–158

Beck, K., Eisner, G., Trescher, D., Dalbey, R.E., Brunner, J., Müller, M. (2001) YidC, an assembly site for polytopic *Escherichia coli* membrane proteins located in immediate proximity to the SecYE translocon and lipids. *EMBO Reports* **2:** 709–714

Begley, T.P. (1994) Photoenzymes: A novel class of biological catalysts. Accounts of chemical research **27:** 394–401.

Benz, J., Rüdiger, W. (1981) Incorporation of ^{14}C-isopentenyldiphosphate, geraniol and farnesol into chlorophyll in plastid membrane fractions of *Avena sativa L. Zeitschrift für Pflanzenphysiologie* **102:** 95–100

Benz, J., Wolf, C., Rüdiger, W. (1980) Chlorophyll biosynthesis: hydrogenation of geranylgeraniol. *Plant Science Letters* **19:** 225–230

Bhaya, D., Dufresne, A., Vaulot, D., Grossman, A. (2002) Analysis of the Hli gene family in marine and freshwater cyanobacteria. *FEMS Microbiology Letters* **215:** 209–219

Blankenship, R.E. (2008) Molecular Mechanisms of Photosynthesis. John Wiley & Sons.

Blankenship, R.E., Madigan, M.T., Bauer, C.E. (1995) Anoxygenic photosynthetic bacteria. Springer.

Boehm, M., Romero, E., Reisinger, V., Yu, J., Komenda, J., Eichacker, L.A., Dekker, J.P., Nixon, P.J. (2011) Investigating the early stages of photosystem II assembly in *Synechocystis* sp. PCC 6803 isolation of CP47 and CP43 complexes. *Journal of Biological Chemistry* 286, 14812–14819

Bogorad, L. (1950) Factors associated with the synthesis of chlorophyll in the dark in seedlings of Pinus jeffreyi. *Botanical Gazette* 221–241.

Bollivar, D.W., Beale, S.I. (1996) The chlorophyll biosynthetic enzyme Mg-protoporphyrin IX monomethyl ester (oxidative) cyclase (characterization and partial purification from *Chlamydomonas reinhardtii* and *Synechocystis* sp. PCC 6803). *Plant Physiology* **112**, 105–114.

Bollivar, D.W., Jiang, Z.-Y., Bauer, C.E., Beale, S.I. (1994a) Heterologous expression of the *bchM* gene product from *Rhodobacter capsulatus* and demonstration that it encodes S-adenosyl-L-methionine: Mg-protoporphyrin IX methyltransferase. *Journal of Bacteriology* **176:** 5290–5296

Bollivar, D.W., Suzuki, J.Y., Beatty, J.T., Dobrowolski, J.M., Bauer, C.E. (1994b) Directed mutational analysis of bacteriochlorophyll *a* biosynthesis in *Rhodobacter capsulatus*. *Journal of Molecular Biology* **237:** 622–640

Bollivar, D.W., Wang, S., Allen, J.P., Bauer, C.E. (1994c) Molecular genetic analysis of terminal steps in bacteriochlorophyll *a* biosynthesis: Characterization of a *Rhodobacter capsulatus* strain that synthesizes geranylgeraniol-esterified bacteriochlorophyll *a*. *Biochemistry* **33:** 12763–12768

Bricker, T.M. (1990) The structure and function of CPa-1 and CPa-2 in photosystem II. *Photosynthesis Research* **24:** 1–13

Bröcker, M.J., Schomburg, S., Heinz, D.W., Jahn, D., Schubert, W.D., Moser, J. (2010) Crystal structure of the nitrogenase-like dark operative protochlorophyllide oxidoreductase catalytic complex (ChlN/ChlB) 2. *Journal of Biological Chemistry* **285:** 27336–27345

Brune, D.C. (1995) Sulfur compounds as photosynthetic electron donors in anoxygenic photosynthetic bacteria. Springer, pp. 847–870

Bryan, S. J., Burroughs, N. J., Shevela, D., Yu, J., Rupperecht, E., Liu, L., Mastroianni, G., Xue, Q., Llorente-Garcia, I., Leake, M.C., Eichacker, L. A., Schnieder, D., Nixon, P. J. and Mullineaux, C. W. (2014) Localisation and interactions of the Vipp1 protein in cyanobacteria. *Molecular Microbiology* **94**: 1179-1195

Buick, R. (2008) When did oxygenic photosynthesis evolve? *Philosophical Transactions of the Royal Society B: Biological Sciences* **363:** 2731–2743

Burda, K., Kruk, J., Schmid, G.H., Strzalka, K. (2003) Inhibition of oxygen evolution in photosystem II by Cu(II) ions is associated with oxidation of cytochrome b559. *Biochemical Journal* **371:** 597-601

Burke, D.H., Alberti, M., Hearst, J.E. (1993a) *bchFNBH* bacteriochlorophyll synthesis genes of Rhodobacter capsulatus and identification of the third subunit of light-independent protochlorophyllide reductase in bacteria and plants. *Journal of Bacteriology* **175:** 2414–2422

Burke, D.H., Alberti, M., Hearst, J.E. (1993b) The *Rhodobacter capsulatus* chlorin reductase-encoding locus, *bchA*, consists of three genes, *bchX*, *bchY*, and *bchZ*. *Journal of Bacteriology* **175:** 2407–2413

Canniffe, D.P., Chidgey, J.W., Hunter, C.N. (2014) Elucidation of the preferred routes of C8-vinyl reduction in chlorophyll and bacteriochlorophyll biosynthesis. *Biochemical Journal* **462:** 433–440

Canniffe, D.P., Jackson, P.J., Hollingshead, S., Dickman, M.J., Hunter, C.N. (2013) Identification of an 8-vinyl reductase involved in bacteriochlorophyll biosynthesis in *Rhodobacter sphaeroides* and evidence for the existence of a third distinct class of the enzyme. *Biochemical Journa*l **450:** 397–405

Chew, A.G.M., Bryant, D.A. (2007) Characterization of a plant-like protochlorophyllide a divinyl reductase in green sulfur bacteria. *Journal of Biological Chemistry* **282:** 2967–2975

Chidgey, J.W., Linhartová, M., Komenda, J., Jackson, P.J., Dickman, M.J., Canniffe, D.P., Konik, P., Pilný, J., Hunter, C.N., Sobotka, R. (2014) A cyanobacterial chlorophyll synthase -HliD complex associates with the Ycf39 protein and the YidC/Alb3 insertase. *The Plant Cell* **26**: 1267-1279

Chitnis, V.P., Xu, Q., Yu, L., Golbeck, J.H., Nakamoto, H., Xie, D.L., Chitnis, P.R. (1993) Targeted inactivation of the gene *psaL* encoding a subunit of photosystem I of the cyanobacterium *Synechocystis* sp. PCC 6803. *Journal of Biological Chemistry* **268:** 11678–11684

Chua, N.-H., Blobel, G., Siekevitz, P., Palade, G.E. (1976) Periodic variations in the ratio of free to thylakoid-bound chloroplast ribosomes during the cell cycle of *Chlamydomonas reinhardtii*. *The Journal of Cell Biology* **71:** 497–514

Cohen-Bazire, G., Sistrom, W.R., Stanier, R.Y. (1957) Kinetic studies of pigment synthesis by non-sulfur purple bacteria. *Journal of Cellular and Comparative Physiology* **49**, 25–68

Coomber, S.A., Chaudhri, M., Connor, A., Britton, G., Hunter, C.N. (1990) Localized transposon Tn5 mutagenesis of the photosynthetic gene cluster of *Rhodobacter sphaeroides*. *Molecular Microbiology* **4**: 977–989

Cooper, D.E., Rands, M.B., Woo, C.P. (1975) Sulfide reduction in fellmongery effluent by red sulfur bacteria. *Journal (Water Pollution Control Federation)* 2088–2100

Davison, P.A., Schubert, H.L., Reid, J.D., Iorg, C.D., Heroux, A., Hill, C.P., Hunter, C.N. (2005) Structural and biochemical characterization of Gun4 suggests a mechanism for its role in chlorophyll biosynthesis. *Biochemistry* **44:** 7603–7612

Dobáková, M., Sobotka, R., Tichý, M., Komenda, J. (2009) Psb28 protein is involved in the biogenesis of the photosystem II inner antenna CP47 (PsbB) in the cyanobacterium *Synechocystis* sp. PCC 6803. *Plant Physiology* **149:** 1076–1086

Dobáková, M., Tichý, M., Komenda, J. 2007. Role of the PsbI protein in photosystem II assembly and repair in the cyanobacterium *Synechocystis* sp. PCC 6803. *Plant Physiology* **145:** 1681–1691

Domanskii, V., Rassadina, V., Gus-Mayer, S., Wanner, G., Schoch, S., Rüdiger, W. (2003) Characterization of two phases of chlorophyll formation during greening of etiolated barley leaves. *Planta* **216:** 475–483

Douglas, S.E. (1998) Plastid evolution: origins, diversity, trends. *Current Opinion in Genetics and Development* **8:** 655–661

Drummond, A.J., Ashton, B., Buxton, S., Cheung, M., Cooper, A., Duran, C., Field, M., Heled, J., Kearse, M., Markowitz, S., others (2011) Geneious v5. 4.

Dühring, U., Ossenbühl, F., Wilde, A. (2007) Late assembly steps and dynamics of the cyanobacterial Photosystem I. *Journal of Biological Chemistry* **282:** 10915–10921

Eichacker, L.A., Helfrich, M., Rüdiger, W., Müller, B. (1996) Stabilization of chlorophyll *a*-binding apoproteins P700, CP47, CP43, D2, and D1 by chlorophyll *a* or Zn-pheophytin *a*. *Journal of Biolological Chemistry* **271:** 32174–32179

El Bissati, K., Delphin, E., Murata, N., Etienne, A.L., Kirilovsky, D. (2000) Photosystem II fluorescence quenching in the cyanobacterium *Synechocystis* PCC 6803: involvement of two different mechanisms. *Biochimica et Biophysica Acta - Bioenergetics* **1457:** 229–242

Ellsworth, R.K., Dullaghan, J.P. (1972) Activity and properties of S-adenosyl-l-methionine:magnesium-protoporphyrin IX methyltransferase in crude homogenates from wheat seedlings. *Biochimica et Biophysica Acta - Enzymology* **268:** 327–333

Ermakova-Gerdes, S., Vermaas, W. (1999) Inactivation of the open reading frame *slr0399* in *Synechocystis* sp. PCC 6803 functionally complements mutations near the Q_A niche of photosystem II a possible role of Slr0399 as a chapterone for quinone binding. *Journal of Biological Chemistry* **274:** 30540–30549

Ferreira, K.N., Iverson, T.M., Maghlaoui, K., Barber, J., Iwata, S. (2004) Architecture of the photosynthetic oxygen-evolving center. *Science* **303:** 1831–1838

Fischer, N., Boudreau, E., Hippler, M., Drepper, F., Haehnel, W., Rochaix, J.D. (1999) A large fraction of PsaF Is nonfunctional in photosystem I complexes lacking the PsaJ Subunit. *Biochemistry* **38:** 5546–5552

Frank, H.A., Bautista, J.A., Josue, J., Pendon, Z., Hiller, R.G., Sharples, F.P., Gosztola, D., Wasielewski, M.R. (2000) Effect of the solvent environment on the spectroscopic properties and dynamics of the lowest excited states of carotenoids. *Journal of Physical Chemistry B* **104:** 4569–4577

Freer, A., Prince, S., Sauer, K., Papiz, M., Lawless, A.H., McDermott, G., Cogdell, R., Isaacs, N.W. (1996) Pigment–pigment interactions and energy transfer in the antenna complex of the photosynthetic bacterium *Rhodopseudomonas acidophila*. *Structure* **4:** 449–462

Fujimori, T., Higuchi, M., Sato, H., Aiba, H., Muramatsu, M., Hihara, Y., Sonoike, K. (2005) The mutant of *sll1961*, which encodes a putative transcriptional regulator, has a defect in regulation of photosystem stoichiometry in the cyanobacterium *Synechocystis* sp. PCC 6803. *Plant Physiology* **139**: 408–416

Garcia-Gil, L.J., Gich, F.B., Fuentes-Garcia, X. (2003) A comparative study of *bchG* from green photosynthetic bacteria. *Archives of Microbiology* **179:** 108–115

Gibson, L.C., Hunter, C.N. (1994) The bacteriochlorophyll biosynthesis gene, *bchM*, of *Rhodobacter sphaeroides* encodes *S*-adenosyl-L-methionine: Mg protoporphyrin IX methyltransferase. *FEBS Letters* **352:** 127–130

Gibson, L.C., Willows, R.D., Kannangara, C.G., von Wettstein, D., Hunter, C.N. (1995) Magnesium-protoporphyrin chelatase of *Rhodobacter sphaeroides*: Reconstitution of activity by combining the products of the *bchH*, *-I*, and *-D* genes expressed in *Escherichia coli*. *Proceedings of the National Academy of Sciences* **92:** 1941–1944

Gill, S.C., Von Hippel, P.H. (1989) Calculation of protein extinction coefficients from amino acid sequence data. *Analytical Biochemistry* **182:** 319–326

Göhre, V., Ossenbühl, F., Crèvecoeur, M., Eichacker, L.A., Rochaix, J.D. (2006) One of two Alb3 proteins is essential for the assembly of the photosystems and for cell survival in *Chlamydomonas*. *The Plant Cell* **18:** 1454–1466

González-Leiza, S.M., Pedro, M.A. de, Ayala, J.A. (2011) AmpH, a bifunctional dd-endopeptidase and dd-carboxypeptidase of *Escherichia coli*. *Journal of Bacteriology* **193:** 6887–6894

Greco, W.R., Hakala, M.T., (1979) Evaluation of methods for estimating the dissociation constant of tight binding enzyme inhibitors. Journal of Biological Chemistry **254:** 12104–12109

Griffin, B.M., Schott, J., Schink, B. (2007) Nitrite, an electron donor for anoxygenic photosynthesis. *Science* **316:** 1870–1870

Guskov, A., Kern, J., Gabdulkhakov, A., Broser, M., Zouni, A., Saenger, W. (2009) Cyanobacterial photosystem II at 2.9-Å resolution and the role of quinones, lipids, channels and chloride. *Nature Structural and Molecular Biology* **16:** 334–342

Havaux, M. (1998) Carotenoids as membrane stabilizers in chloroplasts. *Trends in Plant Science* **3:** 147–151

Helfrich, M., Rüdiger, W., (1992) Various metallopheophorbides as substrates for chlorophyll synthetase. *Zeitschrift für Naturforschung C. A journal of biosciences* **47:** 231–238

Helfrich, M., Shoch, S., Lempert, U., Cmiel, E., Rüdiger, W. (1994) Chlorophyll synthetase cannot synthesize chlorophyll *a*'. *European Journal of Biochemistry* **219:** 267–275

He, Q., Dolganov, N., Björkman, O., Grossman, A.R. (2001) The high light-inducible polypeptides in *Synechocystis* PCC 6803 expression and function in high light. *Journal of Biological Chemistry* **276**: 306–314

Herbstová, M., Tietz, S., Kinzel, C., Turkina, M.V., Kirchhoff, H. (2012) Architectural switch in plant photosynthetic membranes induced by light stress. *Proceedings of the National Academy of Sciences* **109:** 20130–20135

Heyes, D.J., Hunter, C.N. (2005) Making light work of enzyme catalysis: protochlorophyllide oxidoreductase. *Trends in Biochemical Sciences* **30:** 642–649

Heyes, D.J., Kruk, J., Hunter, C.N. (2006) Spectroscopic and kinetic characterization of the light-dependent enzyme protochlorophyllide oxidoreductase (POR) using monovinyl and divinyl substrates. *Biochemical Journal* **394:** 243-248

Hollingshead, S., Kopečná, J., Jackson, P.J., Canniffe, D.P., Davison, P.A., Dickman, M.J., Sobotka, R., Hunter, C.N. (2012) Conserved chloroplast open-reading frame ycf54 is required for activity of the magnesium protoporphyrin monomethylester oxidative cyclase in *Synechocystis* PCC 6803. *Journal of Biological Chemistry* **287:** 27823–27833

Islam, M.R., Aikawa, S., Midorikawa, T., Kashino, Y., Satoh, K., Koike, H. (2008) *slr1923* of *Synechocystis* sp. PCC 6803 is essential for conversion of 3, 8-divinylprotochlorophyllide to 3-monovinylprotochlorophyllide. *Plant Physiology* **148**: 1068–1081

Ito, H., Yokono, M., Tanaka, R., Tanaka, A. (2008) Identification of a novel vinyl reductase gene essential for the biosynthesis of monovinyl chlorophyll in *Synechocystis* sp. PCC 6803. *Journal of Biological Chemistry* **283:** 9002–9011

Jensen, P.E., Gibson, L.C., Henningsen, K.W., Hunter, C.N. (1996) Expression of the *chlI*, *chlD*, and *chlH* genes from the cyanobacterium *Synechocystis* PCC 6803 in *Escherichia coli* and demonstration that the three cognate proteins are required for magnesium-protoporphyrin chelatase activity. *Journal of Biological Chemistry* **271:** 16662–16667

Johnson, M.P., Vasilev, C., Olsen, J.D., Hunter, C.N. (2014) Nanodomains of cytochrome b_6f and photosystem II complexes in spinach grana thylakoid membranes. *The Plant Cell* **26:** 3051–3061

Jordan, P., Fromme, P., Witt, H.T., Klukas, O., Saenger, W., Krauss, N. (2001) Three-dimensional structure of cyanobacterial photosystem I at 2.5 Å resolution. *Nature* **411:** 909–917

Kallberg, Y., Oppermann, U., Jörnvall, H., Persson, B. (2002) Short-chain dehydrogenases/reductases (SDRs). *European Journal of Biochemistry* **269:** 4409–4417

Kaneko, T., Sato, S., Kotani, H., Tanaka, A., Asamizu, E., Nakamura, Y., Miyajima, N., Hirosawa, M., Sugiura, M., Sasamoto, S. (1996) Sequence analysis of the genome of the unicellular cyanobacterium *Synechocystis* sp. strain PCC 6803. II. Sequence determination of the entire genome and assignment of potential protein-coding regions. *DNA Research* **3**: 109–136

Karger, G.A., Reid, J.D., Hunter, C.N. (2001) Characterization of the binding of deuteroporphyrin IX to the magnesium chelatase H subunit and spectroscopic properties of the complex. *Biochemistry* **40**: 9291–9299

Ke, S. H., Madison, E.L. (1997) Rapid and efficient site-directed mutagenesis by single-tube “megaprimer”PCR method. *Nucleic Acids Research* **25:** 3371–3372

Kim, E. J., Lee, J.K. (2010) Competitive inhibitions of the chlorophyll synthase of *Synechocystis* sp. strain PCC 6803 by bacteriochlorophyllide *a* and the bacteriochlorophyll synthase of *Rhodobacter sphaeroides* by chlorophyllide *a*. *Journal of Bacteriology* **192:** 198–207

Kim, J., Klein, P.G., Mullet, J.E. (1994) Synthesis and turnover of photosystem II reaction center protein D1. Ribosome pausing increases during chloroplast development. *Journal of Biological Chemistry* **269:** 17918–17923

Klinkert, B., Ossenbühl, F., Sikorski, M., Berry, S., Eichacker, L., Nickelsen, J. (2004) PratA, a periplasmic tetratricopeptide repeat protein involved in biogenesis of photosystem II in *Synechocystis* sp. PCC 6803. *Journal of Biological Chemistry* **279:** 44639–44644

Klostermann, E., Carde, J., Schunemann, D. (2002) The thylakoid membrane protein ALB3 associates with the cpSecY-translocase in *Arabidopsis thaliana*. *Biochemical Journal* **368:** 777–781

Knoppová, J., Sobotka, R., Tichý, M., Yu, J., Konik, P., Halada, P., Nixon, P.J., Komenda, J. (2014) Discovery of a chlorophyll binding protein complex involved in the early steps of photosystem II assembly in *Synechocystis*. *The Plant Cell* **26:** 1200–1212

Komenda, J., Hassan, H.A.G., Diner, B.A., Debus, R.J., Barber, J., Nixon, P.J. (2000) Degradation of the photosystem II D1 and D2 proteins in different strains of the cyanobacterium *Synechocystis* PCC 6803 varying with respect to the type and level of *psbA* transcript. *Plant Molecular Biology* **42:** 635–645

Komenda, J., Nickelsen, J., Tichý, M., Prášil, O., Eichacker, L.A., Nixon, P.J. (2008) The cyanobacterial homologue of HCF136/YCF48 Is a component of an early photosystem II assembly complex and is important for both the efficient assembly and repair of photosystem II in *Synechocystis* sp. PCC 6803. *Journal of Biological Chemistry* **283:** 22390–22399

Komenda, J., Sobotka, R., Nixon, P.J. (2012) Assembling and maintaining the Photosystem II complex in chloroplasts and cyanobacteria. *Current Opinion in Plant Biology* **15:** 245–251

Komenda, J., Tichý, M., Prášil, O., Knoppová, J., Kuviková, S., Vries, R. de, Nixon, P.J. (2007) The exposed N-terminal tail of the D1 subunit is required for rapid D1 degradation during photosystem II repair in *Synechocystis* sp PCC 6803. *The Plant Cell* **19:** 2839–2854

Kopečná, J., Komenda, J., Bučinská, L., Sobotka, R. (2012) Long-term acclimation of the cyanobacterium *Synechocystis* sp. PCC 6803 to high light is accompanied by an enhanced production of chlorophyll that Is preferentially channeled to trimeric photosystem I. *Plant Physiology* **160:** 2239–2250

Kopečná, J., Sobotka, R., Komenda, J. (2013) Inhibition of chlorophyll biosynthesis at the protochlorophyllide reduction step results in the parallel depletion of photosystem I and photosystem II in the cyanobacterium *Synechocystis* PCC 6803. *Planta* **237:** 497–508

Kroll, D., Meierhoff, K., Bechtold, N., Kinoshita, M., Westphal, S., Vothknecht, U.C., Soll, J., Westhoff, P. (2001) *VIPP1*, a nuclear gene of *Arabidopsis thaliana* essential for thylakoid membrane formation. *Proceedings of the National Academy of Sciences* **98:** 4238–4242

Kulkarni, R.D., Golden, S.S. (1997) mRNA stability is regulated by a coding-region element and the unique 5' untranslated leader sequences of the three *Synechococcus psbA* transcripts. Molecular Microbiology **24:** 1131–1142

Laemmli, U.K., (1970) Cleavage of structural proteins during the assembly of the head of bacteriophage T4. Nature **227:** 680–685

Lang, H.P., Hunter, C.N. (1994) The relationship between carotenoid biosynthesis and the assembly of the light-harvesting LH2 complex in *Rhodobacter sphaeroides*. *Biochemical Journal* **298:** 197–205

Lascelles, J. (1966) The accumulation of bacteriochlorophyll precursors by mutant and wild-type strains of *Rhodopseudomonas spheroides*. *Biochemical Journal* **100:** 175–183

Lebedev, N., Timko, M.P. (1998) Protochlorophyllide photoreduction. *Photosynthesis research* **58:** 5–23

Li, H., Kaneko, Y., Keegstra, K. (1994) Molecular cloning of a chloroplastic protein associated with both the envelope and thylakoid membranes. *Plant Molecular Biology* **25:** 619–632

Link, S., Engelmann, K., Meierhoff, K., Westhoff, P. (2012) The atypical short-chain dehydrogenases HCF173 and HCF244 are jointly involved in translational initiation of the *psbA* mRNA of *Arabidopsis*. *Plant Physiology* **160:** 2202–2218

Masuda, T., Fujita, Y. (2008) Regulation and evolution of chlorophyll metabolism. *Photochemical and Photobiological Sciences* **7:** 1131–1149.

Masuda, T., Fusada, N., Oosawa, N., Takamatsu, K., Yamamoto, Y.Y., Ohto, M., Nakamura, K., Goto, K., Shibata, D., Shirano, Y. (2003) Functional analysis of isoforms of NADPH: protochlorophyllide oxidoreductase (POR), PORB and PORC, in *Arabidopsis thaliana*. *Plant and cell physiology* **44:** 963–974

McGlynn, P., Hunter, C.N. (1993) Genetic analysis of the *bchC* and *bchA* genes of *Rhodobacter sphaeroides*. *Molecular and General Genetics* **236:** 227–234

van de Meene, A.M.L., Hohmann-Marriott, M.F., Vermaas, W.F.J., Roberson, R.W. (2006) The three-dimensional structure of the cyanobacterium *Synechocystis* sp. PCC 6803. *Archives of Microbiology* **184:** 259–270

Minamizaki, K., Mizoguchi, T., Goto, T., Tamiaki, H., Fujita, Y. (2008) Identification of two homologous genes, *chlAI* and *chlAII*, that are differentially involved in isocyclic ring formation of chlorophyll *a* in the cyanobacterium *Synechocystis* sp. PCC 6803. *Journal of Biological Chemistry* **283:** 2684–2692

Müller, A.H., Gough, S.P., Bollivar, D.W., Meldal, M., Willows, R.D., Hansson, M. (2011) Methods for the preparation of chlorophyllide *a*: An intermediate of the chlorophyll biosynthetic pathway. *Analytical Biochemistry* **419:** 271–276

Müller, B., Eichacker, L.A. (1999) Assembly of the D1 precursor in monomeric photosystem II reaction center precomplexes precedes chlorophyll *a*–triggered accumulation of reaction center II in barley etioplasts. *The Plant Cell* **11:** 2365–2377

Müller, P., Li, X.-P., Niyogi, K.K. (2001) Non-photochemical quenching. A response to excess light energy. *Plant Physiology* **125:** 1558–1566. doi:10.1104/pp.125.4.1558

Mullineaux, C.W., Emlyn-Jones, D. (2005) State transitions: an example of acclimation to low-light stress. *Journal of Experimental Botany* **56**: 389–393

Muraki, N., Nomata, J., Ebata, K., Mizoguchi, T., Shiba, T., Tamiaki, H., Kurisu, G., Fujita, Y. (2010) X-ray crystal structure of the light-independent protochlorophyllide reductase. *Nature* **465:** 110–114

Nagamori, S., Smirnova, I.N., Kaback, H.R. (2004) Role of YidC in folding of polytopic membrane proteins. The Journal of Cell Biology **165:** 53–62

Nagata, N., Tanaka, R., Satoh, S., Tanaka, A. (2005) Identification of a vinyl reductase gene for chlorophyll synthesis in *Arabidopsis thaliana* and implications for the evolution of *Prochlorococcus species*. *The Plant Cell* **17:** 233–240

Nakanishi, H., Nozue, H., Suzuki, K., Kaneko, Y., Taguchi, G., Hayashida, N. (2005) Characterization of the *Arabidopsis thaliana* mutant pcb2 which accumulates divinyl chlorophylls. *Plant and Cell Physiology* **46:** 467–473

Nasrulhaq-Boyce, A., Griffiths, W.T., Jones, O.T. (1987). The use of continuous assays to characterize the oxidative cyclase that synthesizes the chlorophyll isocyclic ring. *Biochemical Journal* **243:** 23–29

Naylor, G.W., Addlesee, H.A., Gibson, L.C.D., Hunter, C.N. (1999) The photosynthesis gene cluster of *Rhodobacter sphaeroides*. *Photosynthesis Research* **62:** 121–139

Nelson, N., Ben-Shem, A. (2004) The complex architecture of oxygenic photosynthesis. *Nature Reviews Molecular Cell Biology* **5:** 971–982

Nelson, N., Yocum, C.F. (2006) Structure and function of photosystems I and II. *Annual Review of Plant Biology* **57:** 521–565

Nickelsen, J., Rengstl, B., Stengel, A., Schottkowski, M., Soll, J., Ankele, E. (2011) Biogenesis of the cyanobacterial thylakoid membrane system – an update. *FEMS Microbiology Letters* **315:** 1–5

Niederman, R.A., Mallon, D.E., Langan, J.J. (1976) Membranes of *Rhodopseudomonas sphaeroides IV*. Assembly of chromatophores in low-aeration cell suspensions. *Biochimica et Biophysica Acta - Bioenergetics* **440:** 429–447

Nixon, P.J., Michoux, F., Yu, J., Boehm, M., Komenda, J. (2010) Recent advances in understanding the assembly and repair of photosystem II. *Annals of Botany* **106**: 1-16

Nomata, J., Mizoguchi, T., Tamiaki, H., Fujita, Y. (2006) A second nitrogenase-like enzyme for bacteriochlorophyll biosynthesis reconstitution of chlorophyllide *a* reductase with purified X-protein (BchX) and YZ-protein (BchY-BchZ) from Rhodobacter capsulatus. Journal of Biological Chemistry **281:** 15021–15028

Nomata, J., Swem, L.R., Bauer, C.E., Fujita, Y. (2005) Overexpression and characterization of dark-operative protochlorophyllide reductase from *Rhodobacter capsulatus*. *Biochimica et Biophysica Acta - Bioenergetics* **1708**: 229–237

Ohad, I., Kyle, D.J., Arntzen, C.J. (1984) Membrane protein damage and repair: removal and replacement of inactivated 32-kilodalton polypeptides in chloroplast membranes. *Journal of Cell Biology* **99**: 481–485

Ossenbühl, F., Inaba-Sulpice, M., Meurer, J., Soll, J., Eichacker, L.A. (2006) The *Synechocystis* sp PCC 6803 *oxa1* homolog is essential for membrane integration of reaction center precursor protein pD1. *The Plant Cell* **18:** 2236–2246

Oster, U., Bauer, C.E., Rüdiger, W. (1997) Characterization of chlorophyll *a* and bacteriochlorophyll *a* synthases by heterologous expression in *Escherichia coli*. *Journal of Biological Chemistry* **272:** 9671–9676

Oster, U., Rüdiger, W. (1997) The G4 gene of *Arabidopsis thaliana* encodes a chlorophyll synthase of etiolated plants. *Botanica Acta* **110:** 420–423

Ouchane, S., Steunou, A.-S., Picaud, M., Astier, C. (2004) Aerobic and anaerobic Mg-protoporphyrin monomethyl ester cyclases in purple bacteria a strategy adopted to

bypass the repressive oxygen control system. *Journal of Biological Chemistry* **279:** 6385–6394

Paddock, T.N., Mason, M.E., Lima, D.F., Armstrong, G.A. (2010) *Arabidopsis* protochlorophyllide oxidoreductase A (PORA) restores bulk chlorophyll synthesis and normal development to a *porB porC* double mutant. *Plant Molecular Biology* **72**: 445–457

Pandey, A., Andersen, J.S., Mann, M. (2000) Use of mass spectrometry to study signaling pathways. *Science Signaling* 2000, pl1.

Pasch, J.C., Nickelsen, J., Schünemann, D. (2005) The yeast split-ubiquitin system to study chloroplast membrane protein interactions. *Applied Microbiology and Biotechnology* **69**: 440–447

Peter, E., Salinas, A., Wallner, T., Jeske, D., Dienst, D., Wilde, A., Grimm, B. (2009) Differential requirement of two homologous proteins encoded by *sll1214* and *sll1874* for the reaction of Mg protoporphyrin monomethylester oxidative cyclase under aerobic and micro-oxic growth conditions. *Biochimica et Biophysica Acta - Bioenergetics* **1787**: 1458–1467.

Pinta, V., Picaud, M., Reiss-Husson, F., Astier, C. (2002) *Rubrivivax gelatinosus acsF* (previously orf358) codes for a conserved, putative binuclear-iron-cluster-containing protein involved in aerobic oxidative cyclization of Mg-protoporphyrin IX monomethylester. *Journal of Bacteriology* **184:** 746–753

Porra, R.J. (1997) Recent progress in porphyrin and chlorophyll biosynthesis. *Photochemistry and Photobiology* **65:** 492–516

Porra, R.J., Schäfer, W., Gad'on, N., Katheder, I., Drews, G., Scheer, H. (1996) Origin of the two carbonyl oxygens of bacteriochlorophyll *a*. *European Journal of Biochemistry* **239**, 85–92

Porra, R.J., Schäfer, W., Katheder, I., Scheer, H. (1995). The derivation of the oxygen atoms of the 13^1-oxo and 3-acetyl groups of bacteriochlorophyll *a* from water in *Rhodobacter sphaeroides* cells adapting from respiratory to photosynthetic

conditions: evidence for an anaerobic pathway for the formation of isocyclic ring E. *FEBS letters* **371:** 21–24

Promnares, K., Komenda, J., Bumba, L., Nebesarova, J., Vacha, F., Tichy, M. (2006) Cyanobacterial small chlorophyll-binding protein ScpD (HliB) is located on the periphery of photosystem II in the vicinity of PsbH and CP47 subunits. Journal of Biological Chemistry 281, 32705–32713.

Pudek, M.R., Richards, W.R., (1975) A possible alternate pathway of bacteriochlorophyll biosynthesis in a mutant of *Rhodopseudomonas sphaeroides*. *Biochemistry* **14**: 3132–3137

Qian, P., Addlesee, H.A., Ruban, A.V., Wang, P., Bullough, P.A., Hunter, C.N. (2003) A reaction center-light-harvesting 1 complex (RC-LH1) from a *Rhodospirillum rubrum* mutant with altered esterifying pigments: characterization by optical spectroscopy and cryo-electron microscopy. *Journal of Biological Chemistry* **278:** 23678–23685

Qian, P., Papiz, M.Z., Jackson, P.J., Brindley, A.A., Ng, I.W., Olsen, J.D., Dickman, M.J., Bullough, P.A., Hunter, C.N. (2013) Three-dimensional structure of the *Rhodobacter sphaeroides* RC-LH1-PufX complex: Dimerization and quinone channels promoted by PufX. *Biochemistry* **52:** 7575–7585

Rapoport, T.A., (2007) Protein translocation across the eukaryotic endoplasmic reticulum and bacterial plasma membranes. *Nature* **450:** 663–669

Reid, J.D., Hunter, C.N. (2004) Magnesium-dependent ATPase activity and cooperativity of magnesium chelatase from *Synechocystis* sp. PCC 6803. Journal of Biological Chemistry **279:** 26893–26899

Reid, J.D., Siebert, C.A., Bullough, P.A., Hunter, C.N. (2003) The ATPase activity of the ChlI subunit of magnesium chelatase and formation of a heptameric AAA+ ring. *Biochemistry* **42:** 6912–6920.

Richards, W.R., Lascelles, J. (1969) Biosynthesis of bacteriochlorophyll. The characterization of latter stage intermediates from mutants of *Rhodopseudomonas spheroides*. *Biochemistry* **8:** 3473–3482

Rowe, J.D., Griffiths, W.T. (1995) Protochlorophyllide reductase in photosynthetic prokaryotes and its role in chlorophyll synthesis. *Biochemical Journal* **311:** 417–424

Rüdiger, W. (1987) Chlorophyll synthetase and its implication for regulation of chlorophyll biosynthesis, in: Progress in Photosynthesis Research. Springer, pp. 461–467.

Rüdiger, W. (1997) Chlorophyll metabolism: from outer space down to the molecular level. *Phytochemistry* **46:** 1151–1167

Rüdiger, W., Benz, J., Guthoff, C. (1980). Detection and partial characterization of activity of chlorophyll synthetase in etioplast membranes. *European Journal of Biochemistry* **109:** 193–200

Rzeznicka, K., Walker, C.J., Westergren, T., Kannangara, C.G., von Wettstein, D., Merchant, S., Gough, S.P., Hansson, M. (2005). Xantha-l encodes a membrane subunit of the aerobic Mg-protoporphyrin IX monomethyl ester cyclase involved in chlorophyll biosynthesis. *Proceedings of the National Academy of Sciences* **102**: 5886–5891

Sachelaru, I., Petriman, N.A., Kudva, R., Kuhn, P., Welte, T., Knapp, B., Drepper, F., Warscheid, B., Koch, H.G. (2013) YidC occupies the lateral gate of the SecYEG translocon and is sequentially displaced by a nascent membrane protein. *Journal of Biological Chemistry* **288**: 16295–16307

Sambrook, J., Fritsch, E.F., Maniatis, T. (1989) Molecular cloning. Cold spring harbor laboratory press New York.

Schmid, H.C., Oster, U., Kögel, J., Lenz, S., Rüdiger, W. (2001). Cloning and characterisation of chlorophyll synthase from *Avena sativa*. *Biological Chemistry* **382**: 903–911

Schmid, H.C., Rassadina, V., Oster, U., Schoch, S., Rüdiger, W. (2002) Pre-loading of chlorophyll synthase with tetraprenyl diphosphate is an obligatory step in chlorophyll biosynthesis. *Biological Chemistry* **383**: 1769–1776

Schneider, C.A., Rasband, W.S., Eliceiri, K.W. (2012) NIH Image to ImageJ: 25 years of image analysis. *Nature Methods* **9**: 671–675

Schoch, S. (1978) The esterification of chlorophyllide a in greening bean leaves. *Zeitschrift für Naturforschung C* **33**: 712–714

Schoch, S., Hehlein, C., Rüdiger, W. (1980) Influence of anaerobiosis on chlorophyll biosynthesis in greening oat seedlings (*Avena sativa L*.). *Plant physiology* **66:** 576–579.

Schoch, S., Oster, U., Mayer, K., Feick, R., Rüdiger, W. (1999) Subtrate specificity of overexpressed bacteriochlorophyll synthase from chloroflexus aurantiacus, in: The Chloroplast: From Molecular Biology to Biotechnology. Springer, pp. 213–216.

Schoch, S., Schäfer, W. (1978) Tetrahydrogeranylgeraniol, a precursor of phytol in the biosynthesis of chlorophyll a: localization of the double bonds. *Zeitschrift für Naturforschung C*. **33**: 408–412

Schottkowski, M., Gkalympoudis, S., Tzekova, N., Stelljes, C., Schünemann, D., Ankele, E., Nickelsen, J., (2009) Interaction of the periplasmic PratA factor and the PsbA (D1) protein during biogenesis of photosystem II in *Synechocystis* sp. PCC 6803. *Journal of Biological Chemistry* **284**: 1813–1819

Shalygo, N., Czarnecki, O., Peter, E., Grimm, B. (2009) Expression of chlorophyll synthase is also involved in feedback-control of chlorophyll biosynthesis. *Plant Molecular Biology* **71**: 425–436

Shpilyov, A.V., Zinchenko, V.V., Shestakov, S.V., Grimm, B., Lokstein, H. (2005) Inactivation of the geranylgeranyl reductase (*chlP*) gene in the cyanobacterium *Synechocystis* sp. PCC 6803. *Biochimimica et Biophysica Acta* **1706**: 195–203

Siefert, E., Irgens, R.L., Pfennig, N. (1978) Phototrophic purple and green bacteria in a sewage treatment plant. *Applied and Environmental Microbiology* **35**: 38–44

Silva, P., Thompson, E., Bailey, S., Kruse, O., Mullineaux, C.W., Robinson, C., Mann, N.H., Nixon, P.J. (2003) FtsH is involved in the early stages of repair of photosystem II in *Synechocystis* sp PCC 6803. *The Plant Cell* **15:** 2152–2164

Sirijovski, N., Olsson, U., Lundqvist, J., Al-Karadaghi, S., Willows, R., Hansson, M. (2006) ATPase activity associated with the magnesium chelatase H-subunit of the chlorophyll biosynthetic pathway is an artefact. *Biochemical Journal* **400**: 477–484

Smith, C.A., Suzuki, J.Y., Bauer, C.E. (1996) Cloning and characterization of the chlorophyll biosynthesis gene chlM from *Synechocystis* PCC 6803 by complementation of a bacteriochlorophyll biosynthesis mutant of *Rhodobacter capsulatus*. *Plant Molecular Biology* **30**: 1307–1314

Sobotka, R. (2014) Making proteins green; biosynthesis of chlorophyll-binding proteins in cyanobacteria. *Photosynthesis Research* **119**: 223–232

Soll, J., Schultz, G., Rüdiger, W., Benz, J. (1983) Hydrogenation of geranylgeraniol: two pathways exist in spinach chloroplasts. *Plant Physiology* **71**: 849–854

Spence, E., Bailey, S., Nenninger, A., Møller, S.G., Robinson, C. (2004) A homolog of Albino3/OxaI is essential for thylakoid biogenesis in the cyanobacterium *Synechocystis* sp. PCC 6803. *Journal of Biological Chemistry* **279**: 55792–55800

Spyropoulos, I.C., Liakopoulos, T.D., Bagos, P.G., Hamodrakas, S.J. (2004) TMRPres2D: high quality visual representation of transmembrane protein models. *Bioinformatics* **20**, 3258–3260

Suzuki, J.Y., Bauer, C.E. (1995). A prokaryotic origin for light-dependent chlorophyll biosynthesis of plants. *Proceedings of the National Academy of Sciences* **92**: 3749–3753

Thornton, L.E., Ohkawa, H., Roose, J.L., Kashino, Y., Keren, N., Pakrasi, H.B. (2004) Homologs of plant PsbP and PsbQ proteins are necessary for regulation of photosystem II activity in the cyanobacterium *Synechocystis* 6803. *The Plant Cell* **16**: 2164–2175

Tottey, S., Block, M.A., Allen, M., Westergren, T., Albrieux, C., Scheller, H.V., Merchant, S., Jensen, P.E. (2003) *Arabidopsis* CHL27, located in both envelope and thylakoid membranes, is required for the synthesis of protochlorophyllide. *Proceedings of the National Academy of Sciences* **100**: 16119–16124

Tsukatani, Y., Yamamoto, H., Harada, J., Yoshitomi, T., Nomata, J., Kasahara, M., Mizoguchi, T., Fujita, Y., Tamiaki, H. (2013) An unexpectedly branched biosynthetic pathway for bacteriochlorophyll *b* capable of absorbing near-infrared light. *Scientific Reports* **3**: 1217

Tucker, J.D., Siebert, C.A., Escalante, M., Adams, P.G., Olsen, J.D., Otto, C., Stokes, D.L., Hunter, C.N. (2010) Membrane invagination in *Rhodobacter sphaeroides* is initiated at curved regions of the cytoplasmic membrane, then forms both budded and fully detached spherical vesicles. *Molecular Microbiology* **76**: 833–847

Umena, Y., Kawakami, K., Shen, J.-R., Kamiya, N. (2011) Crystal structure of oxygen-evolving photosystem II at a resolution of 1.9 Å. *Nature* **473**: 55–60

Uniacke, J., Zerges, W. (2007) Photosystem II assembly and repair are differentially localized in chlamydomonas. *The Plant Cell* **19**: 3640–3654

Van Bloois, E., Dekker, H.L., Fröderberg, L., Houben, E.N., Urbanus, M.L., de Koster, C.G., de Gier, J.W., Luirink, J. (2008) Detection of cross-links between FtsH, YidC, HflK/C suggests a linked role for these proteins in quality control upon insertion of bacterial inner membrane proteins. *FEBS letters* **582**: 1419–1424

Van Niel, C.B. (1962) The present status of the comparative study of photosynthesis. *Annual Review of Plant Physiology* **13**: 1–25.

Vavilin, D., Vermaas, W. (2007) Continuous chlorophyll degradation accompanied by chlorophyllide and phytol reutilization for chlorophyll synthesis in *Synechocystis* sp. PCC 6803. *Biochimica et Biophysica Acta - Bioenergetics* **1767**: 920–929

Vermaas, W.F.J., Ikeuchi, M., Inoue, Y. (1988) Protein composition of the photosystem II core complex in genetically engineered mutants of the cyanobacterium *Synechocystis* sp. PCC 6803, in: Molecular Biology of Photosynthesis. Springer, pp. 389–405.

Walker, C.J., Mansfield, K.E., Smith, K.M., Castelfranco, P.A. (1989) Incorporation of atmospheric oxygen into the carbonyl functionality of the protochlorophyllide isocyclic ring. *Biochemical Journal* **257**: 599–602

Walters, R.G. (2005) Towards an understanding of photosynthetic acclimation. *Journal of Experimental Botany* **56**: 435–447

Wang, P., Gao, J., Wan, C., Zhang, F., Xu, Z., Huang, X., Sun, X., Deng, X. (2010). Divinyl chlorophyll(ide) a can be converted to monovinyl chlorophyll(ide) a by a divinyl reductase in rice. *Plant Physiology* **153**: 994–1003

Wang, P., Wan, C., Xu, Z., Wang, P., Wang, W., Sun, C., Ma, X., Xiao, Y., Zhu, J., Gao, X., others (2013) One divinyl reductase reduces the 8-vinyl groups in various intermediates of chlorophyll biosynthesis in a given higher plant species, but the isozyme differs between species. *Plant Physiology* **161**: 521–534

Westphal, S., Heins, L., Soll, J., Vothknecht, U.C. (2001) Vipp1 deletion mutant of *Synechocystis*: A connection between bacterial phage shock and thylakoid biogenesis? *Proceedings of the National Academy of Sciences* **98**: 4243–4248

Wittig, I., Karas, M., Schägger, H. (2007). High resolution clear native electrophoresis for in-gel functional assays and fluorescence studies of membrane protein complexes. *Molecular and Cellular Proteomics* **6**: 1215–1225

Wong, Y.S., Castelfranco, P.A., (1984) Resolution and reconstituion of Mg-protoporphyrin IX monomethyl ester (oxidative) cyclase, the enzyme system responsible for the formation of the chlorophyll isocyclic ring. *Plant Physiology* **75**: 658-661

Wong, Y.-S., Castelfranco, P.A., Goff, D.A., Smith, K.M. (1985) Intermediates in the formation of the chlorophyll isocyclic ring. Plant Physiology **79**: 725–729

Xiong, J., Fischer, W.M., Inoue, K., Nakahara, M., Bauer, C.E. (2000) Molecular evidence for the early evolution of photosynthesis. *Science* **289**: 1724–1730

Xu, H., Vavilin, D., Funk, C., Vermaas, W. (2004) Multiple deletions of small cab-like proteins in the cyanobacterium *Synechocystis* sp. PCC 6803 consequences for pigment biosynthesis and accumulation. *Journal Biologial Chemistry* **279**: 27971–27979

Yamazaki, S., Nomata, J., Fujita, Y. (2006) Differential operation of dual protochlorophyllide reductases for chlorophyll biosynthesis in response to

environmental oxygen levels in the cyanobacterium *Leptolyngbya boryana*. *Plant Physiology* **142**: 911–922

Yang, Z.M., Bauer, C.E. (1990) *Rhodobacter capsulatus* genes involved in early steps of the bacteriochlorophyll biosynthetic pathway. *Journal of Bacteriology* **172**: 5001–5010.

Yao, D., Kieselbach, T., Komenda, J., Promnares, K., Prieto, M.A.H., Tichy, M., Vermaas, W., Funk, C. (2007) Localization of the small CAB-like proteins in photosystem II. *Journal of Biological Chemistry* **282**: 267–276

Yu, J., Smart, L.B., Jung, Y.-S., Golbeck, J., McIntosh, L. (1995) Absence of PsaC subunit allows assembly of photosystem I core but prevents the binding of PsaD and PsaE in *Synechocystis* sp. PCC 6803. *Plant Mololecular Biology* **29**: 331–342

Zhang, S., Shen, G., Li, Z., Golbeck, J. H. and Bryant, D. A. (2014) Vipp1 is essential for the biogenesis of Photosystem I but not thylakoid membranes in *Synechococcus sp.* PCC 7002. *Journal of Biological Chemistry* **289**: 15904-15914

Zouni, A., Witt, H.T., Kern, J., Fromme, P., Krauss, N., Saenger, W., Orth, P. (2001) Crystal structure of photosystem II from *Synechococcus* elongatus at 3.8 Å resolution. *Nature* **409**: 739–743